

1963

X-ray studies of lime-bentonite reaction products

George Rembert Glenn
Iowa State University

Follow this and additional works at: <https://lib.dr.iastate.edu/rtd>

 Part of the [Civil Engineering Commons](#), and the [Geology Commons](#)

Recommended Citation

Glenn, George Rembert, "X-ray studies of lime-bentonite reaction products " (1963). *Retrospective Theses and Dissertations*. 2532.
<https://lib.dr.iastate.edu/rtd/2532>

This Dissertation is brought to you for free and open access by the Iowa State University Capstones, Theses and Dissertations at Iowa State University Digital Repository. It has been accepted for inclusion in Retrospective Theses and Dissertations by an authorized administrator of Iowa State University Digital Repository. For more information, please contact digirep@iastate.edu.

This dissertation has been 64-3868.
microfilmed exactly as received

GLENN, George Rembert, 1923-
X-RAY STUDIES OF LIME-BENTONITE REAC-
TION PRODUCTS.

Iowa State University of Science and Technology
Ph.D., 1963
Engineering, civil
Geology

University Microfilms, Inc., Ann Arbor, Michigan

X-RAY STUDIES OF LIME-BENTONITE REACTION PRODUCTS

by

George Rembert Glenn

A Dissertation Submitted to the
Graduate Faculty in Partial Fulfillment of
The Requirements for the Degree of
DOCTOR OF PHILOSOPHY

Major Subject: Soil Engineering

Approved:

Signature was redacted for privacy.

In Charge of Major Work

Signature was redacted for privacy.

Head of Major Department

Signature was redacted for privacy.

Dean/bf Graduate College

Iowa State University
Of Science and Technology
Ames, Iowa

1963

TABLE OF CONTENTS

	Page
INTRODUCTION	1
REVIEW OF LITERATURE	2
Lime-Bentonite Reaction	2
Calcium Aluminates	7
X-ray analysis	7
Differential thermal analysis	12
Infrared spectroscopy	13
Calcium Silicates	15
X-ray analysis and electron microscopy	17
Differential thermal analysis	21
Electron microscopy	23
Infrared spectroscopy	24
MATERIALS AND METHODS	30
Materials	30
Lime-bentonite materials	31
Sample curing	31
Specimen preparation	31
Synthesis of tobermorite	32
Methods	32
Hydrothermal reaction procedure	32
X-ray diffraction	33
Differential thermal analysis	33
Electron microscopy	34
Infrared spectroscopy	35
Electron probe analysis	35

	Page
RESULTS	37
X-ray Diffraction	37
Resolution of 8 Å peak	37
8 Å peak changes with atmosphere	38
Slow scan of 3Å peak	38
Summary of d-spacings of mixtures	43
Otay bentonite	44
Room cured mixtures of lime-bentonite	44
Calcitic lime plus bentonite	44
Dolomitic monohydrated lime plus bentonite	46
Dolomitic dihydrated lime plus bentonite	48
Hydrothermally reacted mixtures of lime-bentonite	50
Freshly prepared mixtures	50
Cured mixtures	59
Differential Thermal Analysis	78
Otay bentonite	79
Unreacted mixtures of lime-bentonite	79
Room cured mixtures of lime-bentonite	80
Calcitic lime plus bentonite	80
Dolomitic monohydrated lime plus bentonite	80
Dolomitic dihydrated lime plus bentonite	81
Hydrothermally reacted mixtures of lime-bentonite	82
Freshly prepared mixtures	82
Cured mixtures	86
Electron Microscopy	97

	Page
Synthetic tobermorite	97
Hydrothermally reacted cured mixtures of lime-bentonite	103
Room cured mixtures of lime-bentonite	109
Infrared Spectroscopy	119
Pure compounds	119
Dry mixtures of lime-bentonite	121
Room cured mixtures of lime-bentonite	121
Calcitic lime plus bentonite	121
Dolomitic monohydrated lime plus bentonite	124
Dolomitic dihydrated lime plus bentonite	124
Hydrothermally reacted cured mixtures of lime-bentonite	127
Calcitic lime plus bentonite	127
Dolomitic monohydrated lime plus bentonite	130
Dolomitic dihydrated lime plus bentonite	134
Electron Probe Analysis	138
Summary of Results	139
DISCUSSION	145
Calcium Aluminate Hydrates	145
Calcium Silicate Hydrates	147
CONCLUSIONS	151
REFERENCES	155
ACKNOWLEDGMENTS	162

INTRODUCTION

This study is concerned with the characterization of the products of the reaction between hydrated lime of several types and pure bentonite, cured at room temperature $23^{\circ} \pm 2^{\circ}\text{C}$ and under conditions approaching 100 per cent relative humidity. For correlation purposes the cured samples and other freshly prepared samples were also hydrothermally reacted. Hydrated lime added to silicious-aluminous materials often reacts to produce cementitious products in what is called a pozzolanic reaction, and such strength gains have been obtained from mixtures of clay and hydrated lime in the form $\text{Ca}(\text{OH})_2$. Addition of $\text{Ca}(\text{OH})_2$ (2% for calcium bentonite) sufficient to neutralize weakly acidic clay OH^- groups is the minimum amount required for pozzolanic reaction to start, known as the "lime retention point" (Hilt and Davidson 29 and Ho and Handy 31, 32).

Based on these criteria, all mixtures in this study were expected to yield crystalline products, probably calcium aluminate and silicate hydrates.

REVIEW OF LITERATURE

Calcium aluminate hydrates are mostly relatively low temperature compounds, whereas the calcium silicate hydrates may be prepared at either room temperature or under hydrothermal conditions. Extensive study has been done on the systems dealing with the pure forms of these compounds, believed to be involved in the principal Portland cement hydration reactions. Pertinent portions of these studies will be reviewed with particular reference to the systems $\text{CaO-Al}_2\text{O}_3\text{-H}_2\text{O}$ (called CAH) and $\text{CaO-SiO}_2\text{-H}_2\text{O}$ (called CSH) at ordinary or room temperature conditions. In addition, review of a limited number of hydrothermal studies in the system CSH will be presented in the temperature range below 175°C .

The literature which deals with the lime-bentonite reaction and products is restricted to relatively few papers.

Lime-Bentonite Reaction

The lime-clay reaction producing the hydrates under consideration has been termed "pozzolanic". Lea's (41) definition of a pozzolan as modified in the ASTM standard on hydraulic cement, ASTM designation C-219-55 (1) is: "Pozzolan shall be a siliceous or siliceous aluminous material, which in itself

possesses little or no cementitious value, but will, in finely divided form and in the presence of moisture, chemically react with calcium hydroxide at ordinary temperatures to form compounds possessing cementitious properties". This definition would include natural and artificial materials. Whether clay meets the specifications and can be called a pozzolanic material is determined then on the basis of whether the products of the hydrated lime-clay reaction possess cementitious properties. It has long been known that lime added to clayey soils produces a beneficial reaction from the standpoint of workability and strength. Rapid depression of the plasticity index contributes to improved workability and is usually attributed to cation exchange and ion adsorption phenomena. The reasons for the strength gain have never been fully understood. Long-term cementation has been attributed to the products of the reaction of lime and the siliceous-aluminous minerals.

Hilt and Davidson (29) showed that montmorillonitic soils retain Ca(OH)_2 far in excess of their cation exchange capacities measured at pH 7, and that this higher requirement must be satisfied before any lime is available for cementitious reactions. Ho and Handy (30) showed that slurry viscosity and floc size reach a maximum at this point and termed this

the "lime retention point". From x-ray and differential thermal analysis (DTA) studies, the Ca(OH)_2 utilized in this reaction no longer appears as the hydroxide. In a later study Ho and Handy (31) postulate the physico-chemical phenomena. Small amounts of Ca(OH)_2 added to bentonite increase the negative charge on the clay particles, probably by dissociation of OH^- groups. Further additions of Ca(OH)_2 allow Ca^{++} adsorption to gradually compensate the increased negative charge and cause a strong floc formation. Both a high pH and the presence of polyvalent cations are required for this type of flocculation but complete Ca^{++} saturation is unnecessary. The flocculation and partial exchange occur rapidly but complete interlayer cation exchange is comparatively slow and probably continues by diffusion. The dissociation of clay OH^- groups and accompanying adsorption of Ca^{++} ions reach a maximum at the "lime retention point". Lime added in excess of this amount remains crystalline until needed to replenish the system as the dissolved or adsorbed lime is used up in slow pozzolanic reactions.

Studies have been made on the products of lime-clay systems but usually under higher temperature conditions than expected in field situations ($\sim 40^\circ\text{C}$) (2, 3, 14, 15, 16, 42).

Eades and Grim (15) and Eades, Nichols and Grim (16) found unidentified calcium silicate hydrates in hydrothermally treated lime-clay mineral and lime-soil mixtures. D-spacings found were 5.09, 3.04, 2.8 and 1.8 Å. No mix containing a montmorillonite mineral under field conditions was shown to give this product.

McCaleb (42) did x-ray diffraction and electron microscope studies on lime-montmorillonite clay systems but he included no d-spacings observed for "traces of tobermorite" in the room cured samples, and only two electron micrographs were used to compare room cured with hydrothermally treated samples. Examination of the two micrographs he shows for room-cured samples leaves much to be desired insofar as determination of tobermorite. His results for hydrothermally treated samples include x-ray d-spacings of only the first observed basal reflection for tobermorite with a 11.3-11.6 Å spacing. In this instance, his electron micrographs of lime-illite mixtures are more convincing, as he reports the formation of a poorly crystallized tobermorite.

No record was found of electron diffraction studies having been performed on mixtures of lime and clay minerals.

Products of the lime-clay mineral reaction (probably aluminates) under ordinary temperatures were studied by Hilt

and Davidson (28) and by Glenn and Handy (22). In both studies, single crystal x-ray techniques were used as well as powder methods; DTA was used in the latter study.

Diamond (14) shows that the reaction product of a Ca(OH)_2 plus montmorillonite mixture at 60°C for 55 days gives peaks at $2.74 \overset{\circ}{\text{A}}$ and $3.06 \overset{\circ}{\text{A}}$, which he identifies as CSH. No evidence of C_3AH_6 is present. For the same mixture reacted at 45°C for 55 days, no x-ray pattern was shown; peaks were found at $3.02 \overset{\circ}{\text{A}}$, attributed to CSH, and several were attributed to the $7.6 \overset{\circ}{\text{A}}$ calcium aluminate.

Diamond (14) also studied by DTA the reaction product of Ca(OH)_2 plus montmorillonite reacted at 60°C for 55 days. The pattern shows a weak endotherm at 160°C and weak endothermic bulges at 520 and 760°C . A strong exotherm occurs at 940°C . Another curve for the same mixture reacted at 45° for 60 days shows Ca(OH)_2 and CaCO_3 present with a small exotherm at 890°C , attributed to CSH.

Eades and Grim (15) give a DTA curve for a lime-Wyoming bentonite mixture, hydrothermally reacted at 45°C for 72 hours, with a weak very broad endotherm at 160° , a sequence of weak endotherms at 430, 490 and 550° with a medium broad endotherm at 680°C . A very strong exotherm appears at 930°C .

Diatomaceous earth mixtures with equal weights of hydrated lime were reacted by Gaze (20) hydrothermally at 165°C. Crinkly foils of CSH I were identified in electron micrographs; little change occurred with prolonged treatment at 165°C.

Calcium Aluminates

X-ray analysis and electron microscopy

The calcium aluminates crystallize more readily than the silicates in the hydration of Portland cement. Although much study has been done on the system CAH, the structure of only one of the aluminates has been determined exactly according to Taylor (56). A tentative structure has been proposed for another by Tilley, Megaw and Hey (59). The basic study initiated by Wells, Clarke and McMurdie (64) has been supplemented from time to time but the powder x-ray method which has been employed yields cell parameters of uncertain validity. Roberts (51), Buttler, Glasser and Taylor (10) and Aruja (4) have contributed in recent years to clarification of aluminate phases by x-ray and electron diffraction studies of single crystals.

The phase equilibria of the calcium aluminates under room conditions are better understood than those of the silicates.

The principal known compounds are listed in Table 1 which summarizes the material presented here.

Steinour's (53) review of the $\text{CaO-Al}_2\text{O}_3\text{-H}_2\text{O}$ (CAH) system in the literature before 1952 was comprehensive. Selected references are given here to cover this period and others since that time.

Wells, Clarke, and McMurdie (64) reported in 1943 on the System C-A-H at 21°C - 90°C . They determined the solubility curves of hexagonal C_4AH_{13} and of the cubic form, C_3AH_6 , and indexed the 8.2 \AA d-spacing as the first order basal spacing of C_4AH_{13} . D'Ans and Eick (13) later designated it the α polymorph.

More recent work (1953) by D'Ans and Eick (13) on the system CAH at 20° defines the solubility curves for both polymorphs, α and β , of C_4AH_{13} as well as C_3AH_6 and C_2AH_8 . They found that C_3AH_6 is the only stable aluminate. The α form was found to have a very high formation velocity, Midgley (47) gave the three strongest d-spacings as 2.30, 2.04 and 5.14 \AA .

In 1959, Buttler, Glasser and Taylor (10) gave results of single crystal x-ray and electron diffraction studies of the β polymorph of C_4AH_{13} . They report from x-ray powder data that the longest and strongest spacing is 7.92 \AA , indexed (00.1),

Table 1. Hydrated calcium aluminates

Composition	Dimensions, Å		Morphology	d-spacing, Å (47, 51)		
	a	c		Longest	Strongest	
α C ₂ AH ₈	5.7	10.7	(S) ^a	Hexagonal	10.7	10.7
β C ₂ AH ₈	5.7	10.4	(S)	with excellent	10.4	--
α C ₄ AH ₁₃	5.7	8.2	(S)	0001 cleavage (56)	8.2 (6)	8.2
β C ₄ AH ₁₃	5.74	7.92	(S)	Hexagonal (10)	7.92	7.92
C ₄ AH ₁₁	--	--		Hexagonal (10)	7.4 (51)	--
C ₄ AH ₇	--	--		Hexagonal (10)	7.4 (51)	--
C ₄ AH ₁₉	5.7	10.6	(S)	Hex. with 0001 cleavage (62)	10.6 (51)	--
α_1 C ₄ AH ₁₉	5.77	64.08	(U.C.) ^b	Hex. (possibly rhombohedral) (4)	10.82 (4)	10.82
α_2 C ₄ AH ₁₉	5.77	21.37	(U.C.)	Hexagonal (4)	10.84 (4)	2.885
CAH ₁₀	--	--		Hex. prisms (56)	14.3	14.3
C ₃ AH ₆	a 12.576		(U.C.)	Cubic	5.14	2.300
C ₄ A ₃ H ₃	Probably orthohombic			Tablets	3.58 (6)	3.58

^aS - Structural element.

^bU.C. - unit cell.

followed in intensity by 3.99 \AA (00.2) and 2.87 \AA (11.). In the same system at 25°C , Roberts (51) reported in 1957 that a new hydrate C_4AH_{19} is the only tetra-calcium aluminate that exists in the aqueous system at that temperature; the 13, 11, and 7 H_2O hydrates form as dehydrated aluminate products under varying drying conditions. The 19 H_2O hydrate is relatively easily dehydrated to give a mixture of the α and β forms of C_4AH_{13} , characterized by longest basal spacings of 8.2 and 7.9 \AA respectively. The next two strongest spacings for the α form are 4.1 and 3.9 \AA (Bogue 6); for the β form, they are 3.99 and 2.87 \AA (Buttler, Glasser and Taylor 10). As there is little difference in stability between the two forms, there is no way to predict the relative amount of each which may be formed. The 11 and 7 H_2O hydrates both give longest basal spacings of 7.4 \AA . In the same study, Roberts (51) reported two forms of the dicalcium aluminate hydrate, C_2AH_8 , which also occur in the aqueous system C-A-H at 25°C . The α and β forms are characterized by longest basal spacings of 10.7 and 10.4 \AA respectively, with the α form the more stable of the two; an earlier work by Wells, Clarke and McMurdie (64) had reported this spacing as 10.6, indexed as (001). The 7.5 H_2O , 5 H_2O and 4 H_2O hydrates of C_2AH_8 form in lower states of hydration and

give longest basal spacings of 10.6, 8.7 and 7.4 Å, respectively. Aruja (4) reported in 1961 on unit cell and space group determinations of the α_1 and α_2 polymorphs of C_4AH_{19} . The α_1 form is hexagonal (possibly rhombohedral) with structural elements $\underline{a} = 5.77$ and $\underline{c} = 64.08$ Å; the α_2 form is hexagonal with $\underline{a} = 5.77$ and $\underline{c} = 21.37$ Å. In a mimeographed Note No. A92 (private communication), longest d-spacings of the α_1 and α_2 forms are 10.82 Å, indexed (00.6), and 10.84 Å, indexed (00.2), respectively.

Carlson and Berman (11) did recent studies on calcium aluminate carbonate hydrates.

CAH_{10} and C_2AH_8 are relatively unstable with respect to each other in the aqueous phase under conditions near that of the present study. Jones (33) reported in 1960 that the transition temperature is 22°C, with the 10 H₂O hydrate stable below and the other stable above that temperature. Solubility relations of CAH_{10} at 21° is given by Percival and Taylor (50). For its three strongest spacings, Midgley (47) gives 14.3, 7.16 and 3.57 Å.

The three strongest spacings for $C_4A_3H_3$ are given by Bogue (6) as 3.58, 3.26 and 2.80 Å.

As noted above and in Table 1 the length of the structural

element a tends to be the same dimension, 5.7 \AA , regardless of the hydration state; c is found to vary between 7.9 and 10.8 \AA . For these reasons and stacking variations, determinations of these structural elements rather than the crystallographic unit cell is more meaningful. These studies cover principally the stable or metastable products. At room temperature the only thermodynamically stable compound noted is C_3AH_6 . The compounds C_4AH_{19} , C_2AH_8 and CAH_{10} , are however readily formed and do not change quickly to give the stable C_3AH_6 , or $Ca(OH)_2$ or gibbsite, which are also stable in this system. Taylor (56) states that before 1957, the compound now described as C_4AH_{19} was considered to be C_4AH_{13} . Roberts (51) found that dehydration of C_4AH_{19} to give C_4AH_{13} occurs very easily, as soon as the solid has been separated from its mother liquor.

Differential thermal analysis

A differential thermal analysis curve for C_3AH_6 by Kalousek, Davis and Schmertz (36) shows but one peak, a medium endotherm at 310°C .

The DTA of the pure compound C_3AH_6 by Majumdar and Roy (45) shows a very strong endotherm of medium breadth at 330°C followed by a medium endotherm at 490°C . The DTA of $C_4A_3H_3$ shows a medium endotherm of medium breadth at 730°C .

The only DTA of the pure compound C_4AH_{12-13} noted in the literature is shown by Turriziani (61). There are very weak endotherms at 130° and $170^\circ C$ with a strong endotherm at $230^\circ C$. Another weak endothermic peak at $330^\circ C$ is followed by a seemingly broad weak exothermic bulge at about 350° ; the extent is not known as the chart ends there.

Infrared spectroscopy

An infrared spectroscopic pattern for C_4AH_{13} is reproduced by Midgley (48) and is shown in Figure 1. There is a very small broad hydroxyl band at 3.2μ ; no band appears for inter-layer water at 6μ but a broad band at $6.5-7.5\mu$, resembling tobermorite gel. There are two bands giving a broader band at 9.7 and 10.3μ . All bands show less absorption than the CSH products. Two bands at 11.2 and 11.6μ and a very broad band between 12.4 and 13.4μ completes the pattern.

Majumdar and Roy (45) show infrared spectrographs obtained using the K Br disc method of sample preparation on a Perkin-Elmer instrument. The patterns for C_3AH_6 and $C_4A_3H_3$ are both quite complex in the $2-4\mu$ OH region. There are three bands at 2.75 , 3 and 3.3μ , interpreted as indicating a considerable amount of structure, apparently not anticipated. The main unbonded OH position remains at 2.75μ with the removal of 4.5

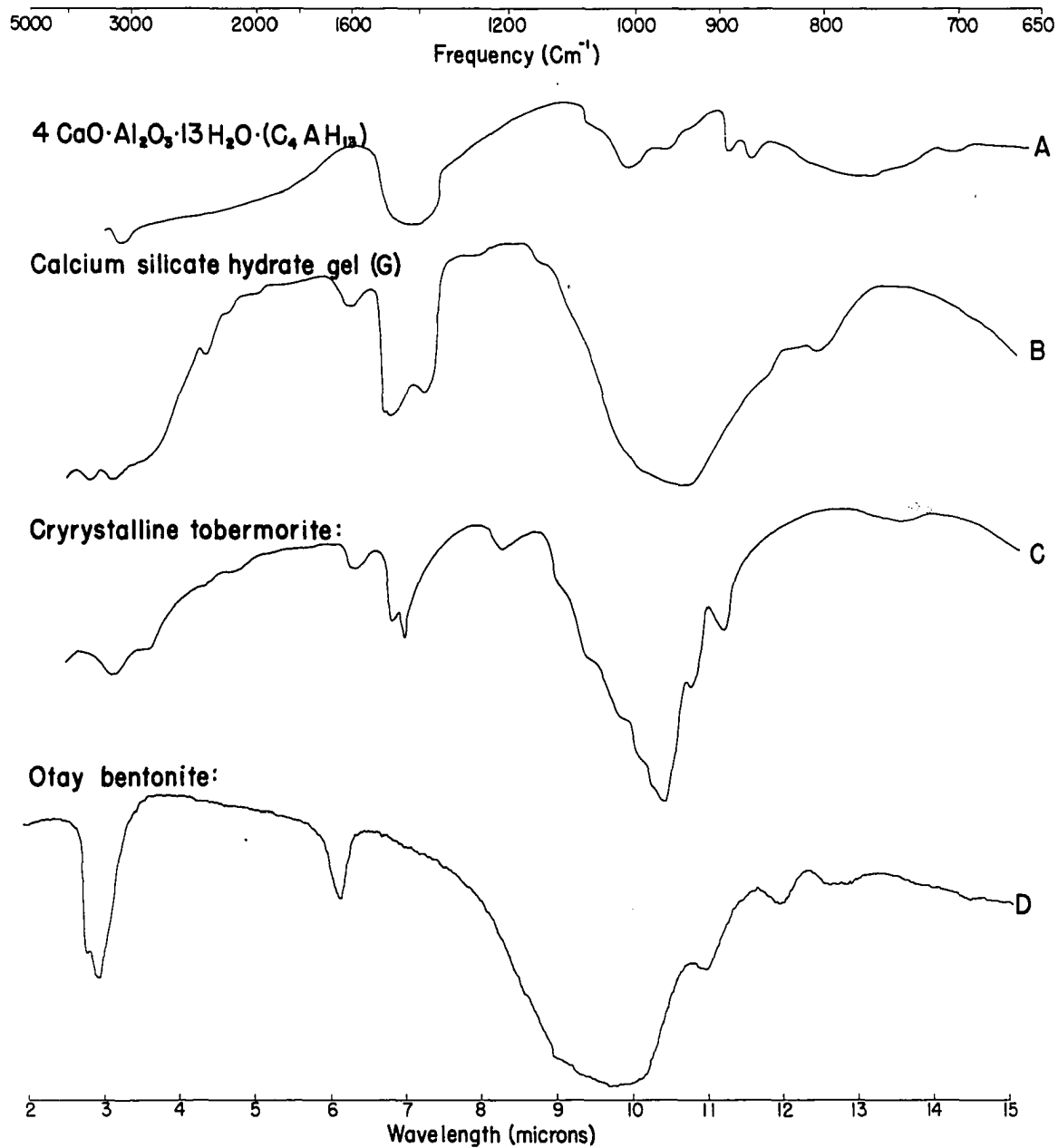


Fig. 1. Infrared spectrographs of pure compounds

molecules of water, the others disappearing. The similarity between the two spectrographs ceases in the upper wave length region. Two distinct bands at 4.4 and 4.7 μ occur on the C₃AH₆ pattern with the 6.2 μ free water absorption band missing but present on C₄A₃H₃. The strongest absorption band occurs at 6.8 μ but only on C₄A₃H₃. Both compounds have 9.3 μ absorption bands and C₄A₃H₃ has a band at 10 μ , which marks the end of the chart.

Calcium Silicates

The reviews of the literature which have been made to date in the CaO-SiO₂-H₂O (CSH) system are in themselves monumental. This review will present pertinent references and abstract relevant details.

The compound now believed to be of greatest significance in Portland cement chemistry is tobermorite. It has been used to designate both the poorly crystallized phases, which are found particularly in room temperature preparations in the CSH system, and the well crystallized phase resembling the rare natural mineral by that name. Formation of hydrated calcium silicates at room temperature was studied comprehensively by Taylor (54).

Diamond's (14) recent thesis is perhaps the most complete survey in some detail and certainly the most helpful in dealing with the confusing terminology inferred above. His study dealt with all the phases of the tobermorite and tobermorite-like calcium silicate hydrates and is an invaluable reference in studies such as the present one. Kalousek has been the principal investigator in much experimental work (34, 35, 36, 37, 38) in recent years in the study of tobermorite and related phases in the CSH system. Original synthesis of the compound (approximate composition $C_5.S_6.H_5$) was by Flint, McMurdie and Wells (17) under hydrothermal conditions. A review of hydrothermal reactions in the CSH system is given by Taylor and Bessey (57). This was followed by Kalousek's synthesis in the 1940's according to Diamond (14) and later synthesis and study in detail by Heller and Taylor (26, 27). The ranges of composition lie between CaO/SiO_2 ratios of 0.8-1.33 (74). Claringbull and Hey (12) first examined the mineral by x-ray diffraction in 1952. Later studies were done by Gard and Taylor (19).

The literature which deals with the poorly crystalline phases of tobermorite overlap those already mentioned; for example, CSH (I) is a distinct compound which may be produced by reaction at room temperature or as a transient phase in

hydrothermal reaction. However, the other two phases related to tobermorite and relevant here, CSH (II) and CSH (G) or Gel, are primarily room temperature preparations according to Diamond (14). CSH (II) was reported as a transient phase in Kalousek's (35) study, and in pure form has been very difficult to synthesize, whereas CSH (I) and CSH (G) or Gel have been relatively easy to synthesize. The ranges of composition for these three compounds vary. The CaO/SiO_2 (C/S) ratio for CSH (I) is near that of tobermorite 0.8-1.33; for CSH (II) and for CSH Gel the ratio is near 1.5. No details of methods of synthesis will be included except to say that the three most prominent are double decomposition, direct synthesis and hydration of individual cement minerals. The nearest analogy to the method usually employed in preparing soil-lime mixtures in the laboratory is known as "paste hydration" as used by Brunauer, Copeland and Bragg (8) for hydration at room temperature. The method of synthesis by McCaleb (42), working with lime and montmorillonitic materials, involved reacting suspensions stirred mechanically and stored or treated hydrothermally.

X-ray analysis

The crystalline character of the calcium silicate hydrates

in relation to their composition and designations or names is presented in Table 2, after the work of Taylor (55).

Table 2. Degrees of crystallinity of calcium silicate hydrates

c/s Ratio of Product	Degree of Crystallinity		
	High	Low	Very Low
	Complete x-ray powder pattern with hkl reflections	Poor x-ray powder pattern with mainly basal and hk or hko reflections	Very poor x-ray powder patterns consisting of one or more hk lines or bands. No basal reflections
0.8-1.33 (Near 0.83 when fully crystalline)	9.3, 11.3 or 14 Å tobermorite. Well crystallized CSH (I)	CSH (I)	Plombierite (natural gel)
1.5-2.0 (Probably 1.5-1.75 when fully crystalline)	"10 or 12.6 Å Tobermorite"	CSH (II)	CSH gel

Although basal d-spacings of these hydrates vary widely, Table 3 shows the relationship between the four principal synthetic compounds presenting d-spacings obtained from selected

Table 3. X-ray diffractometer d-spacings for the principal tobermorite and tobermorite-like calcium silicate hydrates

Synthetic Tobermorite Kalousek (35)	CSH (I)				CSH (II) ^a		CSH Gel ^b	
	Midgley (47)		Diamond (14)		Heller and Taylor (25)		after Diamond (14)	
d-spa., Å ^o Int.	d-spa., Å ^o Int.	d-spa., Å ^o Int.	d-spa., Å ^o Int.	d-spa., Å ^o Int.	d-spa., Å ^o Int.	d-spa., Å ^o Int.	d-spa., Å ^o Int.	
11.1 10	9-14 10			9.8 9				
5.4 2				4.9 2				
3.62 <1								
3.51 <1								
3.33 2								
3.08 6	3.06 10		3.25 2	3.07 10				
			3.02 10			3.03 10 (2.90-3.07)		
2.97 3								
2.81 3	2.81 8			2.85 5				
				2.80 9				

^aPattern by Toropov, Borisenko and Shirokova (60) give a similar pattern with additional spacings at 2.20 and 2.10 Å.

^bPattern by Brunauer (7) shows: 3.07 s vb, 2.80 w and 1.82 Å w.

Table 3. (Continued)

Synthetic Tobermorite Kalousek (35)	CSH (I)				CSH (II) ^a		CSH Gel ^b	
	Midgley (47)		Diamond (14)		Heller and Taylor (25)		after Diamond (14)	
d-spa., Å Int.	d-spa., Å Int.	d-spa., Å Int.	d-spa., Å Int.	d-spa., Å Int.	d-spa., Å Int.	d-spa., Å Int.	d-spa., Å Int.	
			2.78	4				
2.52 <1								
2.43 <1					2.40	4		
2.27 1								
2.12 1								
2.06 <1								
2.00 <1					2.00	6		
1.84 3	1.83	8			1.83	9		
~1.82 1			1.82	3-4			1.82	
							(1.80-1.85)	2
~1.75 <1								
1.65 1	1.67	4	1.66	tr.				
	1.53	2			1.56	5		

references. These data show the variable degree of crystallinity to which reference is made above.

Differential thermal analysis

A quartz-lime mixture with a C/S ratio of 0.33 was reacted hydrothermally at 165°C for an undisclosed period by Gaze (20). The DTA showed a broad, medium exothermic bulge at 410°, a very weak endotherm at 570° with a strong exotherm at 818°C. A paste having equal quantities of lime and diatomaceous earth, giving a C/S ratio of 0.79, was heated at 100° then hydrothermally reacted at 165°C for an undisclosed period. DTA results show a distinct broad exotherm at 330° with a weak endotherm at 770° followed by a weak exotherm at 800°C.

In a continuous hydrothermal study of mixtures of C/S 0.8 at 175°C Kalousek (35) found that the reaction between Ca(OH)_2 and quartz continued after all free Ca(OH)_2 had reacted. At this time less than half the total quartz had reacted. He states that the reaction, after about 6 hours at 175°C, was between the lime-rich phase and the residual quartz. The lime rich phase (C/S = 1.75) gave a very strong exotherm at 850°. Reaction for two hours produced well crystallized tobermorite with no peaks appearing on the DTA pattern.

The differential thermal analysis pattern of pure syn-

thetic tobermorite was shown by Kalousek (35) to be essentially a straight line. Diamond (14) found a noticeable endotherm at 275° and a barely noticeable exotherm at 820°C. He also found that substitutions of various percentages of aluminum in the tobermorite lattice produced the following changes in these peaks: for 3 per cent Al, 810°C medium weak exotherm; for 5 per cent Al, 265°C endotherm, 810°C medium weak exotherm; for 10 per cent Al, 265°C medium endotherm, 630°C weak endothermic bulge and 825°C strong exotherm; for 15 per cent Al, 285, 380°C medium endotherms, about 510°C weak exotherm and 835°C very strong exotherm.

Kalousek (34) noted that there was a distinguishing exothermic peak for CSH (I) in the 835-865°C region; the location of this peak for both room temperature and hydrothermal preparations increases with increase in C/S ratio. His preparations at room temperature give exothermic peaks about 7°C lower than hydrothermal preparations. Diamond's (14) findings for the 15 per cent aluminum substituted tobermorite compounds coincide with Kalousek's (34) preparation of CSH (I) with $C/S = 0.8$.

Van Bemst (63) gives a pattern for CSH II prepared at room temperature. A double set of peaks occurs in the region 340-

380°C, and a slight exothermic bulge occurs around 600°C, with a pair of weak exothermic peaks at 850° and 920°C.

Brunauer and Greenberg (9) report a very strong endotherm near 200°C for CSH Gel preparations. Diamond's (14) results differ; he found that a characteristic small exotherm also occurs between 840 and 865°C, higher than his findings for pure tobermorite and CSH (I). This temperature range coincides with Kalousek's (34) results due to variable C/S ratio.

Electron microscopy

The structures of crystalline compounds formed in the CSH system have been discussed in detail by Bernal (5), Steinour (53) and Bogue (6). Bernal's review at the Third Symposium on the Chemistry of Cement in 1952 emphasized that although a large number of crystal structures had been at least partly resolved for the cement compounds, it would be necessary to develop essentially new x-ray diffraction techniques to attack other compounds of great interest, especially in the CSH system. It was recognized and stated at the time that most of the compounds formed in the reaction of cement with water, including the hydrothermal products formed at elevated temperatures, are available in very low crystalline form. Some results presented at the Third Symposium by Bernal (5) were

later expanded by Grudemo (23, 24). His studies include many micrographs and diffraction patterns obtained by electron diffraction. Diamond's (14) study included several micrographs of calcium silicates and aluminates of interest; however, no detailed analyses were made of the diffraction patterns. Gard, Howison and Taylor (18) examined calcium silicate hydrates having C/S ratios between 0.81 to 1.41. They show electron micrographs for products synthesized at room temperature and hydrothermally. Electron diffraction patterns are given for the latter.

Table 4 is a compilation of d-spacings of selected calcium silicates obtained by electron diffraction, compared with results by x-ray diffraction. More complete compilations may be found in the works cited in the table.

Infrared spectroscopy

Reference is made to Figure 1 showing spectrographs of crystalline tobermorite and CSH Gel compounds after Midgley (48). The infrared spectrum obtained by Kalousek and Roy (38) for synthetic tobermorite ($C_4S_5H_5$) using the Potassium Bromide (K Br) disc procedure of sample preparation showed a broad SiO band with a maximum absorption at about 10.4μ and less absorption at 11.1μ and possibly also at 8.3 to 8.8μ .

Table 4. Selected calcium silicates

1	2	3	4	5	6	7
CSH (I) (23) X-ray	Calculated from basal unit cell ^a	CSH (I) (23) E.D. ^b	CSH (I) E.D. ^c	Tobermorite E.D. ^d	Unsubstituted Tobermorite (14) X-ray	CSH Gel (14) X-ray
12.6 10d					11.2 vs	
5.45 2d					5.47 s	
~4.15 vd		(3.69) sp				
		(3.34) sp			3.50 w	
	3.074 220			3.07 vsb	3.30 w	3.07
3.062 10					3.07 vvs	msb
		3.025 5	3.025 vs			2.9
					2.97 vs	

^aOrthogonal face centered: $5.63 \times 3.67 \text{ \AA}$; indices shown are for a cell double this size, after Megaw and Kelsey (46).

^bE.D. - electron diffraction c/s ratio = 0.92 for samples used in cols. 1, 2, 3, 4; Taylor (54) reports 11.3 \AA instead of 12.6 \AA , col. 1; Grudemo (23) states spacings in parentheses are impurities.

^cD-spacings measured from pattern reproduced on p. 60, Grudemo (23).

^dD-spacings measured from pattern reproduced on p. 93, Diamond (14).

Table 4. (Continued)

1 CSH (I) (23) X-ray	2 Calculated from basal unit cell ^a	3 CSH (I) (34) E.D. ^b	4 CSH (I) E.D. ^c	5 Tobermorite E.D. ^d	6 Unsubstituted Tobermorite (14) X-ray	7 CSH Gel (14) X-ray
2.814 4	2.815 400	2.78 sp	2.76 s	2.78 sp	2.81 vs	
				2.41 wsp	2.52 w	
					2.41 w	
					2.25 w	
					2.14 w	
~2.07 vd		(2.08) sp	2.10 wvd	2.08 sp	2.06 w	
1.836 5	1.835 040	1.846 sp	1.81 s	1.84 sp	2.00 w	1.83 wb
1.673 3	1.671 620	1.664 sp		1.66 sp	1.84 s	1.80
			1.62 m		1.67 m	
1.536 1	1.537 440		1.57 mw	1.55 sp	1.63	
1.407 3	1.408 800				1.53	
			1.37 w	1.38 sp		

A pronounced band at around 6μ was attributed to interlayer water, and another at slightly less than 3μ was attributed to bonded OH groups. Drying did not seem to affect intensities of these latter two bands. Diamond's (14) patterns for tobermorite show better resolution and are more definitive. The main feature is a 10.3μ SiO absorption band, attributed to lattice stretching vibrations, with a smaller band at 11.25μ , attributed to CaCO_3 . Another small band occurred at 10.85μ . The inter-layer water band occurred at 6.18μ , attributed to water deformation vibration. Absorption from the bonded OH groups in the hydroxyl region appeared as a broad weak band between 2.95 and 3.35μ . A similar band was also noted in the 6.95μ region. At the high frequency end of the spectrum, a relatively sharp band occurs at 8.35μ , with a shoulder at 8.55μ . A pair of bands also occurs at 13.5μ and 15.1μ .

Van Bemst (63) reports a very broad absorption band between 8.2 and 11.2μ with a maximum at 10 to 10.5μ for room temperature CSH (I) preparations by the K Br procedure. Kalousek and Roy (38) show infrared spectra for fibrous tobermorites having C/S ratios between 0.8 and 1.5 , the range for CSH (I) composition. The difference in this work and that described above was a broad band between 6.6 and 7μ with

increased absorption with increase in C/S ratio. Diamond's (14) study of CSH (I) shows close similarity to those of his synthetic tobermorites. He found one obvious feature for CSH (I) is the increased absorption of the band near 7μ , often with division into two bands. Whereas his synthetic tobermorites have generally the same absorption on both sides of the SiO band at about 10.3μ , the CSH (I) absorption is more on the longer wave length end of the pattern.

Van Bemst (63) noted that CSH (II) gave a pronounced band at 12.1μ in addition to the common broad SiO band between 8.2 and 11.2μ found for CSH (I). Kalousek and Prebus (37) found CSH (II) absorbs infrared radiation at 2.9μ and between 6.8 - 7.0μ as well.

More extensive study has been done recently on CSH Gel preparations by Diamond (14), Hunt (32) and Midgley (48). Midgley's spectrum is reproduced in this paper in Figure 1 and shows a broad SiO band at 10.6μ . Diamond (14), reporting on other studies noted this same band, attributed to partially linked SiO tetrahedra. The bonded OH group band shown by Midgley (48) is located at 3.1μ . A weak band occurs at 4.4μ and one at 6.3μ due to interlayer water. A broad band around 7μ is divided into two bands of 6.8μ with slightly less

absorption for a band at 7.2μ . A division also occurs in Diamond's (14) findings with more absorption on CSH (I) than Gel. He attributes the longer band to the asymmetrical in-plane vibration of CO_3^{2-} and the shorter to water deformation vibration. The pronounced absorption minimum observed by him for CSH Gel samples at 9μ is not so striking on Midgley's (48) curve, located between 7.5 and 9μ . Whereas the main SiO lattice vibration band at 10.6μ is about the same breadth for both authors, the non-symmetrical pattern is reversed. A distinct band at 12.4μ on the pattern of Midgley (48) also appears, but more broadly, on Diamond's (14) pattern, which he associates with the silicate lattice structure.

MATERIALS AND METHODS

Materials

Table 5, shown below, is a summary and an index to the materials and the methods of analysis employed in this study.

Table 5. Summary of methods and materials

Lime-Bentonite: Water Mixture (weight ratio)	CaO concn. (g/ml)	Theoretical CaO/SiO ₂ (molar ratio)	Analysis*			
			X-ray C H	DTA C H	E.M. C H	I.S. C H
A. Ca(OH) ₂ :Bentonite:H ₂ O 0.45 : 1.00 : 1.62	0.209	0.69	√ √	√ √	√ √	√ √
B. Ca(OH) ₂ + MgO: Bentonite:H ₂ O 0.45 : 1.00 : 1.62	0.136	0.45	√ √	√ √	√ √	√ √
C. Ca(OH) ₂ + Mg(OH) ₂ :Bentonite: H ₂ O 0.45 : 1.00 : 1.62	0.117	0.39	√ √	√ √	- -	√ √

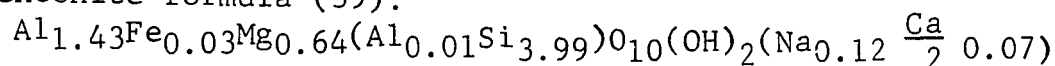
*C - mixtures cured two and one-half to three years at 23°C.

H - hydrothermally reacted at various temperatures up to 170°C.

E.M. - electron microscopy.

I.S. - infrared spectroscopy.

Bentonite formula (39):



When products were large enough, single crystals were isolated under the microscope, mounted and examined by x-ray diffraction and electron probe analysis when desired.

Lime-bentonite materials

The clay mineral used was Otay, California, bentonite, AAPG Reference Clay Mineral number 24 (39, 40). Lime, synthesized from reagent grade laboratory chemicals, was of three types:

- A. High calcium hydrated lime, Ca(OH)_2
- B. Dolomitic monohydrated lime, $\text{Ca(OH)}_2 + \text{MgO}$
- C. Dolomitic dihydrated lime, $\text{Ca(OH)}_2 + \text{Mg(OH)}_2$

Sample curing

Separate slurries of the bentonite were made with each lime and water in the weight ratio 1 : 0.45 : 1.62. The mixtures were sealed in plastic containers to prevent loss of water or entry of carbon dioxide and cured at $23^\circ \pm 2^\circ\text{C}$ for two and one-half to three years.

Specimen preparation

Samples from which specimens were taken were allowed to equilibrate under vacuum over CaCl_2 for twenty-four hours, then ground to approximately 200 mesh size before mounting on

the diffractometer, DTA apparatus or spectrograph. For the x-ray diffraction analysis, duplicate specimens were taken directly from the cured or hydrothermally reacted mixtures and examined under conditions approaching 100 per cent r.h. Denser packing obtained from use of a circular brass ring mount and a 1000 psi pressure gave better reproducibility, so this mounting procedure as reported by Glenn and Handy (22) was used for the moist as well as the vacuum desiccated specimens.

Synthesis of tobermorite

Synthetic tobermorite was prepared hydrothermally at 110-175°C in the laboratory using reagent grade chemicals with a C/S ratio of 0.80 by the patented method of Kalousek (62).

Methods

Hydrothermal reaction procedure

Cured mixtures and some freshly prepared mixtures were reacted hydrothermally in a Pressure Reaction Apparatus, manufactured by Parr Instrument Company, Moline, Illinois, with a maximum range of 1000 psi. Samples were placed in semi-sealed containers which were put in the pressure chamber and sealed. The chamber contained sufficient water to provide steam at its saturated vapor pressure for indicated

temperatures in excess of 100°C, for twelve hours reaction time. Heat was controlled by rheostat, and temperatures were measured in a well provided inside the reaction chamber. To prevent disturbance after reaction, the chamber was cooled in a water bath, after which specimens were taken from each sample for the analyses described below.

X-ray diffraction, differential thermal analysis, electron microscopy and infrared spectroscopy techniques were employed to investigate the reaction products formed.

X-ray diffraction

The equipment used in x-ray diffraction consisted of a General Electric XRD-5 diffractometer, with copper K α radiation for powder samples. Single crystal and powder preparations from single crystals also were mounted in a Siemens Debye-Scherrer camera where Chromium k α radiation was used. Use was made of cited references and x-ray powder data file (1) for identification of compounds.

Differential thermal analysis

The DTA apparatus was equipped with an automatic temperature controller, providing for a heating rate of 10°C per minute to 1000°C. A vertical furnace arrangement is used. The sample block of 18-8 stainless steel, 3/4 in. high by

1 3/4 in. diameter is supported by a hollow ceramic pedestal. Two vertical 3/8 in. diameter by 1/2 in. deep sample holes are symmetrically located with centers 1 in. apart. Number 22 platinum-platinum ten per cent rhodium differential thermocouples are used; the furnace temperature couple is a separate chromel-alumel junction inserted in a 3/8 in. diameter by 1/2 in. deep hole drilled up into the bottom of the block. The inert sample is powdered alumina. Samples were mounted in the remaining hole by application of light pressures on a tamper to give an adequate packing tightness, from which reproducible results were obtainable. The equipment was operated under laboratory atmospheric conditions.

Electron microscopy

The electron microscopic micrographs and diffraction patterns of these materials were made with the assistance of Dr. E. A. Rosauer on the staff of the Ceramic Engineering Department and the Engineering Experiment Station at the University.

The instrument used for the electron microscopic investigations of the lime-montmorillonite mixtures was a Siemens Elmiskop I operated at 80 kilovolts under vacuum $>10^{-4}$ in. Hg. The sample preparation procedure employed ultra-sonic vibration

to assist in dispersion, following a brief mulling of the sample in a mortar. Nebulizing of a drop of the dispersant onto carbon-filmed grids was accomplished by ultrasonic means also. In other instances single crystals of the hexagonal product were crushed and placed on the grids. The purpose of the examination was to obtain electron micrographs of the material, in conjunction with selected area electron diffraction patterns.

The technique resulted in fair dispersion in most instances but with some agglomeration evident, perhaps unavoidable.

Infrared spectroscopy

The infrared spectrophotometer was a model 21, Perkin-Elmer model which was scanned for absorption of wavelengths between two and fifteen microns. Specimen preparation technique was conventional, in which a very small amount was mixed thoroughly with potassium bromide powder. A disc or pellet was formed in a standard Beckman, 15 ton sample die, catalog number 5020.

Electron probe analysis

The electron probe microanalyzer was manufactured by Norelco and utilized the Norelco AMR/3 probe. Samples were single crystals of a hexagonal product of approximately 100

microns width and 5 to 15 microns thickness, glued with a thin film of Duco cement on a graphite base. The analyses were performed by Mr. Richard N. Kniseley, associate chemist in the Ames Laboratory.

RESULTS

X-ray Diffraction

Resolution of 8 \AA° peak

Overlapping reflections or peaks around 8 \AA° are evident from the lack of symmetry which often occurs. Several samples were noted to give this characteristic appearance on x-ray charts so detailed studies were made.

Vacuum dessicated samples of the calcitic lime-montmorillonite mixture having the lowest water : solids ratio showed three peaks, and the intermediate water content samples showed two peaks with only a suggestion of a third peak when scanned at 0.4° per minute by x-ray diffraction. These samples showed no carbonate content when tested with 1N HCl. At room conditions, averages of the three d-spacings were 7.98 \AA° , 7.77 \AA° and 7.58 \AA° , with a range of approximately $\pm 0.05 \text{ \AA}^{\circ}$ for each. The highest and lowest d-spacings observed were 8.03 \AA° and 7.54 \AA° , respectively.

A few samples with the intermediate water : solids ratio of the monohydrated lime-montmorillonite mixture were also examined under room conditions and scanned at 2° per minute; doublet d-spacings were observed at 8.07 \AA° and 7.85 \AA° , about

0.1 Å higher than the calcitic lime. The same mixture at room temperature and humidity for a longer period equilibrated at a single spacing of 7.77 Å.

8 Å peak changes with atmosphere

It was noted in the process of the above investigation that the 8 Å peak in the monohydrated lime-montmorillonite mixture under room conditions slowly changed to 7.77 Å. Under CO₂ free atmosphere for 30 minutes, this peak changed to 7.71 Å. In order to ascertain the influence of an extreme dry atmosphere, a sample of the same mixture which had been desiccated for 6 weeks was placed in a P₂O₅ atmosphere for about ten days except for periodic examination. During this period the lowest d-spacing decreased to about 7.69 Å. Another sample of the same mixture, exposed to the same conditions, gave different results when observed at fast scan only; there was a division of the peak to form the doublet with one d-spacing about 7.7 Å and a lower d-spacing at 7.4 Å. Apparently, the second order peak at 3.9 Å decreases only about 0.02 Å and its spacing seems to be related only to the strongest 1st order reflection.

Slow scan of 3 Å peak

The evidence of a lack of symmetry of the 3 Å peak in

x-ray diffractometer patterns, plus the fact that several compounds have d-spacings in the vicinity, prompted this brief study. The non-symmetrical appearance is evident in fast scan patterns of both room-cured and low temperature hydrothermally treated mixtures, as shown, for example, in Figures 5, 6 and 7. Individual specimens of room-cured samples representing each of the three mixtures shown in Figures 5, 6 and 7 were examined by x-ray diffraction at a scanning rate of 0.4° per minute using high resolution geometry. The results of the average of five scans under CO_2 -free atmosphere is shown by dashed lines in Figures 2, 3 and 4. The upper drawings in the first two figures represent the same specimens left open to laboratory atmosphere for several hours. The heavy lines are sketched to represent possible peaks contributing to the observed pattern. The approximate d-spacings from x-ray of these mixtures under CO_2 free atmosphere are:

	d-spacing, \AA ^o			
$\text{Ca}(\text{OH})_2$ plus bentonite	2.95	2.99	3.04	3.09
$\text{Ca}(\text{OH})_2 + \text{MgO}$ plus bentonite	2.95	2.99	3.04	3.08
$\text{Ca}(\text{OH})_2 + \text{Mg}(\text{OH})_2$ plus bentonite	2.94	2.98	3.04	3.10

X-ray diffraction with fast scan (2° per min.), used in the major part of this study often gives indications of peaks

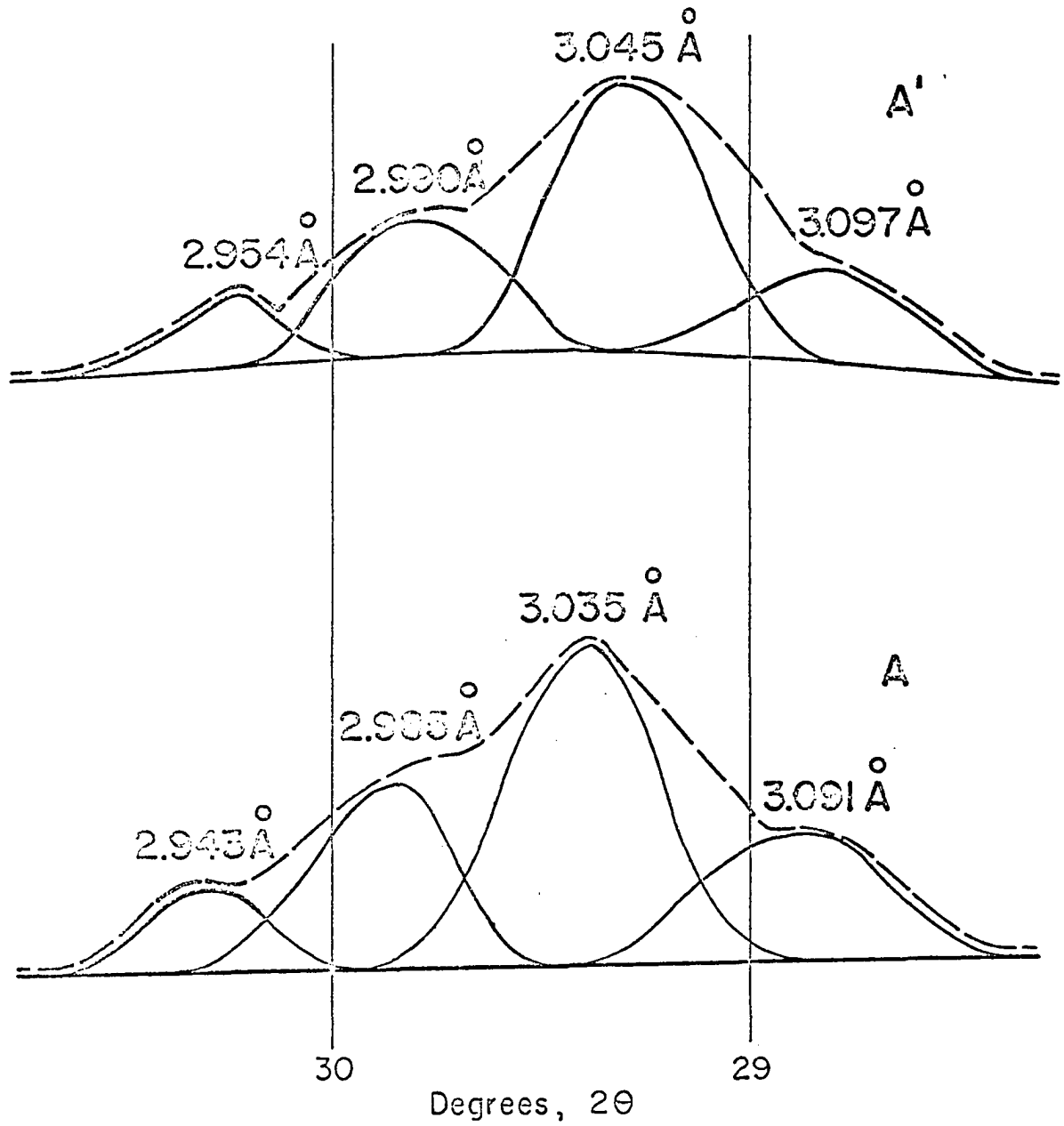


Fig. 2 $\text{Ca}(\text{OH})_2$ + Otay bentonite mixture
X-ray slow scan of 3 Å peak

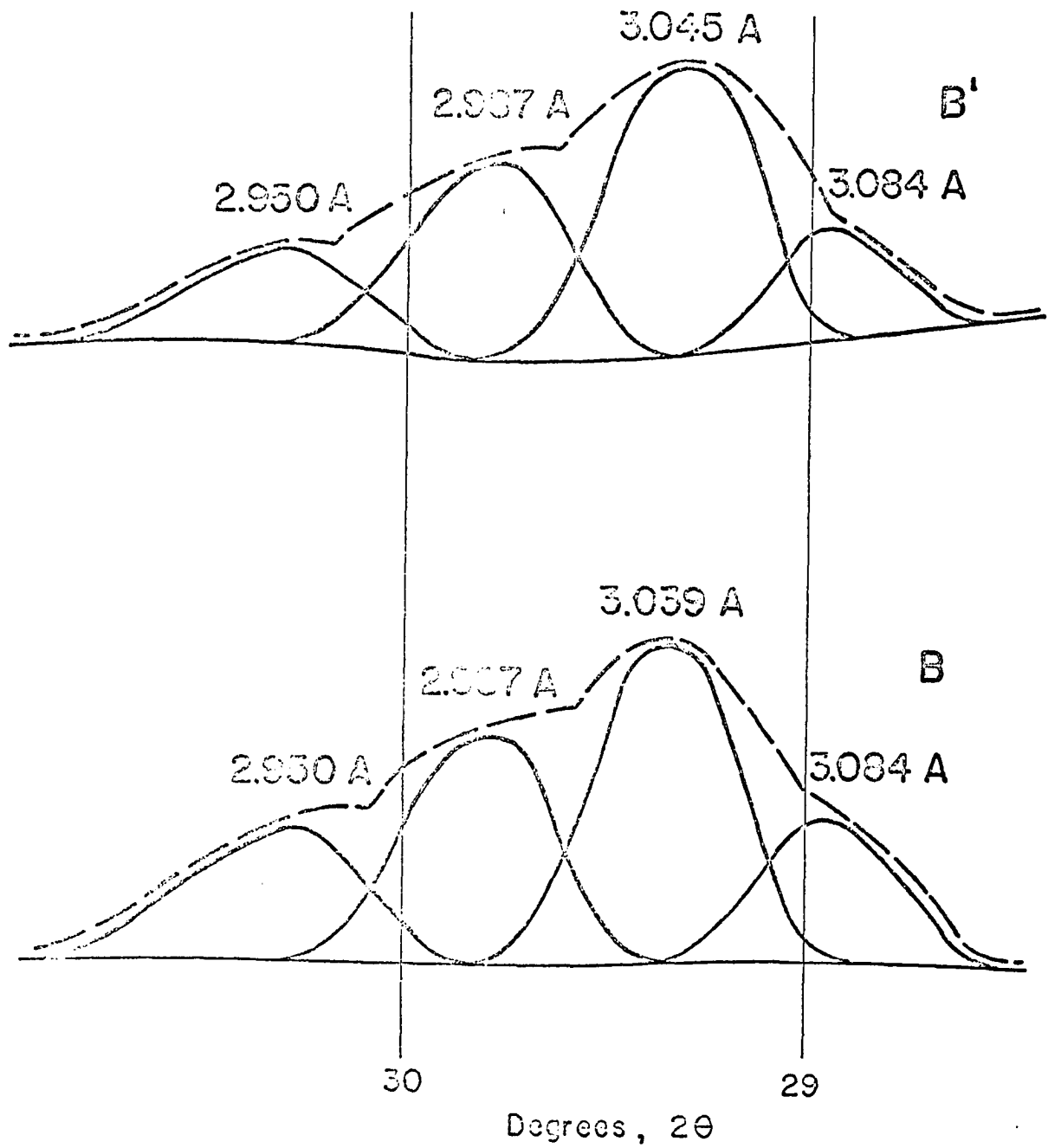


Fig. 3 $\text{Ca(OH)}_2 + \text{MgO} + \text{Otay bentonite}$
X-ray slow scan of 3 Å peak

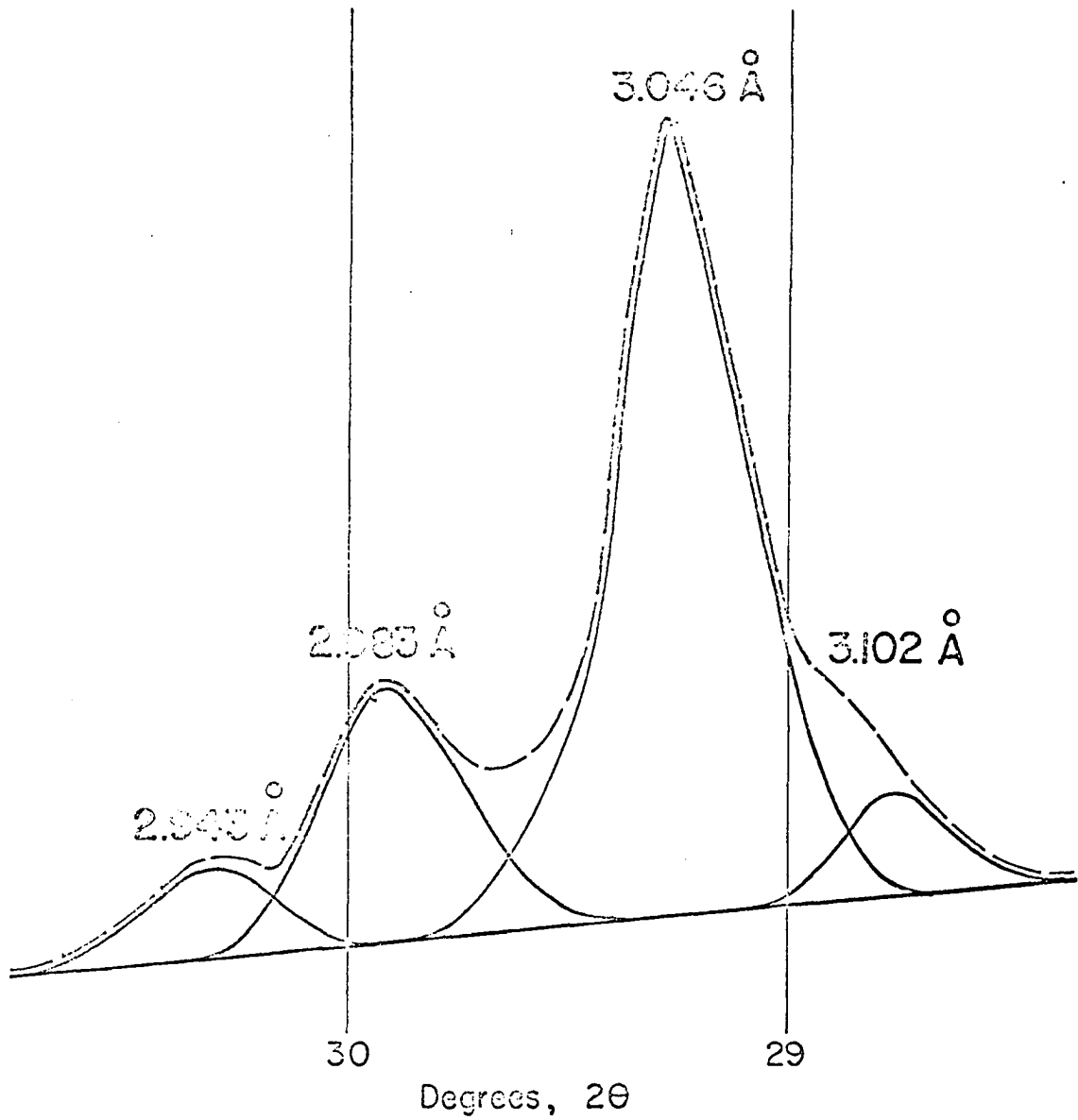


Fig. 4 $\text{Ca(OH)}_2 + \text{Mg(OH)}_2 + \text{Otay bentonite}$
X-ray slow scan of 3 Å peak

near $3 \overset{\circ}{\text{Å}}$ which are not reproduceable. Therefore only the major peak is reported in the data to follow unless there was very strong resolution. When identifying CSH compounds found in the room cured samples, the resolved d-spacing data for the particular mixture will be considered valid.

Summary of d-spacings of mixtures

Identification of d-spacings in the discussion which follows is by compound, such as CSH Gel, CSH I, CSH II or synthetic tobermorite, based on the references cited in Table 3, where all spacings are listed. It will be noted that d-spacings near 3.05 and $1.82 \overset{\circ}{\text{Å}}$ are represented in all CSH compounds. CSH Gel has only these two d-spacings and cannot be positively identified if other spacings appear.

The compound C_4AH_{13} as reported by Buttler, Glasser and Taylor (10) and/or a product isolated by Glenn and Handy (22), is also frequently found in the mixtures. The main d-spacings by both investigators are nearly the same, with the former authors' compilation more extensive. Therefore identification will be based principally on their compilation. The prominent d-spacings are as follows: 7.92 vvs, 3.99 vs, 2.87 s, 2.70 m b, 2.46 s b, 2.24 m, 2.05 m, 1.982 mw, 1.657 ms and $1.438 \overset{\circ}{\text{Å}}$ mw b; twenty-four weaker spacings not listed here appear in

their paper and will be used in identifying C_4AH_{13} . Other references used will be cited in the usual manner.

Otay bentonite

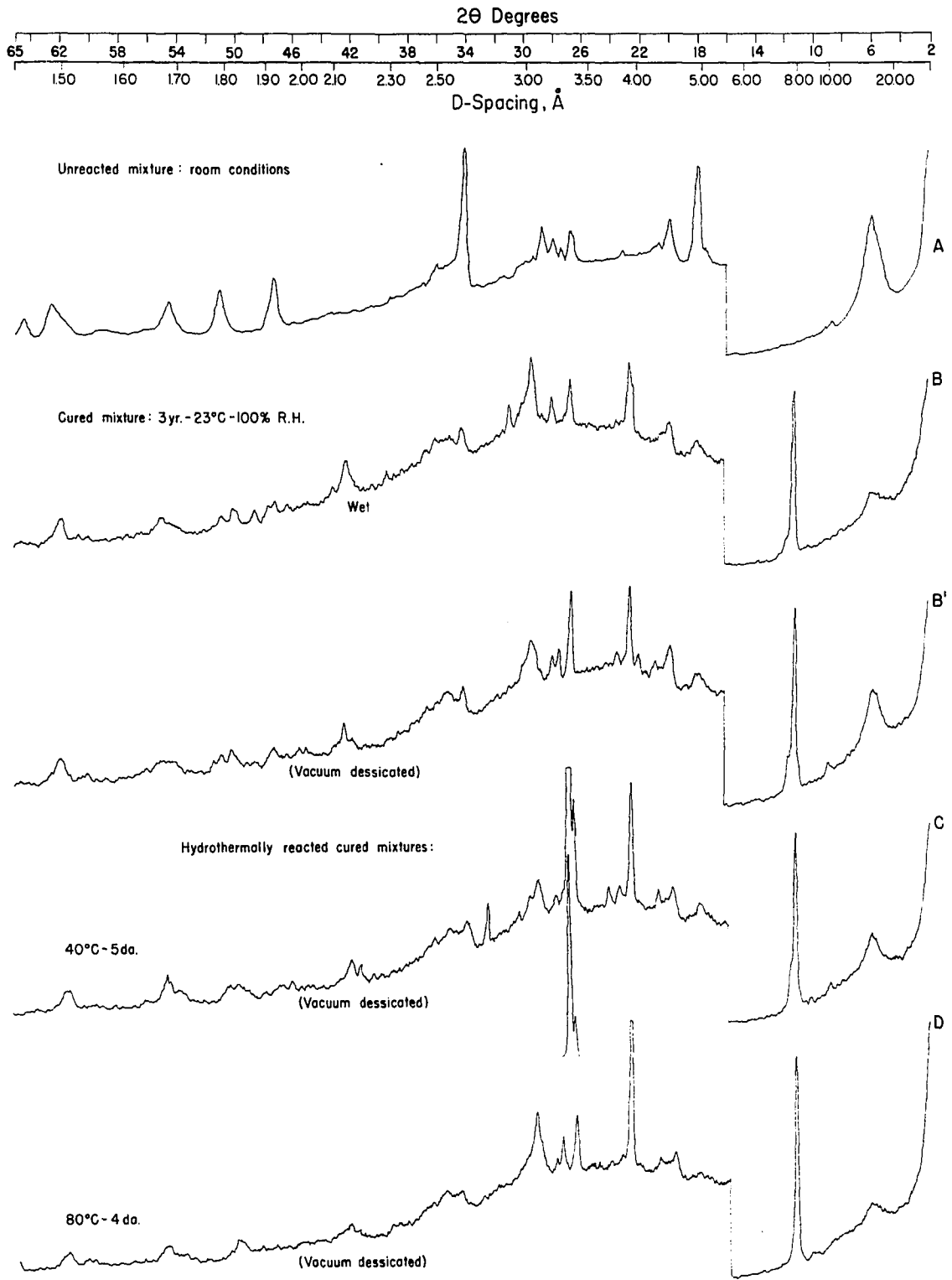
An x-ray diffraction curve for an air dry specimen of Otay bentonite showed peaks at 14.7 vs, 4.48 s, and 2.56 s, 1.69 w and 1.50 \AA° m. Traces of feldspar quartz, mica and calcium carbonate were also present.

Room cured mixtures of lime-bentonite

Calcitic lime plus bentonite The x-ray diffraction curves for this mixture (C/S = 0.69) are shown as curves B and B' in Figure 5. As indicated, curve B' is for a specimen which has been dessicated under vacuum for 24 hr. and curve B for a specimen taken directly from the curing room and x-rayed under conditions approaching 100% r.h. D-spacings for the bentonite in curve B appear at 15.7 m b, 4.48 m, 2.56 mw and $1.499 \text{ \AA}^{\circ}$ mw. The $Ca(OH)_2$ peaks appear at 4.92 w b, 2.62 mw, 1.92 w and 1.79 \AA° w. The strong quartz peak appears at 3.34 \AA° s. $CaCO_3$ peaks appear at 3.04 s b, 2.49 w, 2.28 w and 2.09 \AA° w. The mica peak no longer appears. A feldspar peak appears at 3.19 \AA° m.

Probable reaction product d-spacings are as follows:

7.89 vs, 3.94 s, 3.12 vw, 3.04 s b, 2.85 tr, 2.82 tr, 2.72 tr,



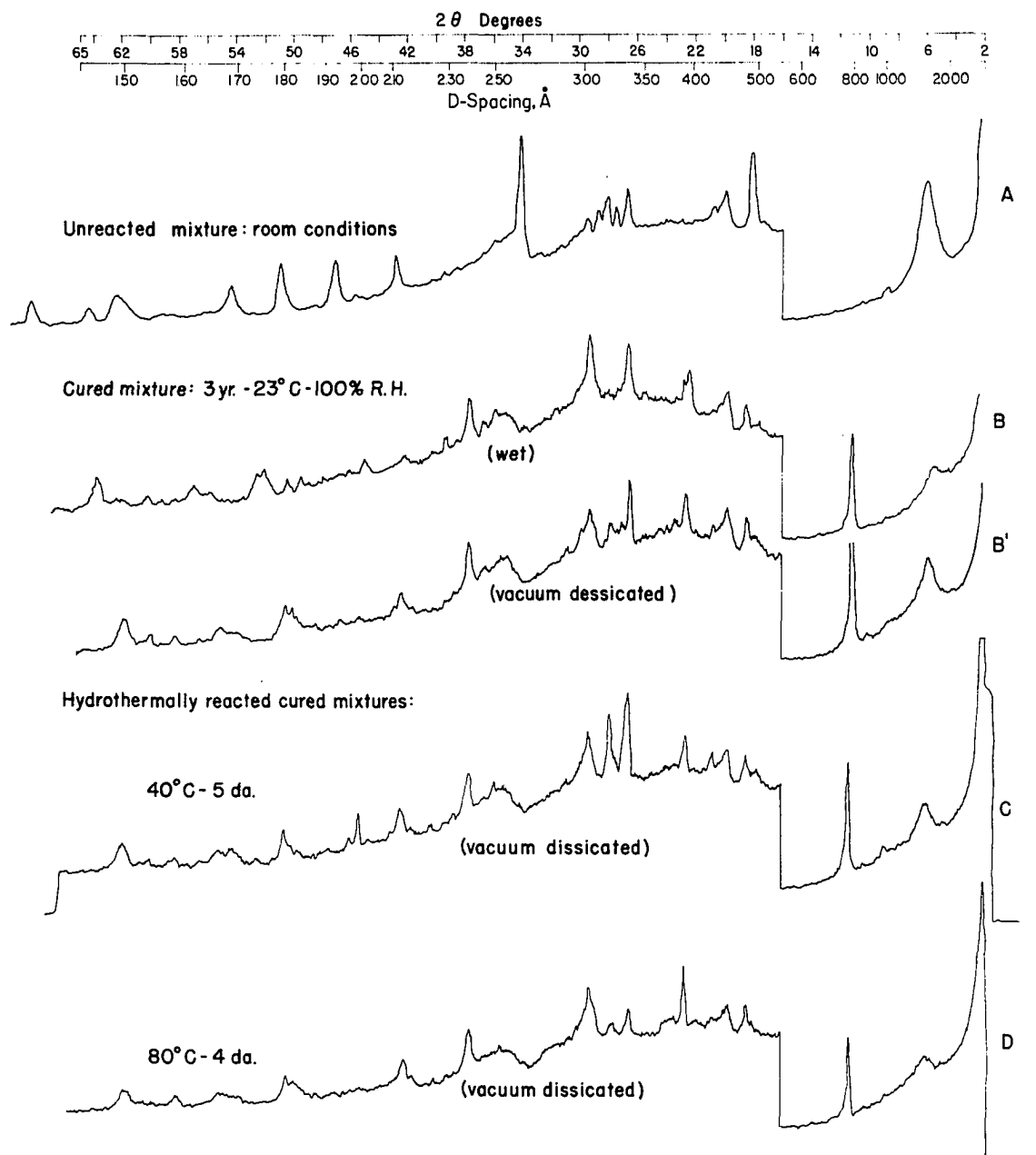
X-ray Diffraction of Mixture

Fig.5 Otay bentonite : Ca(OH)₂ : H₂O (1.00 : 0.45 : 1.62)

2.45 w, 2.90 m, 2.14 ms, 2.02 vw b, 1.82 w b and 1.67 mw b, 1.54 tr, 1.52 Å tr. (2.14 Å peak due to brass ring mount.)

Eleven of the reported d-spacings for C_4AH_{13} correspond to within ± 0.05 Å, to spacings found in this mixture. Four of the five spacings cited in Table 3 for CSH (I) are also present, the 1.82 and 1.67 Å spacings overlapping for these two compounds. As indicated in Table 3, both patterns for CSH (II) indicate the 10 Å spacing. No record was found of this spacing being absent when CSH (II) has been synthesized. All other spacings are present for CSH (II) and CSH Gel.

Dolomitic monohydrated lime plus bentonite The x-ray diffraction curves for this mixture (C/S = 0.45) are shown as curves B and B' in Figure 6. As indicated, curve B' is for a specimen which has been desiccated under vacuum for 24 hr. and curve B for a specimen taken directly from the curing room and x-rayed under conditions approaching 100% r.h. D-spacings for the bentonite appear in curve B at 16.1 mw, 4.48 m, 2.56 mw and 1.499 Å m. The main quartz peak appears at 3.34 Å s. $CaCO_3$ peaks appear at 3.04 s, 2.29 w and 2.10 Å w. No $Ca(OH)_2$ appears. The main peaks of 4.79 m and 2.38 Å m for $Mg(OH)_2$ appear also. The mica peak appears as a trace at 10 Å. Feldspar appears at 3.25 tr.



X-ray Diffraction of Mixture

Fig 6 Otay bentonite : $\text{Ca}(\text{OH})_2 \cdot \text{MgO} \cdot \text{H}_2\text{O}$ (1 : 0.45 : 1.62)

Probable reaction product d-spacings are as follows:

7.89 s, 7.6 w, 4.84 m, 3.9 m, 3.04 s, 2.82 w, 2.54 mw b,
2.50 mw, 2.38 m, 2.00 vw, 1.82 m, 1.67 mw b, 1.62 tr,
1.54 Å^o vw.

Nine d-spacings correspond within 0.05 Å^o to very strong and strong d-spacings of C₄AH₁₃. Another probable aluminate phase found by Hilt and Davidson (28) is also indicated by the 7.6 Å^o spacing and others which overlap those for C₄AH₁₃. If the 3.25 Å^o spacing attributed to feldspar is included, all five CSH (I) spacings are observed for this mixture within ± 0.04 Å^o. The d-spacings for CSH (II) are all represented within ± 0.04 Å^o in those found for this mixture, assuming the 10 Å^o spacing attributed to mica is due in part to this phase.

Dolomitic dihydrated lime plus bentonite The x-ray diffraction curves for this mixture (C/S = 0.39) are shown as curves B and B' in Figure 7. As indicated, curve B is for a specimen which has been desiccated under vacuum for 24 hr. and curve B' for one which was taken directly from the curing room and x-rayed under conditions approaching 100% r.h. D-spacings for the bentonite appear in curve B at 17.3 m b, 4.48 m, 2.56 mw b and 1.499 Å^o m. The quartz peaks appear at 3.36 w and 4.26 Å^o w b. The CaCO₃ peaks appear sharp at 3.04 s, 2.49 vw

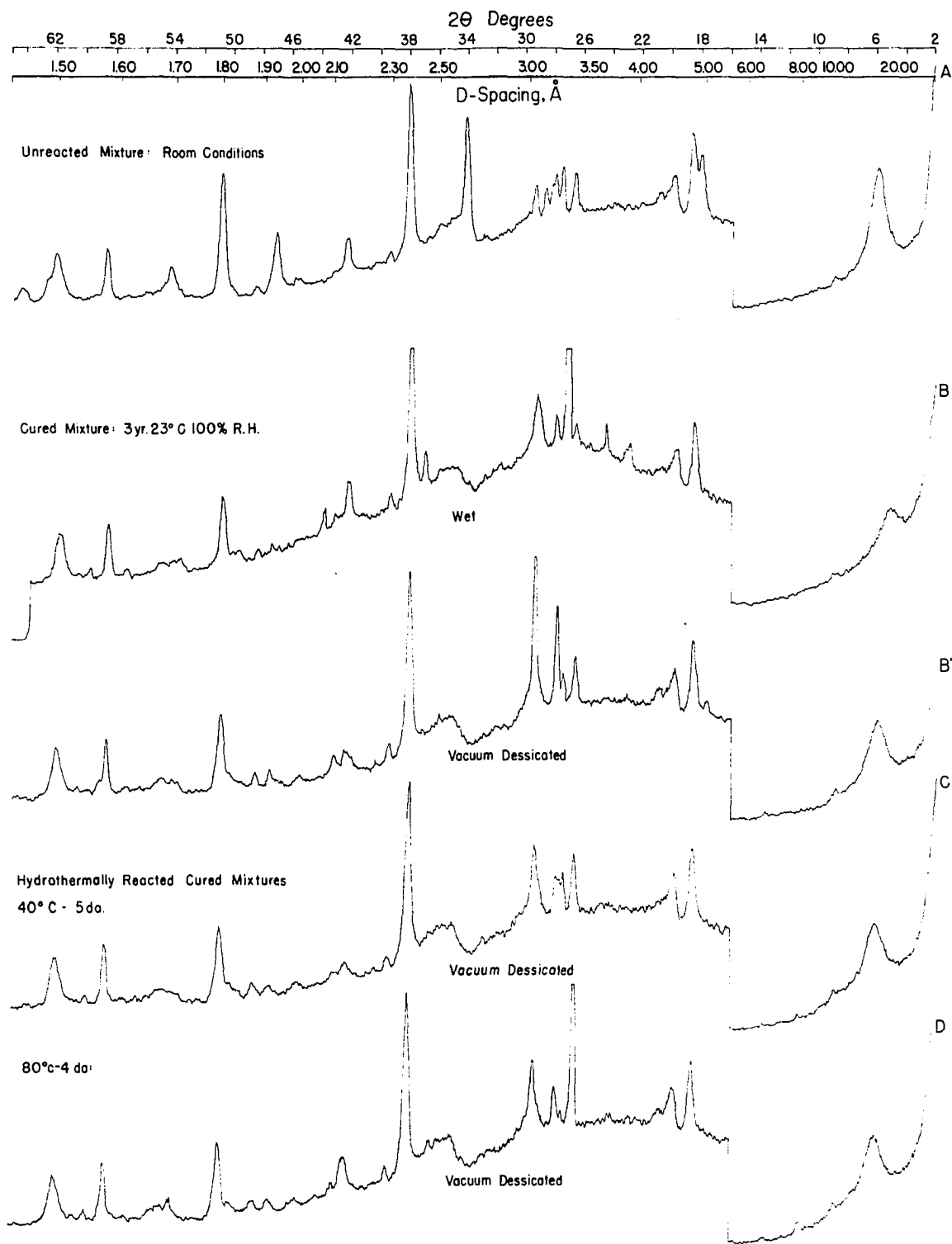


Fig. 7

Xray Diffraction of Mixture
 Otay bentonite: $\text{Ca}(\text{OH})_2 \cdot \text{Mg}(\text{OH})_2 \cdot \text{H}_2\text{O}$
 (1.00:0.45:1.62)

and 2.09 v w. No $\text{Ca}(\text{OH})_2$ appears; the strong peaks at 4.79 s and 2.36 \AA vs for $\text{Mg}(\text{OH})_2$ appear. The mica peak appears very broad at 10.0 \AA tr. Two feldspar peaks appear at 3.18 mw and 3.27 \AA vs.

Probable reaction product d-spacings are as follows:

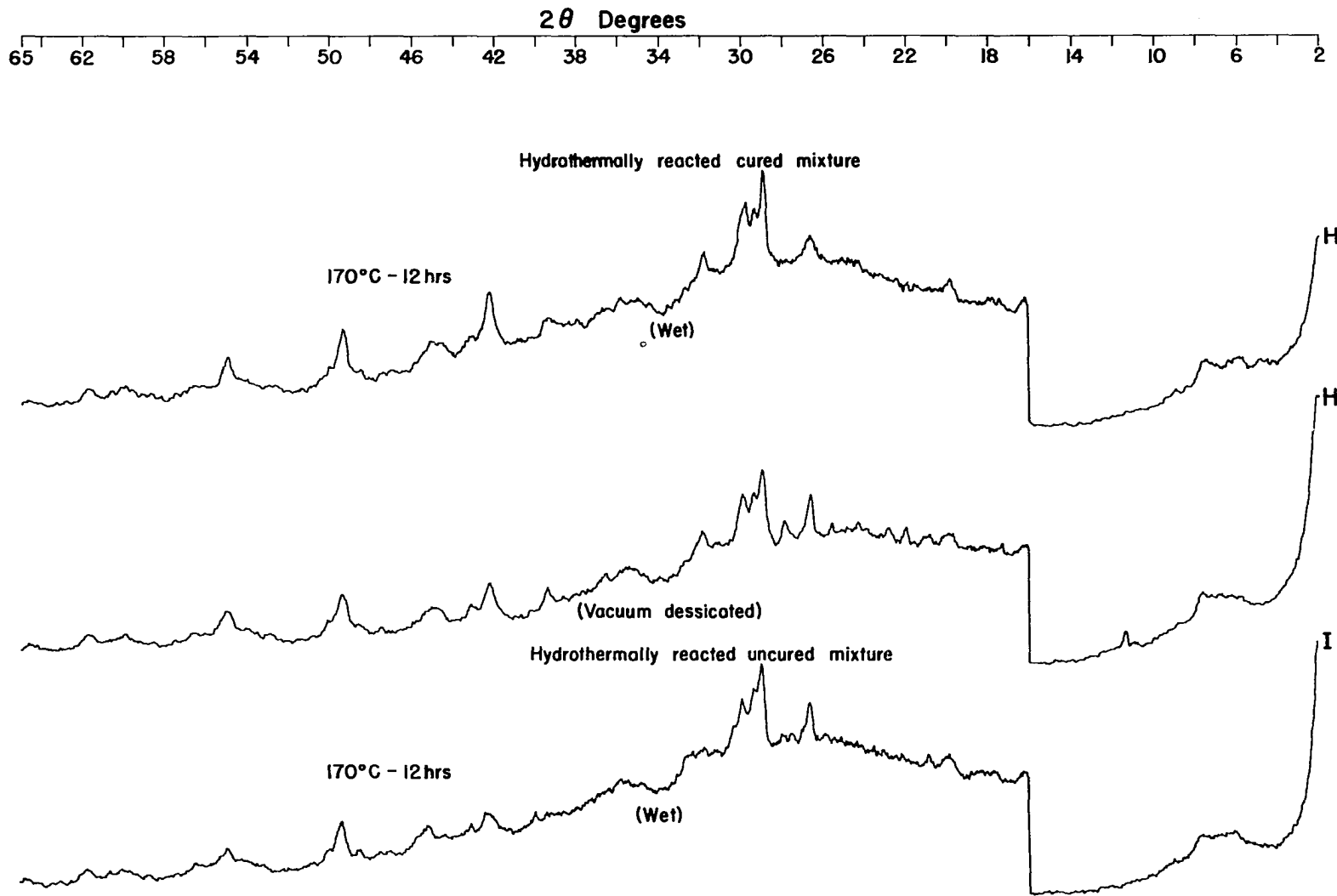
3.04 s b, 2.89 tr, 2.81 w b, 2.42 mw, 2.06 mw, 2.0 tr, 1.83 w, 1.82 vw, 1.70 w b, 1.67 w b and 1.54 \AA w.

D-spacings indicated above correspond within 0.04 \AA to CSH (I), assuming the 3.25 \AA spacing assigned to feldspar belongs to this compound. Except for the two longest spacings for CSH (II), other d-spacings for this compound were found.

Hydrothermally reacted mixtures of lime-bentonite

Freshly prepared mixtures

Calcitic lime plus bentonite The x-ray diffraction curve for this mixture (C/S = 0.69), after hydrothermal treatment for 12 hr. at 170°C, is shown as curve I in Figure 8. As indicated, the curve is for a specimen taken directly from the hydrothermal preparation and x-rayed under conditions approaching 100% r.h. D-spacings for the bentonite in curve I appear at 15.2 w b, 4.46 w, 2.56 w b and 1.502 \AA w b. No $\text{Ca}(\text{OH})_2$ peaks appear. The main quartz peaks appear at 3.34 \AA mw b. CaCO_3 peaks appear at 3.04 ms and 2.28 \AA w. Mica



X-ray diffraction of mixture
Fig. 8 Otay bentonite: Ca(OH)₂ : H₂O (1.00 : 0.45 : 1.62)

appears at 10 \AA° tr. No identifiable feldspar peaks appear.

Probable reaction product d-spacings are as follows:

11.7 mw, 5.46 w, 3.07 s, 3.04 ms, 2.98 mw, 2.81 vw b, 2.74 m b, 2.51 w b, 2.44 w b, 2.25 vw, 2.00 mw, 1.84 m, 1.82 w, 1.67 w, 1.62 vw and 1.54 vw b.

D-spacings found above correspond to synthetic tobermorite. The basal spacing varies due to the moist condition of the sample or to substitution of aluminum in the tobermorite lattice (14).

Except for the 3.25 \AA° d-spacing, the other four for CSH (I) are present in this mixture. Seven of the nine spacings for CSH (II) are also indicated.

Dolomitic monohydrated lime plus bentonite of variable C/S ratio The x-ray diffraction d-spacings for this dolomitic monohydrated lime plus bentonite mixture with a C/S ratio of 0.22, after hydrothermal treatment for 12 hr. at 170°C are as follows. D-spacings for the bentonite are 18.3 s, 4.48 m, 2.56 m and $1.499 \text{ \AA}^{\circ}$ m (overlaps weak $\text{Mg}(\text{OH})_2$ peak). No $\text{Ca}(\text{OH})_2$ appears. $\text{Mg}(\text{OH})_2$ d-spacings are 4.79 m and 2.36 \AA° m. The main quartz peak appears at 3.34 \AA° s. CaCO_3 peaks appear at 3.04 s and 2.28 \AA° vw. The mica peak at 10 \AA° is very weak. The feldspar peaks appear at 3.27 m and 3.20 \AA° m.

Probable reaction product d-spacings are as follows:

3.04 s, 2.24 vw, 2.42 w, 1.82 m, 1.70 w b, 1.67 w b and
 1.54 Å^o vw.

Although principal spacings for the better crystallized CSH compounds listed are missing in the above list, both spacings for CSH Gel are present. Others suggesting a CSH (II) phase are unexplained in any other way. Peaks at 2.24 and 1.70 Å^o remain unidentified.

An x-ray diffraction pattern for dolomitic monohydrated lime plus bentonite with a C/S ratio of 0.45, after hydrothermal treatment for 12 hr. at 170°C, is shown as curve I in Figure 9. As indicated, the curve is for a specimen taken directly from the hydrothermal preparation and x-rayed under conditions approaching 100% r.h. D-spacings for bentonite in curve I appear at 15.2 w b, 4.48 w, 2.57 w and 1.499 Å^o w. No Ca(OH)₂ peaks appear. The Mg(OH)₂ peaks appear at 4.80 mw and 2.37 Å^o m. The main quartz peak appears at 3.34 Å^o s. CaCO₃ peaks appear at 3.04 ms, 2.28 w and 2.10 Å^o w. The mica peak does not appear. A feldspar peak is located at 3.25 Å^o tr.

Probable reaction product d-spacings are as follows:

11.47 m, 5.43 w, 3.53 w, 3.07 s, 3.04 m, 2.97 m s, 2.82 mw b,
 2.71 w, 2.51 w, 2.45 vw, 2.00 mw, 1.84 m, 1.81 w, 1.65 mw,

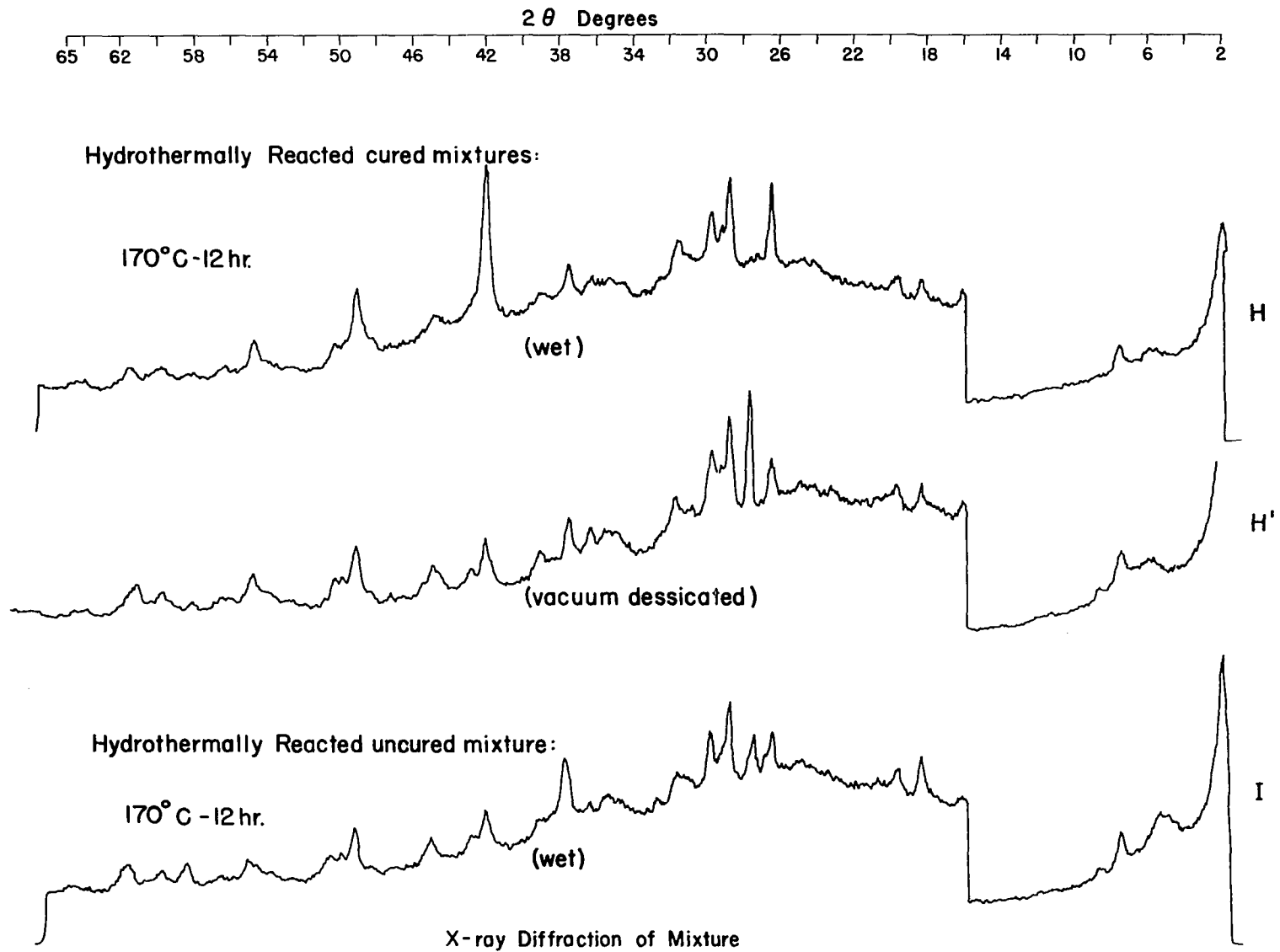


Fig. 9 Otay bentonite : $\text{Ca}(\text{OH})_2 + \text{MgO} : \text{H}_2\text{O}$ (1 : 0.45 : 1.62)

1.62 vw, 1.54 Å^o w.

D-spacings match those for synthetic tobermorite except for minor variations. The basal spacing differs because of moisture condition and/or substitutions in the lattice (14). The d-spacings for CSH (I) are also noted except for the weak 3.25 Å^o spacing attributed above to feldspar. The longest d-spacings as well as the 2.85 Å^o spacing for CSH (II) are missing.

X-ray diffraction d-spacings for this dolomitic monohydrated lime plus bentonite mixture with a C/S ratio of 1.00, after hydrothermal treatment for 12 hr. at 170°C, are as follows. D-spacings for the bentonite are 15.7 wb, 4.48 w, 2.56 w and 1.499 Å^o w (overlaps weak Mg(OH)₂ peak). The main Ca(OH)₂ peak appears at 2.62 w. The main Mg(OH)₂ d-spacings are 4.79 m and 2.36 Å^o s. The main quartz peak is at 3.34 Å^o w. CaCO₃ peaks appear at 3.04 s, 2.28 Å^o vw. The mica peak is at 10 Å^o tr. Feldspar peaks are at 3.29 w and 3.18 Å^o m.

Probable reaction product d-spacings are as follows:

3.04 s b, 2.76 w, 2.24 m, 1.99 w, 1.829 w, 1.67 vw and 1.54 Å^o w.

If the above spacing of 3.29 Å^o attributed to feldspar is attributed to CSH (I), all spacings are present for this phase. Five spacings may be attributed to CSH (II), two of which would

otherwise be unaccounted for.

X-ray diffraction d-spacings for this dolomitic monohydrated lime plus bentonite mixture with a C/S ratio of 1.3, after hydrothermal treatment for 12 hr. at 170°C, are as follows. The only apparent d-spacing for the bentonite, except for a broad very weak hump near 14 Å, appears at 1.499 Å which may be due to Mg(OH)₂ instead. The main Ca(OH)₂ d-spacing appears at 2.62 Å w. The main Mg(OH)₂ spacings appear at 4.79 ms and 2.36 Å s. There is only a trace of quartz evident at 3.34 Å. CaCO₃ peaks appear at 3.04 s b and 2.28 Å w. The mica peak appears as a trace at 10 Å. A feldspar peak appears at 3.19 Å w.

Probable reaction product d-spacings are as follows:

3.04 s, 2.74 mw, 2.72 mw, 2.23 w, 1.99 mw, 1.83 w, 1.70 w, 1.64 w and 1.54 Å w.

X-ray diffraction d-spacings for this dolomitic monohydrated lime plus bentonite mixture with a C/S ratio of 2.00, after hydrothermal treatment for 12 hr. at 170°C, match those for the mixture with a C/S of 1.33 except for considerably more Ca(OH)₂ apparently remaining.

None of the calcium silicate hydrates in the literature match the spacings observed in these two almost identical

patterns. The best fit occurs for CSH (I) except that the weak $3.25 \overset{\circ}{\text{Å}}$ is missing. Only five d-spacings correspond to CSH (II). Unidentified d-spacings are 2.72, 2.23, 1.99 and $1.54 \overset{\circ}{\text{Å}}$.

Dolomitic dihydrated lime plus bentonite The
x-ray diffraction pattern for this mixture (C/S = 0.39), after hydrothermal treatment for 12 hr. at 170°C , is shown as curve I in Figure 10. As indicated the curve is for a specimen taken directly from the hydrothermal preparation and x-rayed under conditions approaching 100% r.h. D-spacings for bentonite in curve I appear at 16.9 s, 4.48 m, 2.55 mw and $1.495 \overset{\circ}{\text{Å}}$ m (overlaps $\text{Mg}(\text{OH})_2$ peak). No $\text{Ca}(\text{OH})_2$ peaks appear. The main $\text{Mg}(\text{OH})_2$ peaks appear at 4.77 ms and $2.36 \overset{\circ}{\text{Å}}$ vs. The main quartz peak appears at 3.34 mw b. CaCO_3 peaks appear at 3.04 ms and $2.28 \overset{\circ}{\text{Å}}$ w. The mica peak appears at $10.04 \overset{\circ}{\text{Å}}$ w. Feldspar peaks are located at 3.18 m, and $3.22 \overset{\circ}{\text{Å}}$ w.

Probable reaction product d-spacings are as follows:
11.18 mw, 5.46 w, 3.08 s, 3.04 s, 2.98 m, 2.83 w, 2.79 w b,
2.46 mw, 2.23 tr, 1.99 mw, 1.83 w, 1.81 w, 1.67 w b, 1.62 tr
and $1.54 \overset{\circ}{\text{Å}}$ w.

Only minor d-spacings are absent in the pattern for this

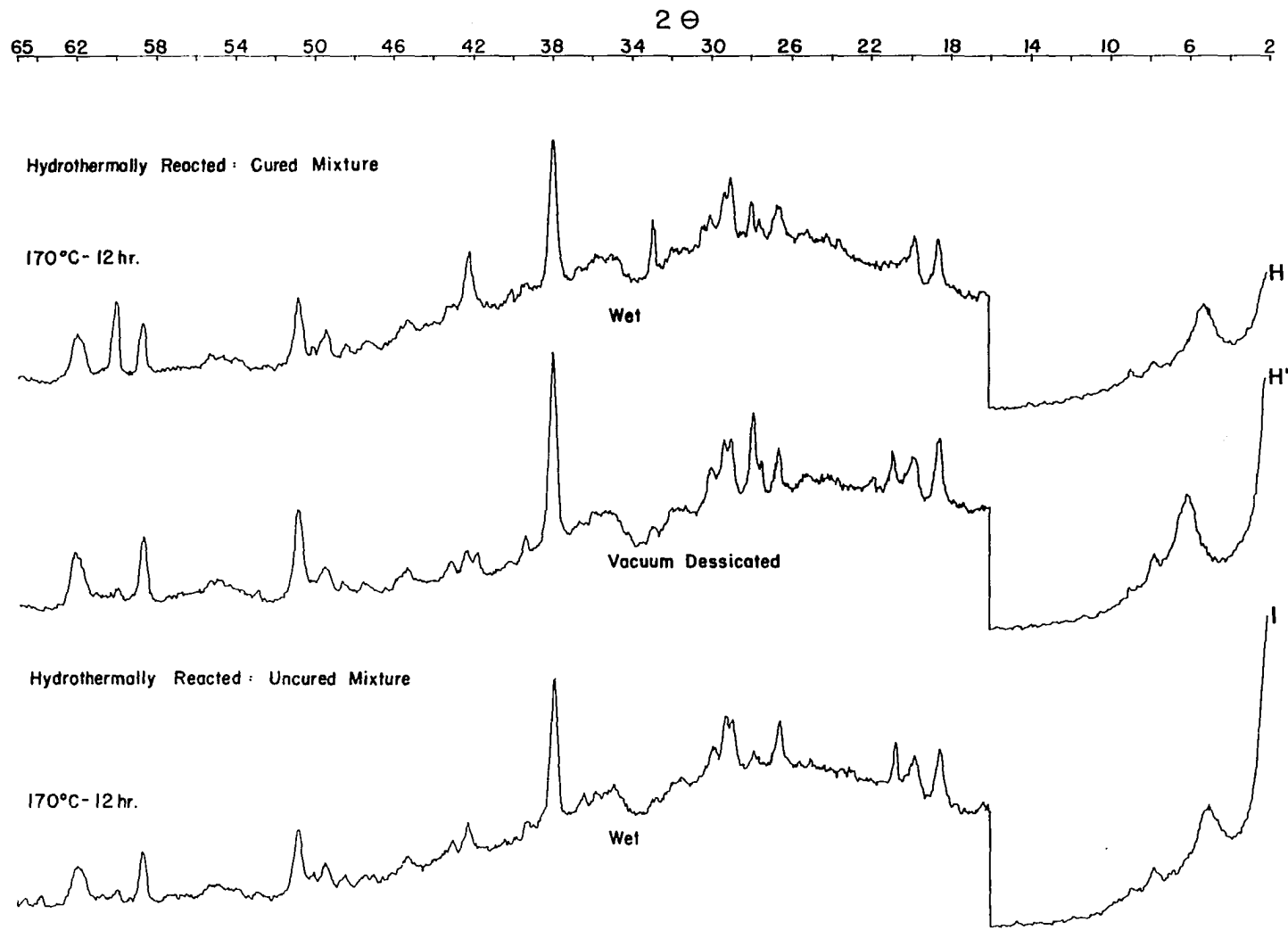


Fig. 10

Xray Diffraction of Mixture
 Otay bentonite : $\text{Ca}(\text{OH})_2 + \text{Mg}(\text{OH})_2 + \text{H}_2\text{O}$
 1 : 0.45 : 1.62

mixture when compared with synthetic tobermorite. All six of the spacings are present for well crystallized CSH (I).

Although most of the d-spacings for CSH (II) are present, the two longest ones are absent.

Cured mixtures

Calcitic lime plus bentonite The x-ray diffraction curves for this mixture with a C/S of 0.69 are given below according to the hydrothermal treatments.

The x-ray diffraction curve for the calcitic lime plus bentonite mixture, reacted for five days at 40°C, is shown as curve C in Figure 5. As indicated, the curve is for a specimen taken from the treatment and vacuum desiccated for 24 hr. before being x-rayed. D-spacings for the bentonite in curve C are 14.7 m, 4.46 mw, 2.53 w and 1.499 Å w b. Ca(OH)₂ peaks appear at 4.93 mw, 2.61 mw, 1.92 w b, 1.79 w b and 1.69 Å w b. The main quartz peaks appear at 3.34 vs and 4.26 Å mw. A CaCO₃ peak appears at 3.04 ms but only a trace at 2.09 Å. The mica peak appears at 10 Å vw. Feldspar peaks appear at 3.20 w.

Probable reaction product d-spacings are as follows:
7.87 vs, 7.6 m, 3.92 vs b, 3.04 s b, 2.98 m, 2.91 w, 2.79 tr,
2.72 m, 2.61 w, 2.53 w, 2.45 w, 2.21 vw, 2.16 w, 1.95 w,

1.81 w b, 1.67 m b, 1.57 tr and 1.54 Å tr.

D-spacings in this pattern correspond within 0.05 Å to very strong and strong spacings obtained for C_4AH_{13} . Strong d-spacings of the product isolated by Hilt and Davidson (28) are also present. The presence of these compounds would account for all the spacings observed except for 2.61 Å w, which may be partially due to $Ca(OH)_2$, with 2.98 Å unexplained. CSH (I) matches the d-spacings as well, so this phase may also be present.

The x-ray diffraction curve for calcitic lime plus bentonite mixture, reacted for four days at 80°C, is shown as curve D in Figure 5. As indicated, the curve is for a specimen taken from the treatment and vacuum desiccated for 24 hr. before being x-rayed. D-spacings for bentonite in curve D appear at 14.2 mw b, 4.48 mw, 2.59 w b and 1.499 Å w b. The main $Ca(OH)_2$ peaks appear displaced to 4.89 vw b and 2.59 Å w b. The main quartz peak appears at 3.34 Å s. $CaCO_3$ peaks appear at 3.04 s and 2.29 Å vw. The mica peak is absent. Feldspar peaks appear at 3.24 m and 3.18 Å vw.

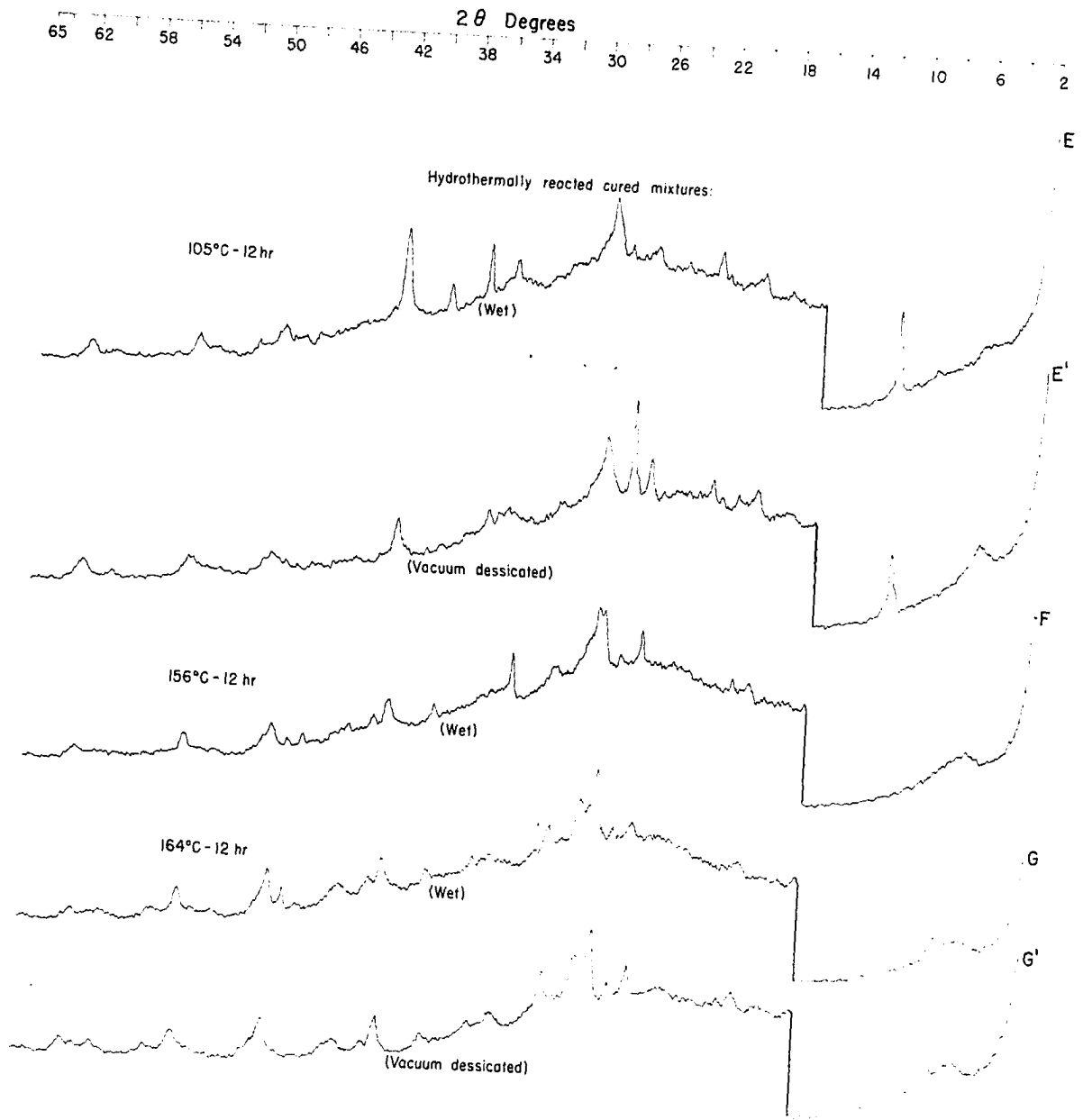
Probable reaction product d-spacings are as follows:
7.77 vs, 3.91 vvs, 3.04 s, 2.97 mw b, 2.79 tr, 2.59 w b,
2.51 mw b, 2.45 vw b, 2.31 vw b, 1.82 w b, 1.80 vw, 1.67 w b

and $1.54 \overset{\circ}{\text{Å}}$ tr.

D-spacings of 7.77 and $3.91 \overset{\circ}{\text{Å}}$ correspond closely to two strong spacings of the product isolated by Hilt and Davidson (28). Other strong spacings are missing so some modified form of this or of the C_4AH_{13} product may be present. Other spacings indicate the presence of CSH (I) but CSH (II) is not indicated. Except for the two longest d-spacings of synthetic tobermorite, all other major spacings for this compound are also present in this pattern.

The x-ray diffraction curve for calcitic lime plus bentonite mixture, after hydrothermal treatment for 12 hr. at 105°C , is shown as curve E in Figure 11. D-spacings for bentonite in curve E appear at 15.7 vw b, 4.48 w b, 2.5 w b and $1.499 \overset{\circ}{\text{Å}}$ w b. The main $\text{Ca}(\text{OH})_2$ peaks appear displaced to positions at 2.6 vw b and $4.89 \overset{\circ}{\text{Å}}$ vw b. The main quartz peaks appear at 3.34 w b and $4.26 \overset{\circ}{\text{Å}}$ tr. CaCO_3 peaks appear at 3.04 ms b and $2.28 \overset{\circ}{\text{Å}}$ mw. The mica peak is $10.0 \overset{\circ}{\text{Å}}$ vw. A feldspar peak appears at $3.21 \overset{\circ}{\text{Å}}$ s.

Probable reaction product d-spacings are as follows:
 7.89 s, 3.93 mw, 3.04 ms b, 2.98 mw b, 2.96 w, 2.90 vw b,
 2.81 vw b, 2.72 vw b, 2.53 mw, 2.42 ms, 2.02 vw b, 1.83 w b,
 1.67 w b, 1.60 vw b, 1.57 vw and $1.54 \overset{\circ}{\text{Å}}$ w.



X-ray Diffraction of Mixture

Fig. 11 Otay bentonite : $\text{Ca}(\text{OH})_2$: H_2O (1.00 : 0.45 : 1.62)

Several d-spacings correspond closely to the C_4AH_{13} with apparent change and weakening of some reflections. The longest d-spacings for well crystallized tobermorite are absent. Only the 3.25 \AA spacing for CSH (I) is absent. Four d-spacings otherwise unaccounted for match CSH (II) three spacings which overlap those of CSH (I).

The x-ray diffraction curve for calcitic lime plus bentonite mixture, after hydrothermal treatment for 12 hr. at 156°C , is shown as curve F in Figure 11. D-spacings for bentonite in curve F appear at 14.7 m b, 4.48 w, 2.54 w b and 1.502 \AA w b. The Ca(OH)_2 peaks are missing. The main quartz peaks are at 4.26 w and 3.34 \AA m w. CaCO_3 peaks appear at 3.04 s b and 2.28 \AA w. The mica peak is absent. A feldspar peak appears at 3.19 w.

Probable reaction product d-spacings are as follows:
 12.6 mw b, 5.46 tr, 3.07 s, 3.04 s, 2.98 m b, 2.79 mw b,
 2.58 m, 2.02 vw b, 1.84 mw b, 1.82 w, 1.72 tr and 1.67 \AA w.

Column 1 of Table 4 lists a 12.6 \AA CSH (I) studied by Grudemo (23). A similar but different pattern having 12.6 \AA as longest spacing was also observed by Taylor (56). Seven d-spacings in the first study mentioned also appear here. Well crystallized tobermorite has nine of the d-spacings

noted, leaving only the 2.58 \AA spacing unaccounted for.

The x-ray diffraction curves for two calcitic lime plus bentonite mixtures, after hydrothermal treatment for 12 hr. at 164° and 170°C , are shown as curves G and H in Figures 11 and 8, respectively. Since the curves are almost identical, the data is combined. D-spacings for bentonite appear at 15.0 w b, 4.46 w b, 2.55 w b and 1.50 \AA w b. The Ca(OH)_2 peaks are absent. The main quartz peak appears at 3.34 \AA w. CaCO_3 peaks appear at 3.03 m and 2.28 \AA w. The mica peak appears as a trace at 10 \AA . A feldspar peak appears at 3.19 w on curve G only and is absent on curve H.

Probable reaction product d-spacings are as follows:

11.7 mw b, 5.50 w b, 3.08 s, 3.03 m, 2.98 ms, 2.88 tr, 2.81 mw b, 2.74 w b (curve G only), 2.44 w b, 2.36 w b (curve H only), 2.01 mw b, 1.84 mw, 1.82 w b, 1.74 tr, 1.67 m b, and 1.54 \AA w b.

D-spacings found for each compound correspond to well crystallized synthetic tobermorite, with deviation in longest spacing (11.7 \AA) accounted for by aluminum substitutions noted earlier (14, 34). CSH (I) is indicated except for the absence of the 3.25 \AA d-spacing. The d-spacing at 2.88 \AA is accounted for by CSH (II), represented in the present mixture by seven spacings, excluding the two longest spacings which

are absent for this compound.

Dolomitic monohydrate lime plus bentonite The
x-ray diffraction curves for this mixture, with a C/S of
0.45, are given below according to the hydrothermal treatments.

The x-ray diffraction curve for the dolomitic monohydrated lime plus bentonite mixture, reacted for five days at 40°C, is shown as curve C in Figure 6. As indicated, the curve is for a specimen taken from the treatment and vacuum desiccated for 24 hr. before being x-rayed. D-spacings for the bentonite in curve C are 14.7 ms, 4.48 m, 2.56 m b and 1.499 Å mw. Ca(OH)₂ peaks appear at 4.89 tr and 2.62 Å vw. Mg(OH)₂ peaks appear at 4.79 mw and 2.38 Å m. The main quartz peak appears at 4.26 mw and 3.36 Å vs. CaCO₃ peak appear at 3.04 s and 2.48 Å w. The mica peak appears 10.0 Å w. Feldspar peaks appear at 3.19 Å s.

Probable reaction product d-spacings are as follows:
7.86 vs, 5.4 tr, 3.93 m, 3.04 s b, 2.98 w, 2.89 vw, 2.8 tr,
2.32 vw, 1.99 m, 1.97 w, 1.83 vw, 1.74 vw, 1.67 w, 1.63 vw,
1.58 w and 1.54 Å w b.

The longest d-spacing corresponds within 0.06 Å to the very strong spacing of C₄AH₁₃. The other main spacings match within 0.02 Å. Some of the lower d-spacings of this product

are weaker, with the 2.46 Å spacing absent.

The d-spacings for CSH Gel are both present, being the strongest evidence for a calcium silicate hydrate with only a trace indicated for the usually medium spacing at 2.8 Å suggests the presence of CSH (I) but in small amount. Four of the other spacings are also present in this pattern.

The x-ray diffraction curve for dolomitic monohydrated lime plus bentonite mixture, reacted for four days at 80°C, is shown as curve D in Figure 6. As indicated, the curve is for a specimen taken from the treatment and vacuum desiccated for 24 hr. before being x-rayed. D-spacings for bentonite appear in curve D at 14.7 mw, 4.48 mw, 2.56 w b and 1.497 Å w b. The main $\text{Ca}(\text{OH})_2$ peaks are at 4.89 w and 2.63 Å w b. The main $\text{Mg}(\text{OH})_2$ peaks appear at 4.81 m b and 2.36 Å m s. The main quartz peak appears 4.26 t r and 3.34 Å m. CaCO_3 peaks appear at 3.04 s and 2.3 Å tr. The mica peak appears 10 Å tr. A feldspar peak appears at 3.21 Å w b.

Probable reaction product d-spacings are as follows:

7.80 vs, 3.93 s, 3.04 s, 2.90 tr, 2.79 vw b, 2.51 vw,
1.99 tr, 1.82 mw b, 1.7 tr, 1.66 w b and 1.54 Å t r.

The longest d-spacing observed at 7.80 Å is apparently a diminished spacing of C_4AH_{13} . The second strongest spacing

is the same and the 2.9 \AA d-spacing appears as a trace. The other main spacing at 1.66 \AA also remains. CSH (I) is indicated by all spacings represented, assuming the 3.21 \AA spacing attributed above to feldspar belongs to this product.

The x-ray diffraction curve for dolomitic monohydrated lime plus bentonite mixture, after hydrothermal treatment for 12 hr. at 105°C , is shown as curve E in Figure 12. D-spacings for bentonite appear at 15.7 w b , 4.48 m b , 2.56 w b and 1.501 \AA mw . The main $\text{Ca}(\text{OH})_2$ peak appears at 2.62 \AA vw . The main $\text{Mg}(\text{OH})_2$ peaks appear at 4.79 m and 2.37 \AA mw . CaCO_3 peaks appear at 3.04 vs and 2.29 \AA w . The mica peak appears at 10.0 \AA vw . A feldspar peak appears at 3.20 \AA mw .

Probable reaction product d-spacings are as follows:

7.85 vvs , 7.6 tr , 3.93 s , 3.04 vs , 2.96 w b , 2.88 w , 2.79 w b , 2.00 tr , 1.83 mw b , 1.81 mw , 1.75 tr , 1.71 tr , 1.67 w b , 1.62 tr and 1.54 \AA vw .

The three strongest reflections are indicated for C_4AH_{13} . Others appear weaker or not at all. Four spacings are evident for Hilt and Davidson's (28) product while others are absent or considerably weakened. There are strong indications for CSH (I) spacings evident whenever a higher crystalline form is present. Unexplained is a 2.96 \AA spacing which is normally

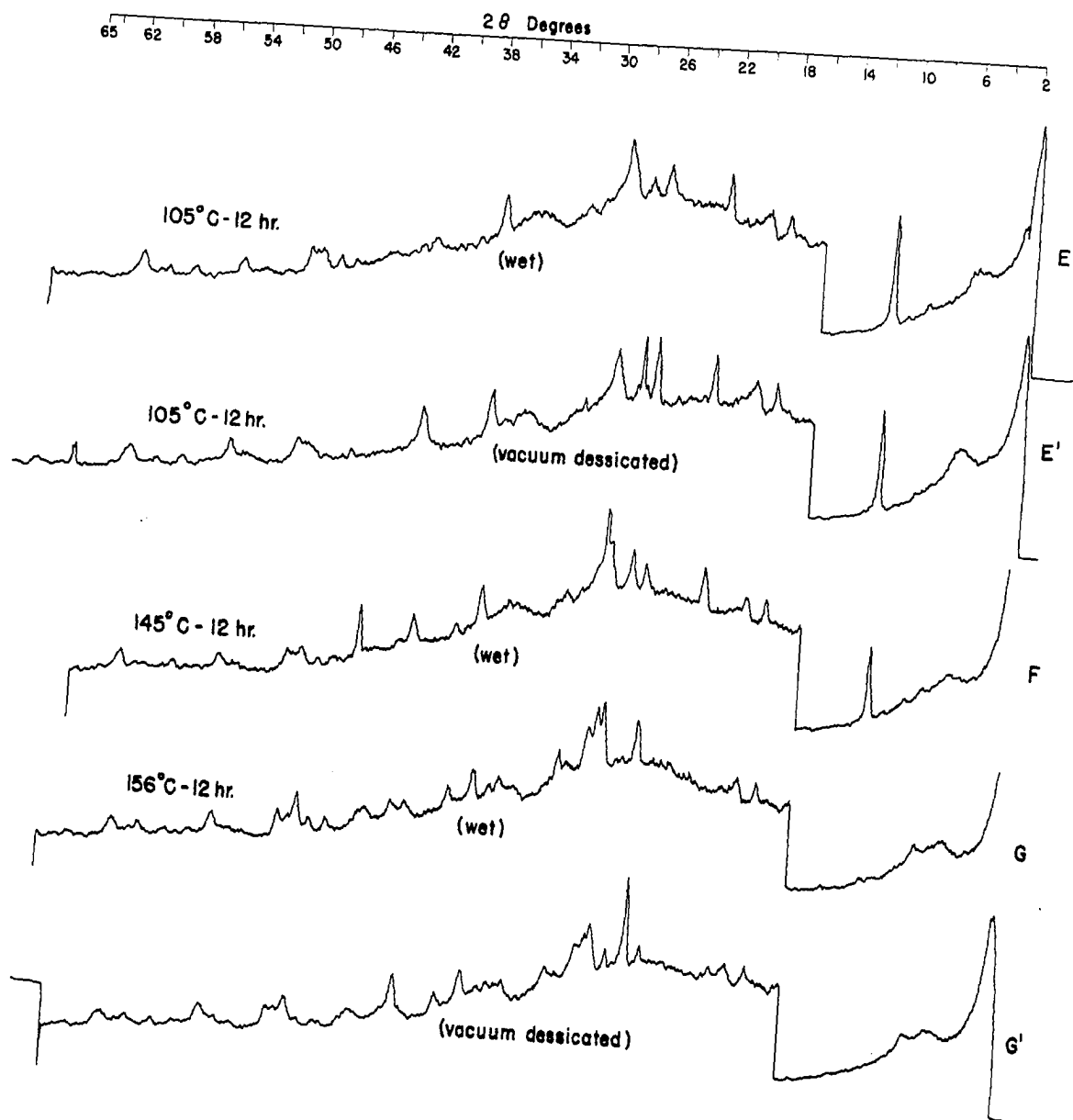


Fig. 12 Otay bentonite: $\text{Ca}(\text{OH})_2 \cdot \text{MgO} \cdot \text{H}_2\text{O}$ (1: 0.45: 1.62) X-ray Diffraction of Mixture

associated with well crystallized CSH.

The x-ray diffraction curve for dolomitic monohydrated lime plus bentonite mixture, after hydrothermal treatment for 12 hr. at 145°C, is shown as curve F in Figure 12. D-spacings for bentonite appear at 14.7 w b, 4.50 mw, 2.56 w b and 1.502 Å w. No Ca(OH)₂ peaks appear. The main Mg(OH)₂ peaks appear at 4.80 m and 2.39 Å s. The main quartz peak appears at 3.34 Å ms. CaCO₃ peaks appear at 3.04 vs and 2.28 Å w. The mica peak is at 10.0 Å vw. A feldspar peak appears at 3.24 Å s.

Probable reaction product d-spacings are as follows:

7.89 vs, 3.93 s, 3.07 s b, 3.04 vs, 2.98 m b, 2.80 w b, 2.33 tr, 1.98 s, 1.83 mw, 1.81 w, 1.70 tr, 1.67 w b, 1.62 tr and 1.54 Å tr.

Only the two longest d-spacings are evident for C₄AH₁₃. CSH (I) is indicated by all d-spacings, reassigning the 3.24 Å spacing to this product. Except for the longest spacings at 9-14 Å, all other spacings match within 0.01 Å. Unidentified is the 1.98 Å d-spacing.

The x-ray diffraction curve for dolomitic monohydrated lime plus bentonite mixture, after hydrothermal treatment for 12 hr. at 156°C, is shown as curve G in Figure 12. D-spacings

for bentonite appear at 15.2 m w b, 4.5 m, 2.57 w b and 1.503 Å w. The $\text{Ca}(\text{OH})_2$ peak does not appear. The main $\text{Mg}(\text{OH})_2$ peak appears at 4.80 m and 2.39 Å ms. The main quartz peak appears at 4.26 tr and 3.35 Å s. CaCO_3 peaks appear at 3.05 vs and 2.29 Å mw b. The mica peak is at 10 Å tr. A feldspar peak appears at 3.25 Å tr.

Probable reaction product d-spacings are as follows:

11.62 w b, 7.8 tr, 5.50 vw b, 3.91 mw, 3.08 ms b, 3.05 vs, 2.98 m, 2.87 t r, 2.81 mw b, 2.46 w, 2.02 w, 2.00 w, 1.84 m, 1.82 w, 1.67 mw, 1.62 vw and 1.54 Å w.

Only trace indications occur for the C_4AH_{13} . Strong d-spacings for synthetic tobermorite indicate its presence in this mixture. Any other phase of CSH is also indicated by these spacings, in combination with the 3.05 Å spacing.

The x-ray diffraction curve for dolomitic monohydrated plus bentonite mixture, after hydrothermal treatment for 12 hr. at 170°C is shown as curve H in Figure 12. D-spacings for bentonite appear at 15.7 w b, 4.48 w b, 2.58 w b and 1.499 Å w b. No $\text{Ca}(\text{OH})_2$ appears. $\text{Mg}(\text{OH})_2$ peaks appear at 4.80 mw and 2.37 Å m b. The mica peak does not appear. No feldspar peaks appear. The main quartz peak is at 3.34 Å vs. CaCO_3 peaks appear at 3.04 m and 2.28 Å w b.

The probable reaction product d-spacings are as follows:
 11.62 m, 5.46 w, 3.08 vs, 3.04 m, 2.98 s, 2.82 ms, 2.73 vw b,
 2.52 w b, 2.46 w b, 2.26 tr, 2.00 w b, 1.84 s b, 1.82 w,
 1.67 mw b and 1.54 $\overset{\circ}{\text{A}}$ w b.

All d-spacings for well crystallized tobermorite and CSH (I) are evident in this mixture. CSH (II) d-spacings appear with maximum deviations of 0.03 $\overset{\circ}{\text{A}}$ with the 10 and 2.85 $\overset{\circ}{\text{A}}$ spacing absent. The strength and breadth of the 1.84 $\overset{\circ}{\text{A}}$ peak suggests overlapping of the several phases which have reflection in this vicinity.

Dolomitic dihydrate lime plus bentonite The x-ray diffraction curves for this mixture, with a C/S of 0.39, are given below according to the hydrothermal treatments.

The x-ray diffraction curve for the dolomitic dihydrate lime plus bentonite mixture, reacted for five days at 40°C, is shown as curve C in Figure 7. As indicated, the curve is for a specimen taken from the treatment and vacuum desiccated for 24 hr. before being x-rayed. D-spacings for the bentonite in curve C are 14.7 ms, 4.45 m, 2.53 mw and 1.495 $\overset{\circ}{\text{A}}$ ms. Faint suggestions for Ca(OH)₂ appear at 2.6 and 1.7 $\overset{\circ}{\text{A}}$. The main Mg(OH)₂ spacings appear at 4.77 s and 2.37 $\overset{\circ}{\text{A}}$ vs. The main quartz peak appears at 3.34 $\overset{\circ}{\text{A}}$ ms. CaCO₃ peaks appear at

3.04 s and 2.29 Å w. The mica peak appears very weak at 10 Å. Feldspar peaks are located at 3.25 m and 3.19 Å m.

Probable reaction product d-spacings are as follows:
7.7 tr, 5.53 w, 3.6 vw b, 3.04 s, 2.74 w b, 2.24 tr, 1.99 w,
1.70 w, 1.67 w b and 1.54 Å tr.

Suggestions of several compounds are present in the pattern for this mixture. All d-spacings ± 0.04 Å are present for CSH (I), assuming the 3.25 Å peak is at least partly due to this product. Deviations up to .04 Å occur but additional weak reflections at 1.99 and 5.53 Å suggest a higher crystalline form. The product of Hilt and Davidson (28) is suggested by a trace at 7.7 Å and several weaker reflections.

The x-ray diffraction curve for dolomitic dihydrated lime plus bentonite mixture, reacted for four days at 80°C, is shown as curve D in Figure 7. As indicated, the curve is for a specimen taken from the treatment and vacuum desiccated for 24 hr. before being x-rayed. D-spacings for bentonite appear at 14.7 s b, 4.48 ms b, 2.55 mw b, 1.495 s b (overlaps Mg(OH)₂). The main Ca(OH)₂ peak appears at 2.62 Å tr. The main Mg(OH)₂ peaks at 4.76 vs and 2.37 Å vvs. The main quartz peaks appear 4.26 w b and 3.36 Å vvs. CaCO₃ peaks appear at 3.04 vs b and 2.27 Å w b. The mica peak appears 10.0 tr.

Feldspar peaks appear at 3.24 w and 3.19 Å s b.

Probable reaction product d-spacings are as follows:

11.6 tr, 7.7 w, 7.1 tr, 6.5 tr, 5.4 tr, 3.9 vw, 3.04 vs,
2.76 vw b, 2.72 vw b, 2.05 tr, 1.99 vw b, 1.81 vw b, 1.67 w b
and 1.54 Å vw.

All d-spacings for CSH (I) appear in the pattern for this mixture reassigning the 3.24 Å spacing to this product. Strong d-spacings CSH (II) are present except for the longest spacing at 9.8 Å. A lime rich phase, α C₂SH, reported by Kalousek (35) is an intermediate phase in 175°C hydrothermal reactions would account for all remaining d-spacings except the 7.7 Å w spacing, suggestive of Hilt and Davidson's (28) product.

The x-ray diffraction curve for dolomitic dihydrated lime plus bentonite mixture, after hydrothermal treatment for 12 hr. at 105°C, is shown as curve E in Figure 13. D-spacings for bentonite appear at 16.6 m b, 4.48 m, 2.54 m b and 1.495 Å m b. The main Ca(OH)₂ peak is 2.6 Å tr. The main Mg(OH)₂ peaks appear at 4.76 s and 2.37 Å vvs. The main quartz peaks appear at 4.26 tr and 3.34 Å s. CaCO₃ peaks appear at 3.03 s b and 2.28 Å vw. The mica peak is 10.0 Å w. Feldspar peaks appear at 3.24 w and 3.18 Å w.

Probable reaction product d-spacings are as follows:

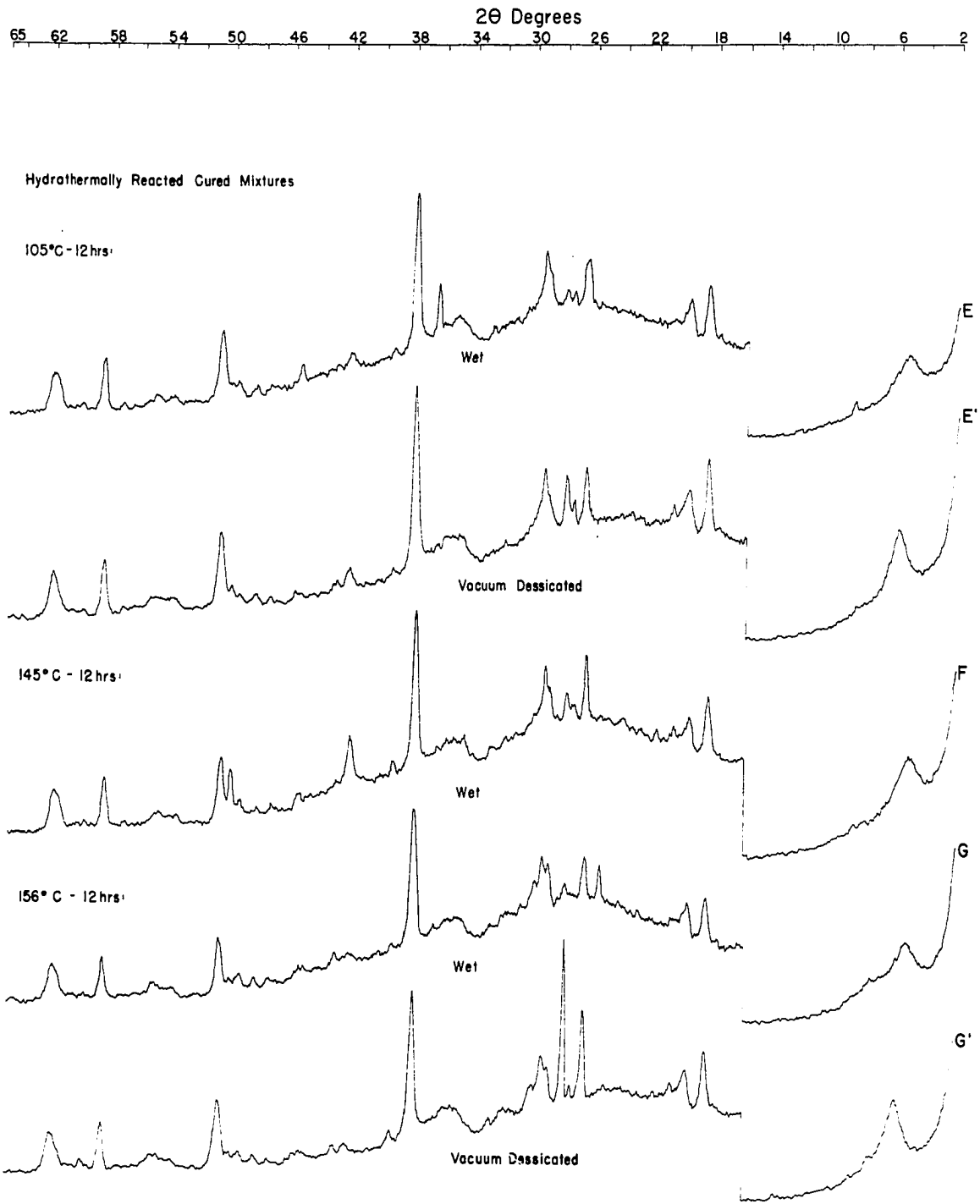


Fig. 13

Xray Diffraction of Mixture
 0.10y bentonite : Ca(OH)₂ · Mg(OH)₂ · H₂O
 (1.00 : 0.45 : 1.62)

5.5 w, 3.03 vs, 2.92 vw b, 2.85 tr, 2.8 vw b, 2.57 w, 2.46 s, 2.24 tr, 1.99 mw, 1.83 w b, 1.82 w, 1.69 w b, 1.67 w b, 1.60 v w and 1.54 Å^o tr.

All d-spacings appear in this pattern for CSH (I) with very small deviations. Strong d-spacings for CSH (II) are also represented except for the longest at 9.8 Å^o. A lime rich phase known as α dicalcium silicate was found by Kalousek (35) to occur briefly in hydrothermal mixtures at higher temperature. If this phase is present, all other lines are accounted for.

The x-ray diffraction curve for dolomitic dihydrated lime plus bentonite mixture, after hydrothermal treatment for 12 hr. at 145°C, is shown as curve F in Figure 13. D-spacings for bentonite appear at 16.9 ms b, 4.48 mw b, 2.5 w b and 1.497 Å^o s b. The main Ca(OH)₂ peak appears at 2.6 Å^o vw. The main Mg(OH)₂ peaks appear at 4.76 s and 2.37 Å^o vvs.

The main quartz peaks appear at 4.26 vw and 3.34 Å^o s. CaCO₃ peaks appear at 3.04 s b and 2.28 Å^o w. The mica peak appears at 10 Å^o tr. Feldspar peaks appear at 3.25 w and 3.20 Å^o mw.

Probable reaction product d-spacings are as follows:

11. tr, 7.2 tr, 5.5 vw, 3.86 w, 3.07 m, 2.98 w b, 2.86 vw b,

2.80 vw, 2.73 w, 1.98 w, 1.83 w, 1.82 s, 1.70 vw, 1.67 wb and 1.54 Å tr.

All of the strong d-spacings for synthetic tobermorite appear with little deviation. The same analysis applies to Diamond's CSH I, attributing the 3.25 Å reflection as at least partially due to this compound. The strongest d-spacings for CSH (II) appear except for the 9.2 Å spacing. Three additional d-spacings at 3.86 w, 2.73 w and 1.70 vw would be accounted for if overlapping spacings could be partially attributed to a lime rich phase, α C₂SH, found by Kalousek (35) to occur after hydrothermal treatment at 175°C for a short period.

The x-ray diffraction curve for dolomitic dihydrated lime plus bentonite mixture, after hydrothermal treatment for 12 hr. at 156°C, is shown as curve G in Figure 13. D-spacings for bentonite appear at 16.6 mw b, 4.48 m, 2.56 w b, 1.496 mw b. The main Ca(OH)₂ peak appears at 2.6 Å tr. The main Mg(OH)₂ peaks appear at 4.76 s and 2.36 Å vvs. The main quartz peaks appear at 4.26 vw and 3.34 Å s. CaCO₃ peaks appear at 3.03 s and 2.29 Å vw b. The mica peak does not appear. A feldspar peak appears at 3.195 Å w b.

Probable reaction product d-spacings are as follows:
11.47 vw b, 5.4 tr, 3.86 w, 3.07 s, 2.98 ms b, 2.90 vw,

2.84 w b, 2.80 vw b, 2.72 vw b, 2.5 w b, 2.45 vw, 2.24 vw b, 2.05 tr, 2.00 w b, 1.84 w, 1.81 vw, 1.69 w b, 1.66 w b and 1.54 Å^o tr.

The x-ray diffraction curve for dolomitic dihydrated lime plus bentonite mixture, after hydrothermal treatment for 12 hr. at 170°C, is shown as curve H in Figure 10. D-spacings for bentonite appear at 16.9 s b, 4.48 m, 2.55 w b and 1.495 Å^o m b. The main Ca(OH)₂ peak appears at 2.6 Å^o tr. Mg(OH)₂ peaks appear at 4.76 ms and 2.36 Å^o vvs. The mica peak appears at 10.0 Å^o vw. Feldspar peaks appear at 3.22 w and 3.18 Å^o m.

Probable reaction product d-spacings are as follows:

11.47 vw b, 7.5 tr, 6.3 tr, 5.4 vw, 3.9 w s, 3.07 s, 2.97 mw, 2.93 w, 2.84 vw, 2.79 w b, 2.71 s, 2.5 w b, 2.44 tr, 2.24 w, 2.00 w b, 1.84 mw b, 1.81 vw, 1.69 vw b, 1.66 w and 1.54 Å^o vs.

The patterns represented by the above data on specimens, hydrothermally reacted at 156°C and 170°C, are nearly identical; therefore these analyses are combined into one. All strong and some weak spacings for synthetic tobermorite are present in these patterns for this mixture. The same analysis applies to CSH (I) except for the missing 3.25 Å^o peak. For CSH (II) only the longest spacing is not evident here.

Differential Thermal Analysis

Differential thermal analysis results were compared with published patterns, in particular, those on the pure aluminate and silicate hydrate compounds.

As Mackenzie (44) has noted regarding such comparisons between results obtained by DTA, reproducibility of technique is absolutely essential. This involves such aspects as particle size, pretreatment and packing of the specimen and equipment characteristics, with the heating rate having the most marked effect upon the DTA pattern. Peak areas and sharpness are important considerations, but perhaps most significant in the present study is the matter of peak temperature; all are affected by heating rate. No correlation procedure is indicated in this reference.

Diamond (14) performed a DTA analysis of the same material on two different instruments. One was used in the major part of his study of pure compounds and had a heating rate of 58°C per min. initially and then varying linearly to 5.4° per min. at 600° , after which it was constant. The other instrument had a heating rate equal to the one used in the present study which was 10°C per min. The 825°C exotherm used to indicate CSH composition in the DTA pattern read 795° on his instrument.

The principal reference to published patterns used in the present study were by Kalousek (34, 35), who apparently standardized his DTA studies and used a heating rate of 7°C per minute initially which varied to 12.5° per minute at 300°C after which this rate was constantly maintained. Van Bemst (63) in his study of CSH (II) used 13°C per minute. Turriziani (61) used 15° per minute. No correlations were found between these rates and the 10° per minute used in this study. Comparisons between data indicate that peaks occur at slightly higher temperatures for the faster heating rate.

Otay bentonite

Differential thermal analysis of Otay bentonite shows a strong endotherm at 160°C , indicating removal of constitutional water. Two medium endothermic peaks at 650° and 855° indicate expulsion of mineral lattice hydroxyl water. CaCO_3 also has an endotherm in the vicinity of the second endotherm. The 990° exotherm is associated with the appearance of the second endothermic peak for bentonite but its exact origin is unknown (44).

Unreacted mixtures of lime-bentonite

Figures 14, 15 and 16 are headed by DTA patterns marked A. These represent dry mixtures of calcitic, dolomitic

monohydrated and dihydrated lime plus bentonite, respectively.

Room cured mixtures of lime-bentonite

Calcitic lime plus bentonite The DTA of this mixture (C/S = 0.69) is shown as curve B in Figure 14. A very strong constitutional water endotherm appears at 110°C. A very weak broad endotherm appears at about 220° and another very broad endotherm appears between 350° and 430°. A weak endotherm is noted at 705°. The only exotherm appears at 840°, and of medium intensity. Laboratory CO₂ level was normal so there was probably carbonation; however the 705° is lower than anticipated for CaCO₃ but about right for antigorite (44). Shifts in this peak position were noted in previous work by Glenn and Handy (22). The difference between peak temperatures may be explained on the basis of the fine particle size of the carbonate formed from the Ca(OH)₂ (44). The low temperature endothermic effects suggest C₄AH₁₃ from patterns by Turriziani (61) and Kalousek (36). The exotherm at 840° is about right for room temperature CSH (I) by Kalousek (35) having a C/S ratio around 1.2.

Dolomitic monohydrated lime plus bentonite The DTA of this mixture (C/S = 0.45) is shown as curve B in Figure 15. The strong constitutional water endotherm occurs at 130°C with

a small shoulder at 160° . Very weak and broad endotherms appear at 315° and 510° ; the latter suggests $\text{Ca}(\text{OH})_2$. The medium endotherm at 740° is attributed to CaCO_3 . A weak exothermic peak appears at 630°C . A medium to strong exotherm occurs at 850° . CSH (I) with a C/S ratio of about 1.25 is indicated by this peak as found in the work of Kalousek (35). Diamond's (14) patterns for CSH Gel prepared at room temperature have exotherms of weak intensity in this range also.

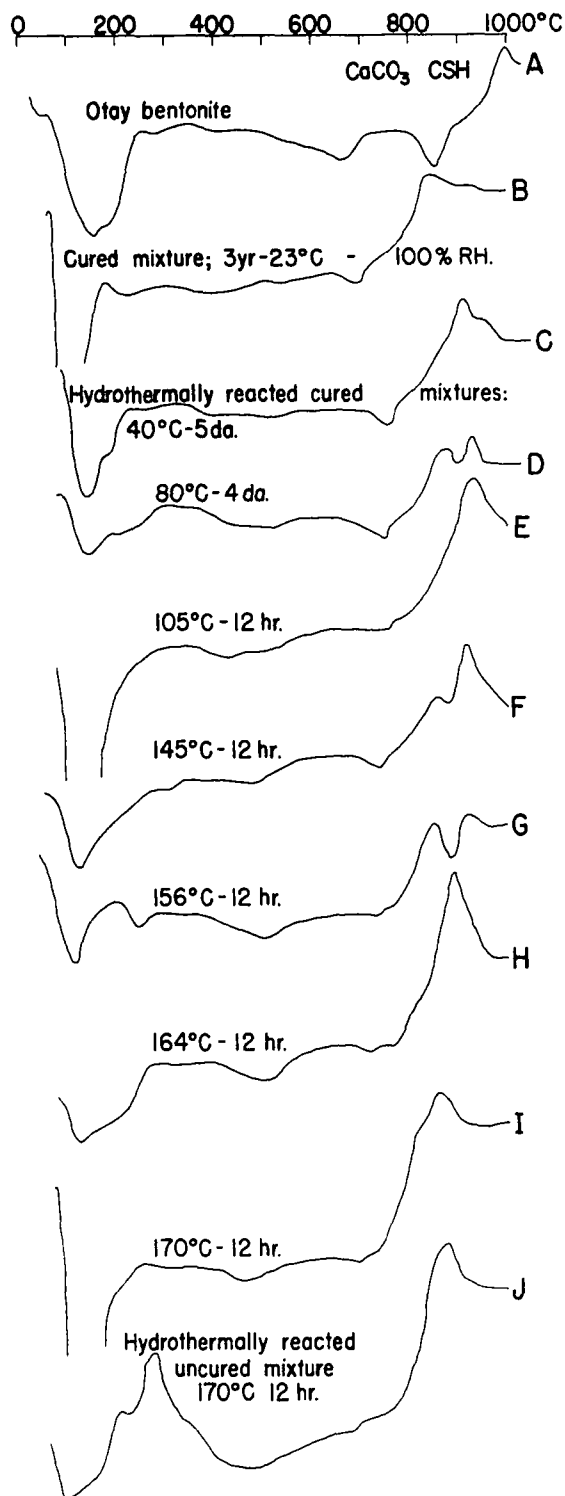
Dolomitic dihydrated lime plus bentonite The DTA of this mixture (C/S = 0.39) is shown as curve B in Figure 16. The strong constitutional water endotherm occurs at 120°C . The strong endotherm at 390° is identified as probably $\text{Mg}(\text{OH})_2$, although Mackenzie (44) reports the usual temperature for expulsion of its lattice water is somewhat higher. Very weak peaks appear at 250° and 600° with a medium weak endotherm at 690° ; the latter is attributed to the presence of carbonate. This curve shows double exothermic effects at 850° and 920° , which are near those reported by Van Bemst (63) for CSH II; however his low temperature exothermic effect is absent. Diamond's (14) CSH Gels gave an exotherm in this range, also.

Hydrothermally reacted mixtures of lime-bentoniteFreshly prepared mixturesCalcitic lime plus bentonite

The DTA of this mixture (C/S = 0.69) after hydrothermal treatment for 12 hours at 170°C is shown as curve J in Figure 14. There is a broad constitutional water endotherm at 100° with broadening near 170°. The second endothermic peak is of medium intensity at 470° and extends between 400° and 550°. Two very weak endotherms at 690° and 770° are probably due to carbonates. A strong exotherm occurs at 280° and a medium-strong exotherm occurs at 870°. None of the patterns described in the literature except CSH (II) by Van Bemst (63) have intense low temperature exothermic effects. Also the exotherm at 870° in the present pattern is intermediate to the double exothermic effects noted at high temperature for this compound. A somewhat weaker exothermic effect in this temperature range was noted by Diamond (14) in his CSH Gel study.

Dolomitic monohydrated lime plus bentonite mixturesof variable C/S ratio

The DTA of the mixture with a C/S ratio of 0.45, after hydrothermal treatment for 12 hours at 170°C, is shown as curve J in Figure 15. The broad constitutional water endotherm has a main strong peak at 100° with a



Note: All samples vacuum desiccated.

Fig. 14. Differential thermal analysis
 Otay bentonite: Ca(OH)₂: H₂O
 (1: 0.45 : 1.62)

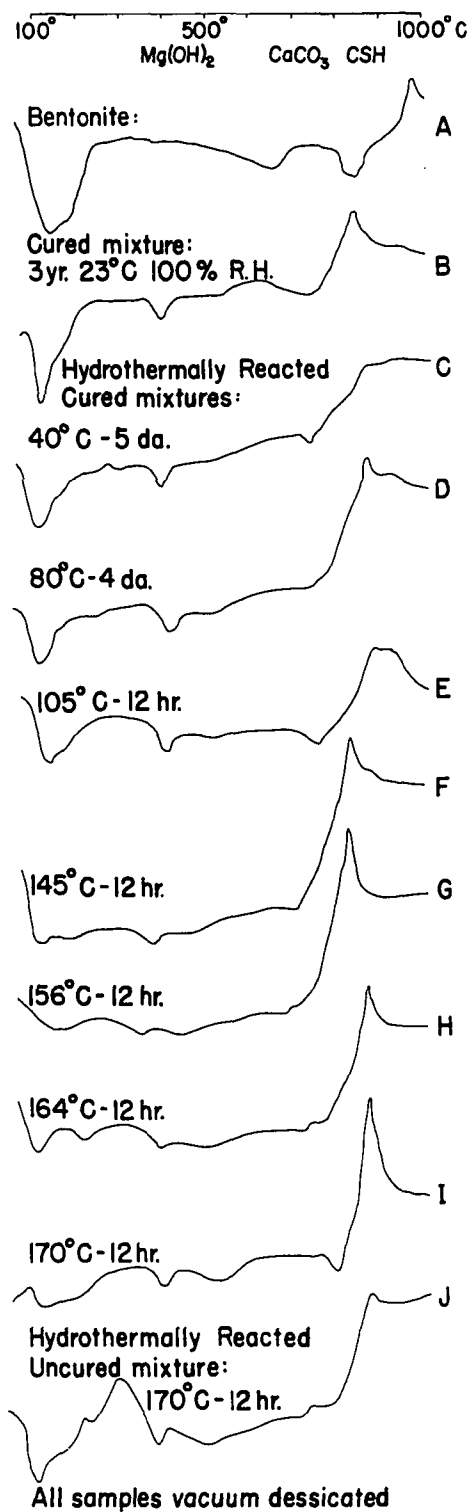


Fig. 15. Differential thermal analysis of mixture
Otay bentonite: Ca(OH)₂ + MgO : H₂O
(1.00 : 0.45 : 1.62)

distinct broad shoulder around 180° . Small exotherms occur near 225° and 400° with a broad endothermic bulge at 500° . A 720° endotherm appears and is probably due to carbonate. A strong exotherm occurs at 300° and a weak exotherm at 880° . The presence of $\text{Mg}(\text{OH})_2$ is probably indicated by the endothermic effect at 500° . Otherwise, this pattern resembles the CSH (II) of Van Bemst (63), with the exotherm at 880° replacing the double effects in his pattern. Diamond's (14) and Kalousek's (34) aluminum substituted (15 to 20%) tobermorite have strong exotherms in this same temperature range.

The DTA of the mixture with a C/S ratio of 1.3, after hydrothermal treatment for 12 hours at 170°C showed a sharp constitutional water endotherm at 110° with a broad shoulder around 150° . A strong endotherm, attributed to $\text{Mg}(\text{OH})_2$, appears at 400° , followed by a very weak endotherm at 470° and a medium endotherm at 760° , the last probably due to CaCO_3 . There is a weak exothermic effect between 870° and 930° and a strong exotherm at 280° . The DTA of the mixture with a C/S ratio of 2.0 has an almost identical pattern to the C/S 1.3 mixture. This pattern suggests the presence of CSH (II), as prepared by Van Bemst (63).

Dolomitic dihydrated lime plus bentonite

The DTA

of this mixture with a C/S ratio of 0.39, after hydrothermal treatment for 12 hours at 170°C is shown as curve J in Figure 16. A strong constitutional water endotherm appears at 110° with a broad shoulder at 180°. Weak endotherms occur at 225°, 500° and 705° with a broad endotherm at 620°. A strong endotherm at 405° is attributed to Mg(OH)₂. There is a strong exotherm at 300°, a weak endotherm at 800° and a medium exotherm at 850°. Features of this pattern resemble that obtained for CSH (II) by Van Bemst (63).

Cured mixturesCalcitic lime plus bentonite (C/S = 0.69)

The DTA

of this mixture after treatment for five days at 40°C is shown as curve C in Figure 14. The strong constitutional water endotherm at 130° is followed by a distinct endothermic shoulder at 180°. Very weak broad endotherms occur at 250° and between 380° and 540°. A medium endotherm occurs at 760° and is attributed to CaCO₃. A medium exothermic effect occurs at 910° followed by a weaker shoulder at 950°. The double effect is unexplained; however, the principal exotherm is near that obtained from products of Kalousek (35) of high C/S ratio.

The DTA of the calcitic lime plus bentonite mixture after

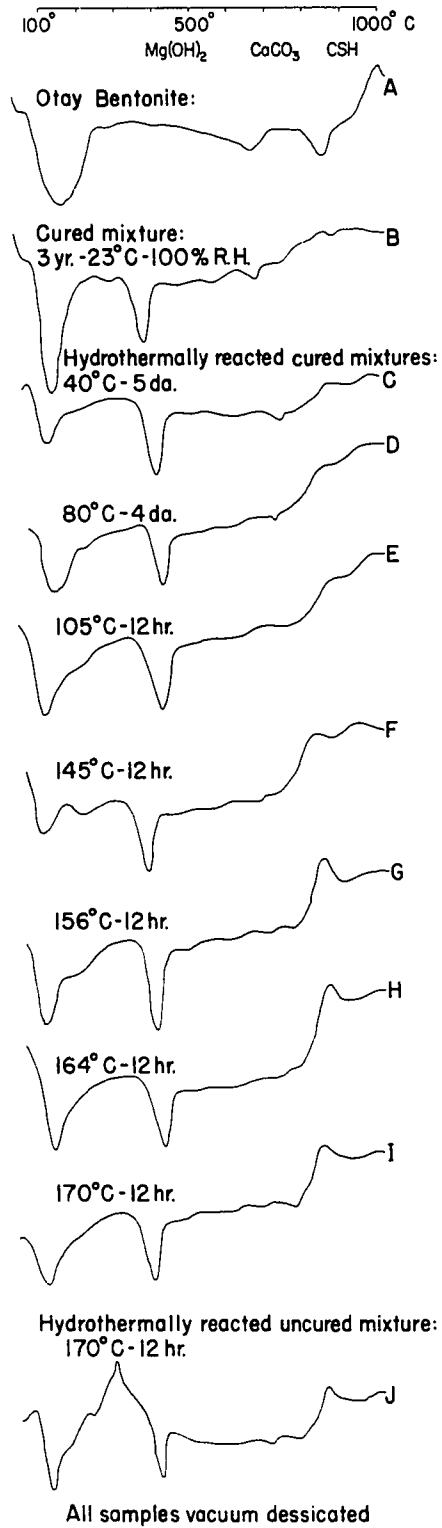


Fig. 16 Differential thermal analysis
Otay bentonite: $\text{Ca}(\text{OH})_2 \cdot \text{Mg}(\text{OH})_2 \cdot \text{H}_2\text{O}$
(1.00 : 0.45 : 1.62)

treatment for four days at 80°C is shown as curve D in Figure 14. The constitutional water endotherm at 130° is of medium intensity and broad. It is followed by a shoulder at 240°. A weak exotherm occurs at 300°. A broad weak endotherm extends between 420° and 530°. This is followed by a weak endotherm at 745° and is attributed to CaCO₃. Two exothermic peaks of weak to medium intensity occur at 870° and 920°. The features of this pattern resemble that for CSH II of Van Bemst (63). However, the possibility exists that two aluminum substituted synthetic tobermorites are represented instead; Kalousek (34) found peaks in this temperature range for 15-20% aluminum substitution.

The DTA of the calcitic lime plus bentonite mixture after hydrothermal treatment for 12 hours at 105° is shown as curve E in Figure 14. The constitutional water endotherm at 130° is very strong. Very weak endothermic effects appear around 420° and 500°. A definite but weak endotherm appears at 760° and is attributed to CaCO₃. This is followed by a strong broad exotherm at 930°. Although low temperature exothermic features are missing, CSH (II) of Van Bemst (63) and high Al₂O₃ substituted tobermorites of Kalousek (34) give exothermic effects around 900°. 1.33 C/S ratio products were noted by Kalousek

(35) also to give similar exothermic effects.

The DTA of the calcitic lime plus bentonite mixture after hydrothermal treatment for 12 hours at 145°C is shown as curve F in Figure 14. A strong constitutional water endotherm appears at 130°. Weak broad endothermic effects appear at 310° and between 420° and 500°. A weak endotherm appears at 740°, and is attributed to CaCO₃. This is followed by a medium exotherm at 850° and a somewhat stronger exotherm at 905°. The high temperature exotherms suggest the presence of CSH (I), found by Kalousek (35) to have C/S ratios around 1.2 and 1.4, respectively.

The DTA of the calcitic lime plus bentonite mixture after hydrothermal treatment for 12 hours at 156°C is shown as curve G in Figure 14. The constitutional water endotherm is of strong intensity at 110°. A definite endothermic peak occurs at 235° followed by a broader endotherm at 500° extending between 450° and 530°. A very weak endothermic effect is noted at 730°, attributed to CaCO₃. This is followed by two medium to strong exotherms at 850° and 920°. Aluminum substituted tobermorites, which were studied by Kalousek (34) and Diamond (14), are suggested by this pattern. There is also the possibility of two CSH compounds having C/S ratios

above 1.25, as noted by Kalousek (35).

The DTA of the calcitic lime plus bentonite mixture after hydrothermal treatment for 12 hours at 164°C is shown as curve H in Figure 14. The constitutional water endotherm appears as a medium broad peak at 110° with a broad shoulder near 220°. A definite broad endotherm appears at 500° which suggests Ca(OH)₂. This is followed by a weak endothermic effect at 730° which is attributed to CaCO₃. A very strong exotherm occurs at 900°, probably representing CSH (I) with C/S ratio near 1.3, prepared by Kalousek (35).

The DTA of the calcitic lime plus bentonite mixture after hydrothermal treatment for 12 hours at 170°C is shown as curve I in Figure 14. A very strong constitutional water endotherm appears at 140°. A definite broad endotherm appears at 450°; this is followed by a weak endotherm at 700° probably due to CaCO₃. A medium to strong exotherm occurs at 850°. The overall pattern resembles Diamond's (14) CSH (I) preparation, tested on an instrument with heating rate similar to the one used here. The exothermic effect appears similar to that found by Diamond (14) for 10% aluminum substituted tobermorite.

Dolomitic monohydrated lime plus bentonite (C/S = 0.45) The DTA of this mixture after treatment for five days

at 40°C is shown as curve C in Figure 15. The strong constitutional water endotherm at 110° has a shoulder at 160°. The medium endotherm at 395° suggests Mg(OH)₂. A very weak endotherm around 520° is probably due to Ca(OH)₂. These are followed by a weak but sharp endotherm at 740°, probably due to CaCO₃. An exothermic effect appears with the usual sharp rise to 870° but this is followed by a leveling effect, giving no definite peak. The latter is unexplained.

The DTA of the dolomitic monohydrated lime plus bentonite mixture after treatment for four days at 80°C is shown as curve D in Figure 15. A strong constitutional water endotherm appears at 110° with a shoulder at 160°. It is followed by broad weak endothermic effects at 250°, 520° and 730°. The 520° endotherm is probably from Ca(OH)₂ and the 730° endotherm is attributed to CaCO₃. A medium endotherm appears at 420° from Mg(OH)₂. A sharp strong exotherm occurs at 890° suggests CSH (I) prepared by Kalousek (35), having a C/S ratio near 1.3.

The DTA of the dolomitic monohydrated lime plus bentonite mixture after treatment for 12 hours at 105°C is shown as curve E in Figure 15. A strong endotherm at 150° is followed by a weak endotherm at 190°, representing the expulsion of constitutional water. Definite medium endotherms occur at

410° and 760°, due to $\text{Mg}(\text{OH})_2$ and CaCO_3 , respectively. A weak broad endotherm at 510° is attributed to $\text{Ca}(\text{OH})_2$. An exotherm occurs as a strong broad peak with the suggestion of double effects at 880° and 920°. These may indicate two CSH (I) products of different C/S ratios, according to Kalousek (35). They appear similar to the high temperature exotherms of Van Bemst's (63) CSH (II); his low temperature exotherm is missing, however.

The DTA of the dolomitic monohydrated lime plus bentonite mixture after hydrothermal treatment for 12 hours at 145°C is shown as curve F in Figure 15. Expulsion of constitutional water is represented by a sharp endotherm at 100° followed by a very slowly rising curve having a shoulder at 170°. This is followed without much rise in the curve by an endotherm at 380°. A broad weak endothermic effect at 470° may be from $\text{Ca}(\text{OH})_2$. The definite endothermic effect appearing at 710° may be attributed to carbonate. A very sharp strong exothermic peak at 830° with a shoulder at 860° may be indicative of two CSH (I) products as prepared by Kalousek (35). In combination with the low temperature endotherm Diamond (14) noted these effects for aluminum substituted tobermorite. Kalousek (35) indicates such an exotherm should appear on a pattern for

CSH (I), having a C/S ratio between 1.0 and 1.25.

The DTA of the dolomitic monohydrated lime plus bentonite mixture after hydrothermal treatment for 12 hours at 156°C is shown as curve G in Figure 15. The constitutional water endotherm consists of but one broad effect noted at 170° with about the same shape as curve F. A definite endotherm appears at 360° followed by a weak broad endotherm around 450° possibly representing $\text{Ca}(\text{OH})_2$. A very weak endothermic effect is noted at 690°, possibly carbonate; this is followed by a very sharp strong exotherm at 815°. The 360° endotherm and the 815° exotherm in combination strongly suggest aluminum substituted tobermorite, as noted by Diamond (14) and Kalousek (34).

The DTA of the dolomitic monohydrated lime plus bentonite mixture after hydrothermal treatment for 12 hours at 164°C is shown as curve H in Figure 15. The constitutional water endotherm is sharper than that of curve G but occurs at a lower temperature of 100°. Definite medium endotherms appear at 230° and 405°, the latter due to $\text{Mg}(\text{OH})_2$. Weaker endothermic effects occur at 510° and 730° which may be attributed to $\text{Ca}(\text{OH})_2$ and CaCO_3 , respectively. A very sharp exothermic peak occurs at 870°. This pattern resembles Kalousek's (34) and Diamond's (14) aluminum substituted tobermorite. Kalousek (34)

also reports such an exothermic effect from CSH compounds having a C/S ratio near 1.25.

The DTA of the dolomitic monohydrated lime plus bentonite mixture after hydrothermal treatment for 12 hours at 170°C is shown as curve I in Figure 15. The constitutional water endotherm is medium and very broad with an effect at 120° followed by a broad shoulder at 190°. A definite endotherm of medium intensity appears sharp at 410° and is attributed to Mg(OH)₂. A broader endothermic peak appears at 530°, suggesting Ca(OH)₂. A sharp endotherm occurs at 800°. A very weak endothermic effect appears at 750° and is probably due to carbonate. A very sharp exothermic effect appears at 880°. The aluminum substituted tobermorite of Kalousek (34) is suggested by the effects at 800° and 880°; the 230° effect which he found does not appear here although one does occur at 190°.

Dolomitic dihydrated lime plus bentonite (C/S = 0.39)

The DTA of this mixture after treatment for five days at 40°C is shown as curve C in Figure 16. The strong endotherm representing the expulsion of constitutional water occurs at 110°. There is a suggestion of a weak endothermic effect at 200° which is followed by a very strong endotherm at 410°; the latter is attributed to Mg(OH)₂. A very weak broad endotherm

appears around 610° . Another definite endothermic effect at 730° is probably due to CaCO_3 . The exothermic effect here is represented by a gently rising curve, flattening at 850° , similar to that occurring in the monohydrated mixture for this same treatment. This is followed by a weak exothermic effect at 970° , sometimes occurring on bentonite patterns (44).

The DTA of the dolomitic dihydrated lime plus bentonite mixture after hydrothermal treatment for four days at 80°C is shown as curve D in Figure 16. A strong endotherm at 130° indicates expulsion of constitutional water. There is an equally strong endotherm at 430° followed by a definite but weak endothermic effect at 720° ; these are attributed to $\text{Mg}(\text{OH})_2$ and CaCO_3 , respectively. The curve showing the exothermic effects is similar to curve C with flattening at 850° but having a weak exothermic peak at 940° ; a somewhat higher temperature exotherm is sometimes associated with bentonite (44).

The DTA of the dolomitic dihydrated lime plus bentonite mixture after hydrothermal treatment for 12 hours at 105°C is shown as curve E in Figure 16. The strong constitutional water endotherm appears at 110° with a suggestion of a shoulder as the curve broadens at 200° . An equally strong endotherm

appears at 430° due to $\text{Mg}(\text{OH})_2$. This is followed by very weak endothermic effects around 610° and 760° ; the latter effect is probably due to carbonate. A strong exothermic effect appears resembling curve D but without definite peaks, being represented instead by two level stretches at 880° and 990° . The latter phenomena may be associated with bentonite (44).

The DTA of the dolomitic dihydrated lime plus bentonite mixture after hydrothermal treatment at 145°C is shown as curve F in Figure 16. A medium endotherm appears at 110° representing the expulsion of constitutional water. This is followed by a definite endothermic effect at 205° followed by a strong endotherm at 395° . A very broad weak endothermic effect is noted around 580° followed by very weak effects at 700° and 740° . Distinct medium exothermic effects are noted at 830° and 940° .

The DTA of the dolomitic dihydrated lime mixture plus bentonite after hydrothermal treatment for 12 hours at 156°C is shown as curve G in Figure 16. The constitution water expulsion is shown by a sharp strong endotherm at 110° followed by a definite weak endothermic effect at 195° . Another sharp and strong endotherm appears at 405° , followed by very

weak effects around 495° , 605° and 710° . A strong exothermic peak occurs at 850° ; this is followed by a shoulder at 1000° .

Patterns for curves F and G are very similar and will be discussed together. The strong endothermic effects around 400°C are attributed to $\text{Mg}(\text{OH})_2$. The weaker endotherms above 700° are associated with the presence of carbonate. The 830 - 850° exotherms are attributed to well crystallized CSH (I) or tobermorite, probably with some aluminum substitution in the lattice, as noted in studies by Kalousek (34, 35) and Diamond (14).

Electron Microscopy

As an aid in identification of data, references were consulted for electron micrographs and diffraction diagrams of some of the products which would possibly appear in the investigation. Tobermorite, synthesized at the same temperature as some of the lime-bentonite mixtures were treated, was examined by electron microscopy for comparison.

Synthetic tobermorite

The synthetic tobermorite prepared in this study was almost identical in its x-ray diffraction pattern to that of Kalousek (35), shown in Table 3, except for a basal spacing of

11.2-11.3 Å^o for a vacuum dessicated sample. Agreement was even closer to that of Diamond (14), shown in column 6 of Table 4.

Figure 17 is an electron micrograph of this preparation showing flexible thin plates with indications of waves and sometimes rolling at the edges. This compares with the micrograph of Kalousek (35). Better dispersion occurred in some instances, as shown in Figure 18. This figure shows a few single crystals, with some tubes and lathlike formations. The large single crystal gave the diffraction diagram showing a distinct cross grating, representing a crystal lying on (001). When the electron beam of intermediate intensity was allowed to bear upon specimens, the pattern soon became too weak to be observed. The hk spacings may be conveniently calculated from a face centered orthogonal unit cell after Megaw and Kelsey (46), if the scale factor is known. In the present investigation, none were determined, but usually the longest d-spacing observed in such diagrams corresponds to the 3.07 Å^o d-spacing, also found by x-ray diffraction of this specimen. Although the 220 reciprocal lattice point is not clearly indicated in Figure 18, the 440 spot corresponding to half this d-spacing, appears strongly and was used for calculation of other d-spacings, based on measurements of the other lattice points in relation to 440. These results (± 0.03 Å^o) are given first, followed by

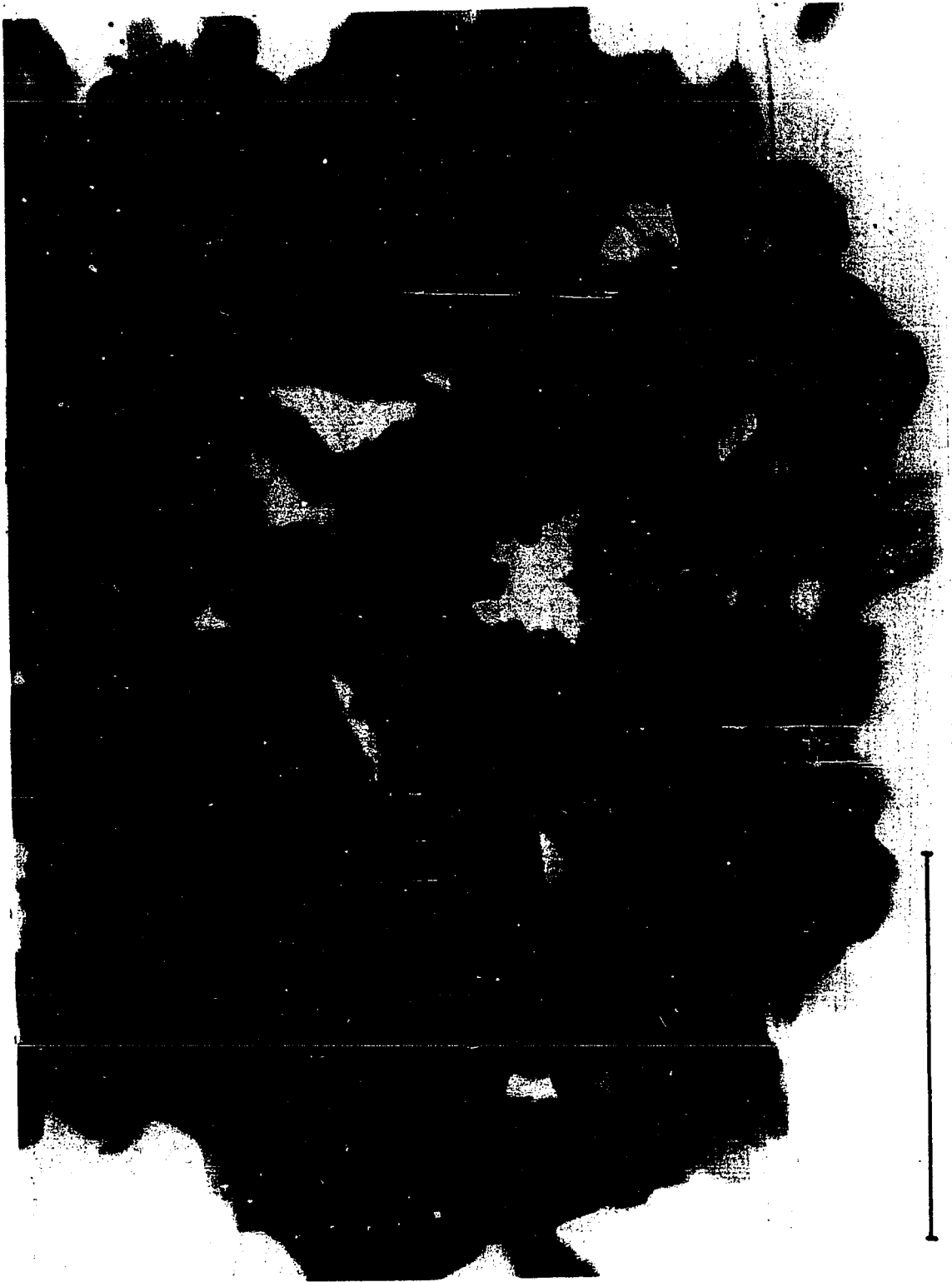


Fig. 17. Electron micrograph of synthetic tobermorite

assigned hk values and x-ray diffractometer d-spacings for a vacuum desiccated sample which probably correspond: (2.79 \AA) 400 (2.82 \AA) , (1.87 \AA) 040 (1.87 \AA) , (1.65 \AA) 620 (1.67 \AA) , (1.54 \AA) 440 (1.54 \AA) , (1.37 \AA) 800 --, (1.09 \AA) 840 --, and (0.93 \AA) 080 --. Gard, Howison and Taylor (18) found spacings for a similar pattern from material having a comparable C/S ratio as (3.05 \AA) 220, (2.80 \AA) 400 and (1.83 \AA) 040.

Figure 19 shows several overlapping flat crystals. Electron diffraction near the center gave three distinct patterns similar to Figure 18 but with fewer spots. These patterns were not persistent for very long under the beam so they were always taken before the micrographs. In this instance, three superimposed patterns are easily distinguishable; they are rotated with respect to each other. A similar phenomenon was reported for two overlapping crystals studied by Gard, Howison and Taylor (18).

Materials were often found in each lime-bentonite mixture which gave very weak diffraction patterns if at all. However, it was usually possible to ascertain the morphology of the samples in micrographs. The scale is shown on each micrograph by a line representing one micron.

Calcium silicate hydrates usually show better crystalliza-

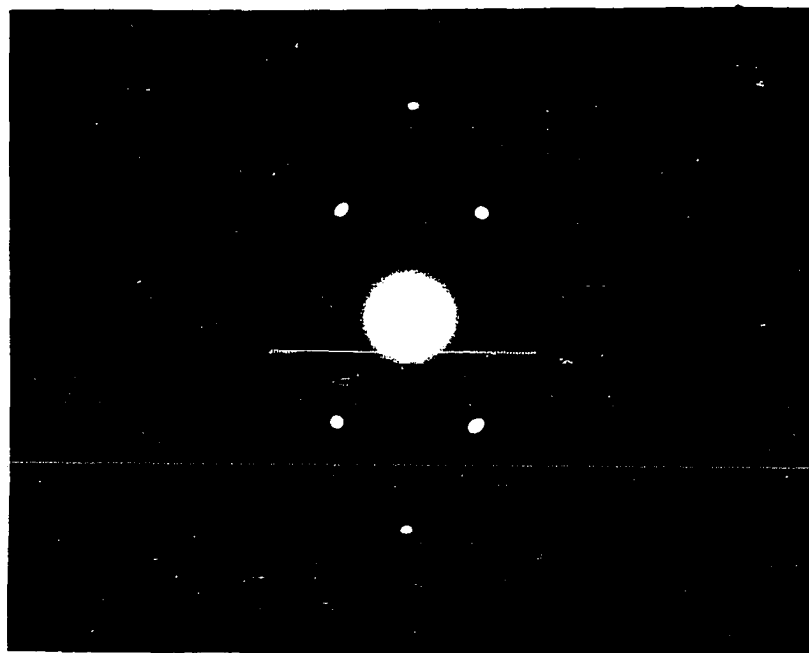


Fig. 18. Electron micrograph and diffraction pattern of synthetic tobermorite

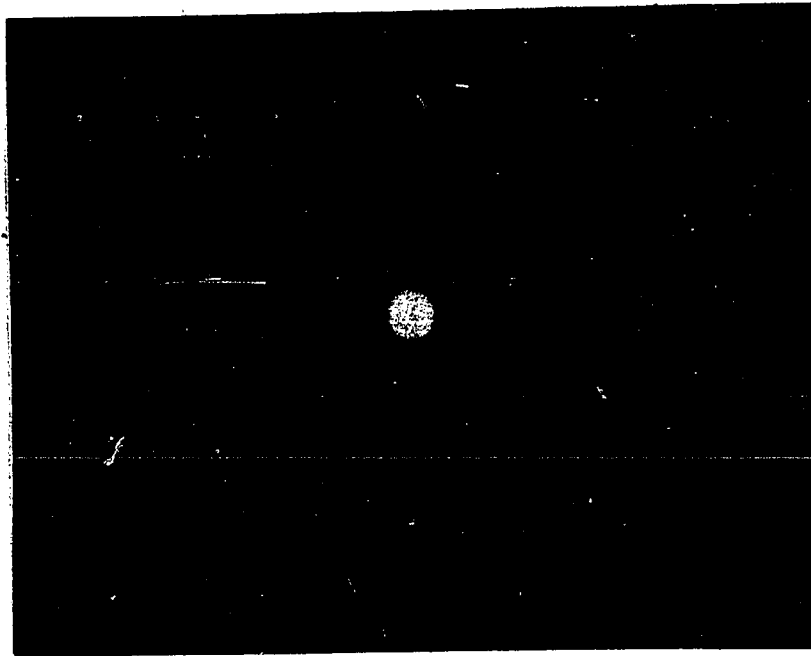


Fig. 19. Electron micrograph and diffraction pattern from overlapping synthetic tobermorite crystals

tion if formed by hydrothermal treatment. Therefore, results from specimens having this treatment are presented first.

Hydrothermally reacted cured mixtures of lime-bentonite

Electron micrographs and diffraction patterns from the hydrothermally (170°C-12 hours) reacted cured mixture of $\text{Ca(OH)}_2 + \text{MgO}$: Otay bentonite are shown in Figures 20 to 22. A view of agglomerates and partially dispersed field of clay and interleaved plates or fibers of tobermorite is shown in Figure 20 with a diffraction pattern of apparently unoriented crystals. The materials in the field view were apparently so poorly crystalline that no interpretable pattern was produced; many attempts resulted in no pattern at all. The morphology suggested in the field view resembles the spheroidal forms found in the ultrasonically dispersed C_3S and other preparations of Bogue (6) in which CSH (I) was found. With better dispersion, specimens with needle-like habit and laths were noted, as shown in Figure 21. Several overlapping crystals are apparent here but not with the preferred orientation noted in Figure 19. In the diffraction pattern the outline of two distinct single crystals is shown, one of which has the appearance of possible hexagonal symmetry. The second crystal may be rotated out of the plane of the photograph having two

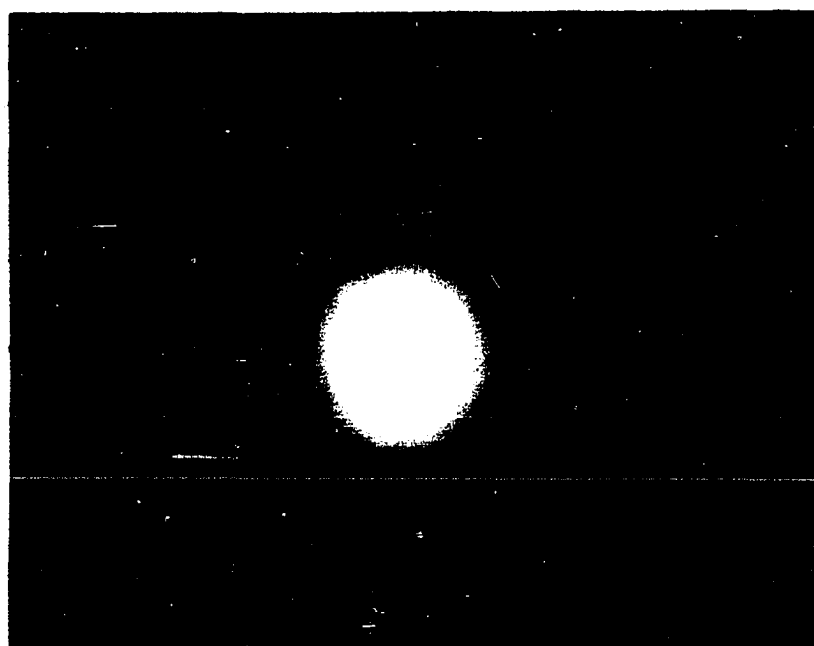


Fig. 20. Electron micrograph and diffraction pattern from $\text{Ca(OH)}_2 + \text{MgO}$: Otay bentonite mixture

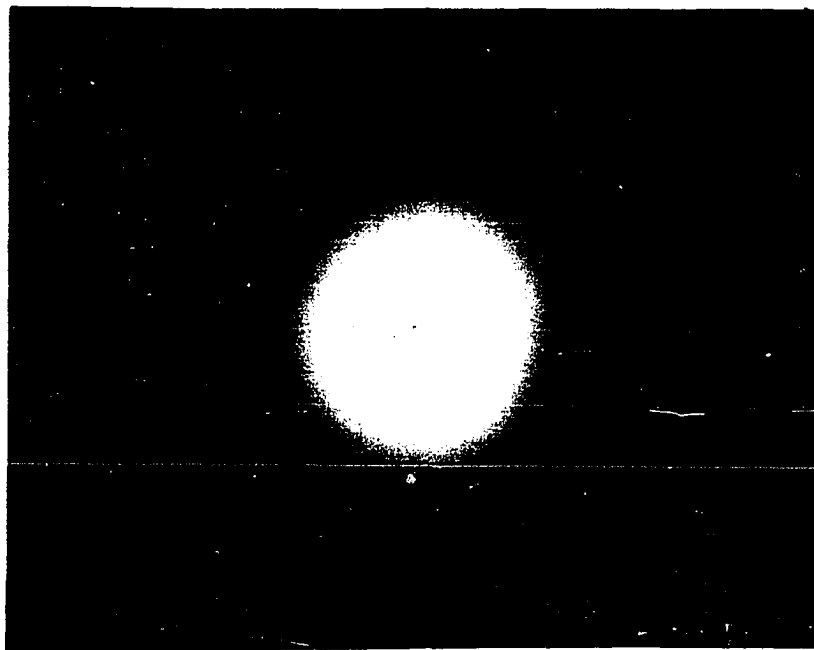
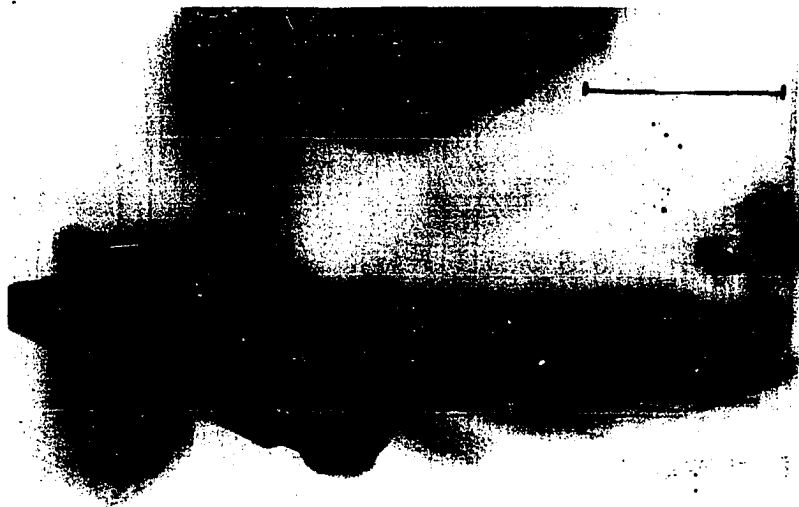


Fig. 21. Electron micrograph and diffraction pattern from $\text{Ca}(\text{OH})_2 + \text{MgO}$: Otay bentonite mixture

diametrically opposite lattice points superimposed on the more regular pattern. This suggests that the second crystal may be composed of a smaller lattice in one dimension or else it may have non-hexagonal symmetry. The extreme brightness of the ring onto which both crystal patterns are superimposed suggests the presence of a number of such disarranged crystals superimposed in the same pattern. Although certainly not a well crystallized sample, the hexagonal pattern could, of course, be one of several other materials with this symmetry but certainly it is not as well crystallized as mica or talc or one of the aluminates; these tend to give sharper and more extended patterns.

Figure 22 shows a diffraction pattern composed of three diffraction rings from the gel-like material shown in the micrograph. A few scattered spots appear in the vicinity of the inside and middle diffraction rings, indicating the possibility of material present with a higher degree of crystallinity. Two possibilities for interpretation exist. No absolute values for d-spacings can be established as was indicated earlier; however, relative values for the two d-spacings anticipated for CSH Gel and two of the strong spacings for poorly crystallized CSH (I) are equal in absolute value

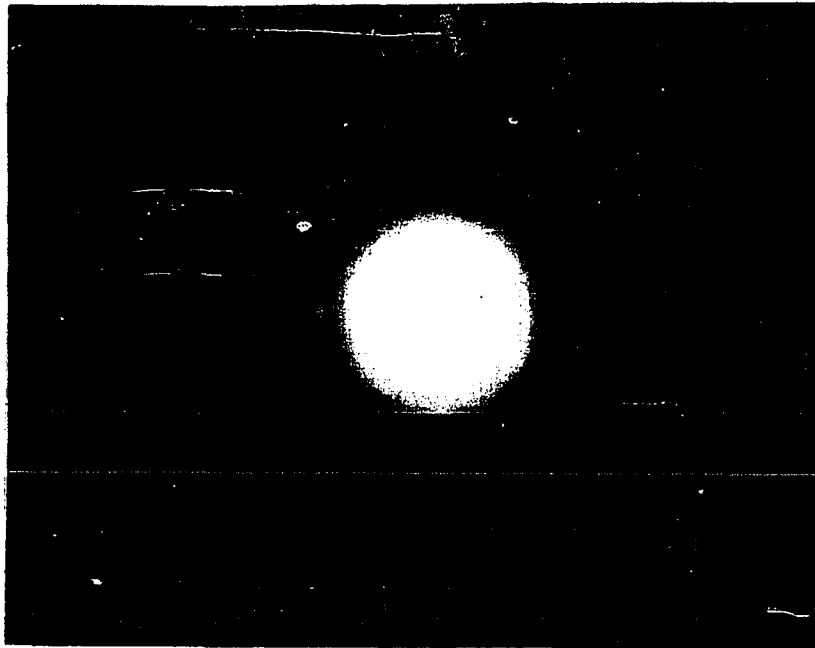
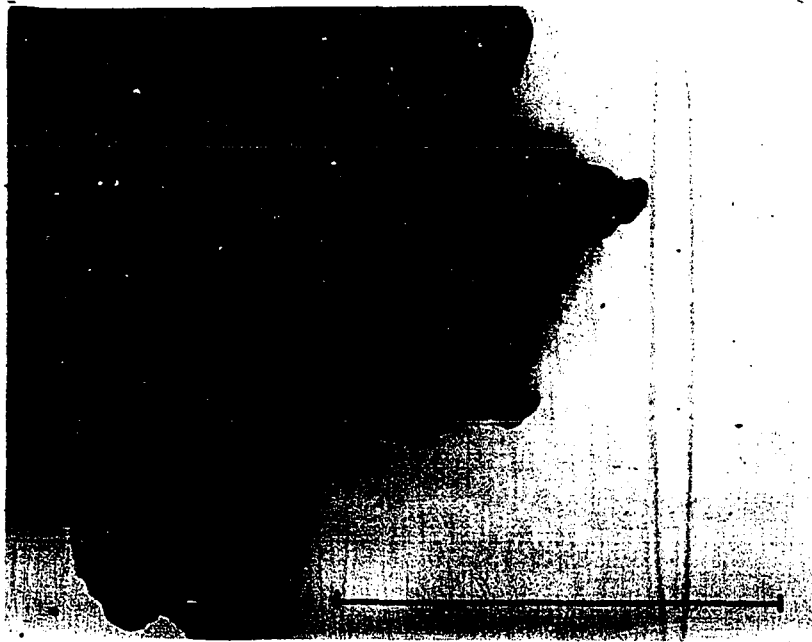


Fig. 22. Electron micrograph and diffraction pattern from $\text{Ca}(\text{OH})_2 + \text{MgO}$: Otay bentonite mixture

to the relative radii of the respective rings in the reciprocal space pattern. Table 4 in the Review of Literature shows three strong lines (col. 4). Diamond (14) in his x-ray was only able to get the same two lines at around $1.8 \overset{\circ}{\text{Å}}$ and $3.0 \overset{\circ}{\text{Å}}$ for his CSH Gel as shown in Table 3. Assuming $3.03 \overset{\circ}{\text{Å}}$ for the inner ring on Figure 22, the second ring gives $1.78 \overset{\circ}{\text{Å}}$ and the outer ring $1.53 \overset{\circ}{\text{Å}}$. Thus identification as CSH Gel or poorly crystallized CSH (I) is possible. It is also of interest to note the appearance of a distinct single crystal diffraction pattern of near hexagonal symmetry superimposed on the rings. An exception is noted below but it may be that the material producing the rings is also the material producing the spots, as indicated by superposition of the two patterns. As a second possibility for interpretation, one may assume the hk reflections from a hexagonal aluminate (C_4AH_{13}) and index on this basis. This would allocate hki indices of $11\cdot$ to the inner ring of $2.87 \overset{\circ}{\text{Å}}$, $30\cdot$ to the second ring of $1.66 \overset{\circ}{\text{Å}}$ and $22\cdot$ to the outer ring of $1.43 \overset{\circ}{\text{Å}}$ for spots actually observed. The spots also index the same. This assumes that long basal spacings are missing, as usual in this type material.

This example suggests the possibility that CSH material can be intimately associated with CAH plates, as was noted in

an overlapping ringed and spotted electron diffraction pattern by Grudemo (24). In the present instance, most if not all the material is identified as C_4AH_{13} . The absence of the sharp and extended pattern to be shown in Figure 24 was attributed to the effects of the hydrothermal treatment. Single crystals picked from this mixture showed only a few lines on a Debye-Scherrer x-ray film using chromium radiation, as compared with unheated crystals.

Room cured mixtures of lime-bentonite

Figure 23 shows a micrograph at the top representing a typical view of a room cured mixture of $Ca(OH)_2 + MgO$: Otay bentonite. Isolated fibers were noted, one of which is also shown; no diffraction pattern could be obtained.

The edge of a crushed hexagonal single crystal is shown in Figure 24. The electron diffraction pattern shown was obtained from the lighter edge. It is the type pattern which a well crystallized hexagonal compound such as mica or talc would give. However, this is also characteristic of the pattern of some of the aluminates; Buttler, Glasser, Dent and Taylor (10) found such a pattern for C_4AH_{13} . In that this material was preferentially selected and mounted, this pattern is identified as one of the tetracalcium aluminate hydrates

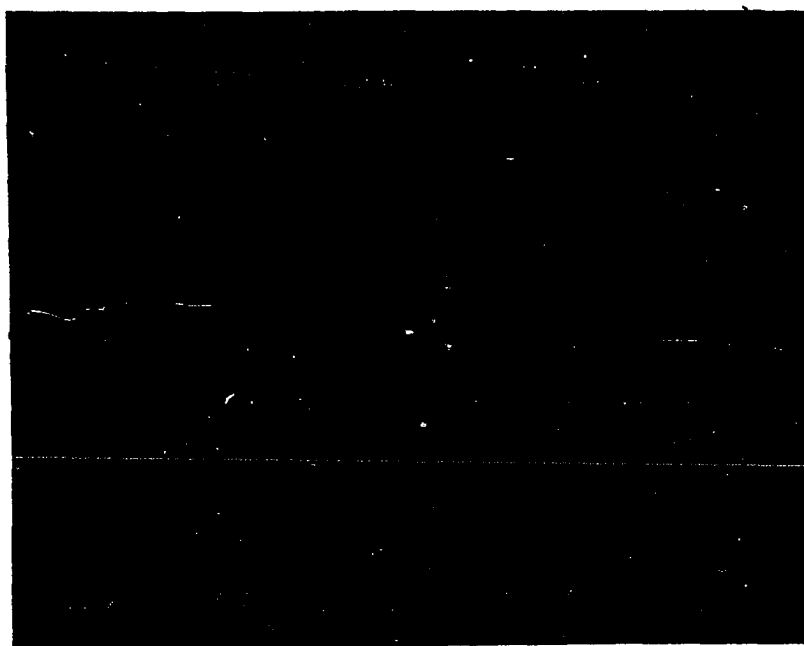


Fig. 23. Electron micrographs from $\text{Ca(OH)}_2 + \text{MgO}$: Otay bentonite mixture

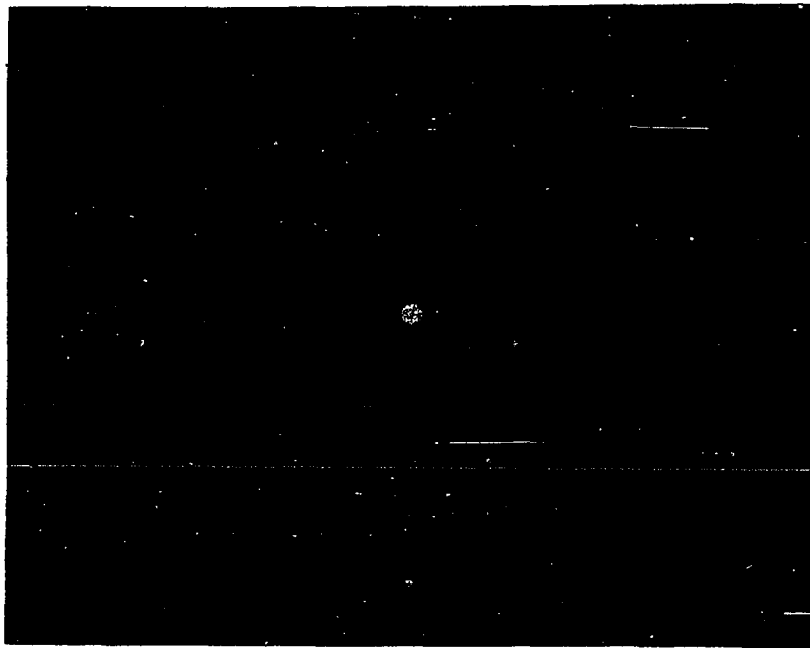
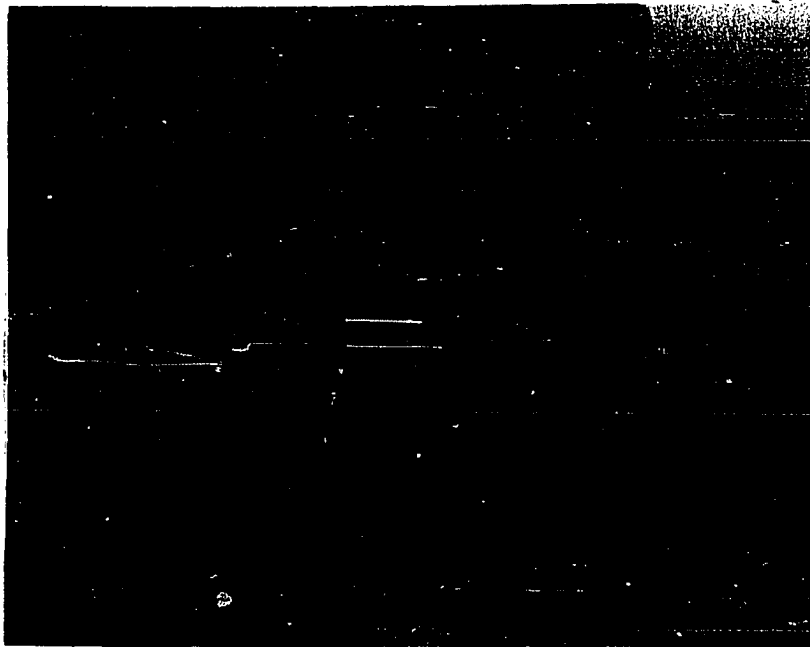


Fig. 24. Electron micrograph and diffraction pattern from $\text{Ca}(\text{OH})_2 + \text{MgO}$: Otay bentonite mixture

given in Table 1.

Another single crystal fragment from an isolated hexagonal compound was placed manually onto one of the grids. A micrograph in Figure 25 shows thin plates with some curled into tubes, giving the appearance of fibers. This was found to be characteristic of CSH (I) by Grudemo (23). Unfortunately this detail was not visually evident under the microscope at high magnification so no diffraction pattern was attempted. In a more recent paper, Grudemo (24) indicates a very intimate association between hexagonal CAH plates, with tobermorite adsorbed on their surfaces.

Another single crystal fragment is shown in Figure 26; it resembled the one shown in Figure 24. Attached material gave the accompanying diffraction diagram. Two rings composed of very diffuse spots may be identified. The ratio of d-spacings for the strongest reflections of calcium carbonate compare favorably with the reciprocal ratio for the diameters of these rings. This sample is on the same grid and is probably one of the same crystals observed the previous day. On that occasion, the edges of fragments of the hexagonal crystals were noted to have a growth forming visibly under 20,000 X magnification. This occurred after the mount had been in the

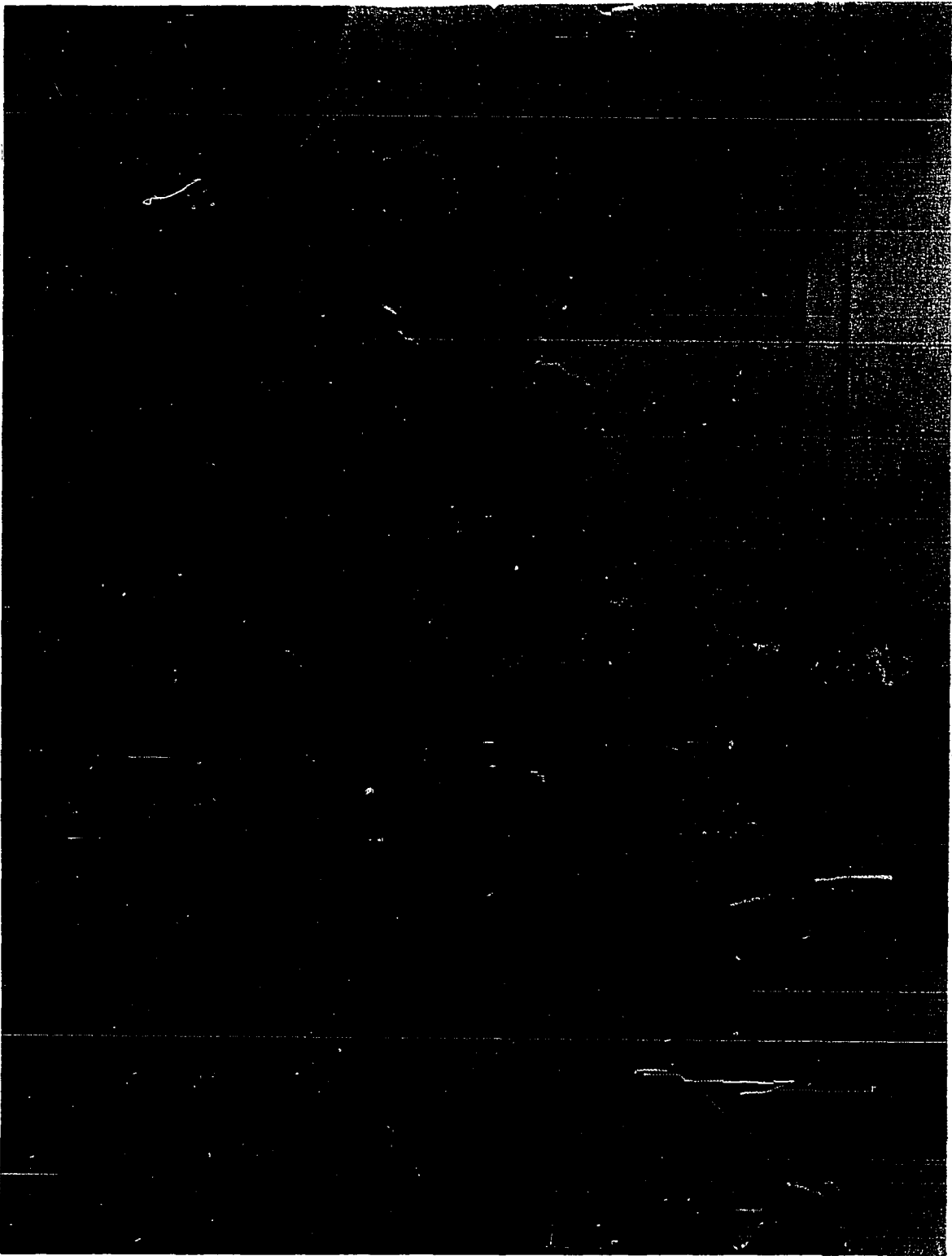


Fig. 25. Electron micrograph from $\text{Ca}(\text{OH})_2 + \text{MgO}$: Otay bentonite mixture

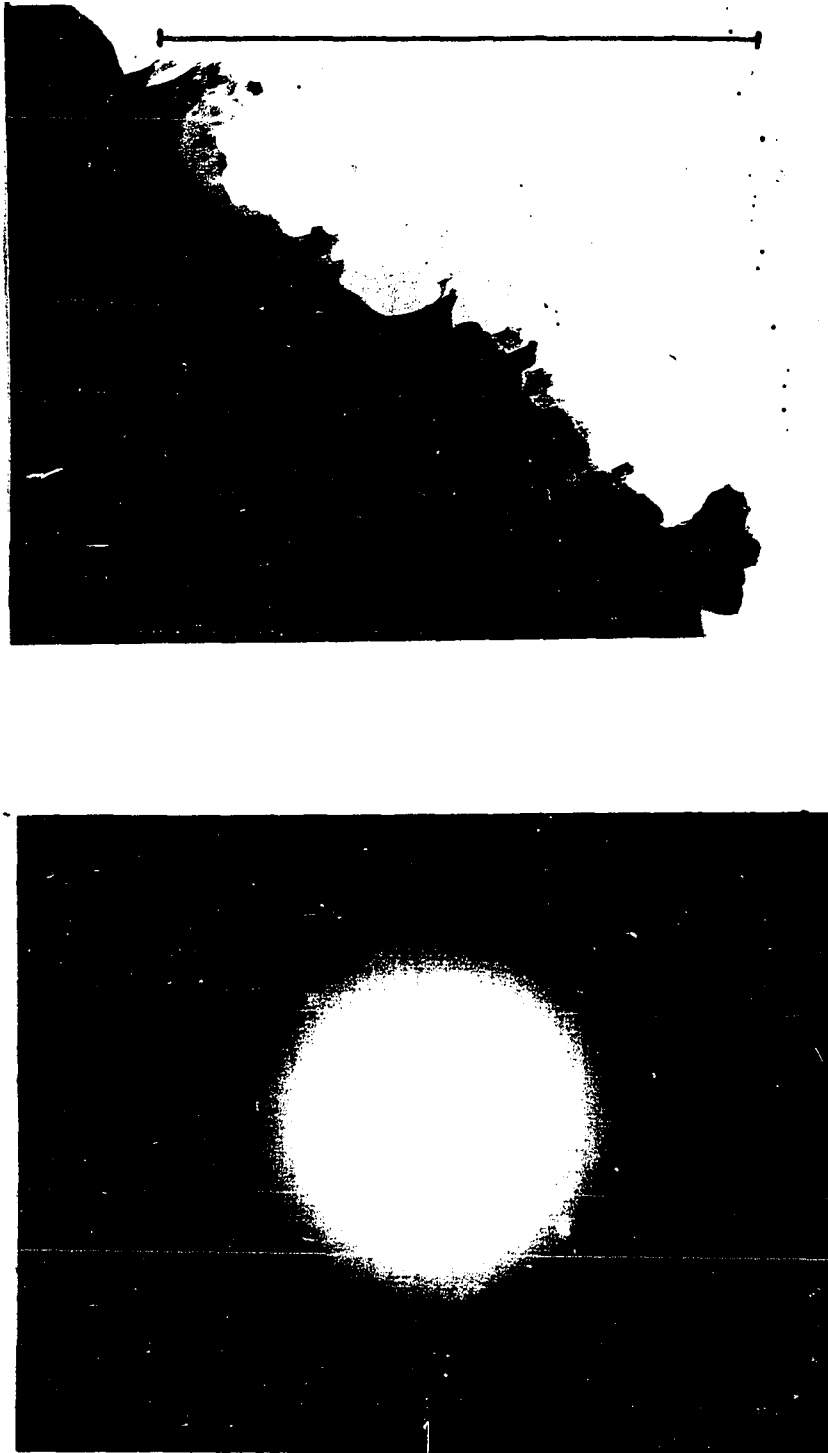


Fig. 26. Electron micrograph and diffraction pattern from $\text{Ca}(\text{OH})_2 + \text{MgO}$: Otay bentonite mixture

beam under vacuum for a total time near one hour. Since carbon dioxide was present in large quantities, the material formed was probably CaCO_3 , resulting from carbonation of released water containing calcium from the parent compound; note also discussion of Figure 24.

Hexagonal crystals similar to those discussed above were removed from a room cured mixture of Ca(OH)_2 : Otay bentonite and crushed. They were placed manually on the grids for observation. Figure 27 shows the edge of a crushed hexagonal single crystal giving an appearance of flat plates and three rolled tubes near the center of the micrograph.

Figure 28 shows an electron micrograph of the space between several crushed hexagonal crystals, with what appears to be extensions of about 0.3μ from the main body of material. These give the appearance of rolls or tubes but without the characteristic flat plates, noted in Figure 25, which usually accompany such formations. The electron diffraction pattern in the absence of a scale factor can only be interpreted by assigning the strongest circle of spots to the strongest d-spacing of possible compounds as was done on other such diagrams. Comparisons were then made by establishing reciprocal ratios of radii of other spotty circles to the



Fig. 27. Electron micrograph of $\text{Ca}(\text{OH})_2$: Otay bentonite mixture

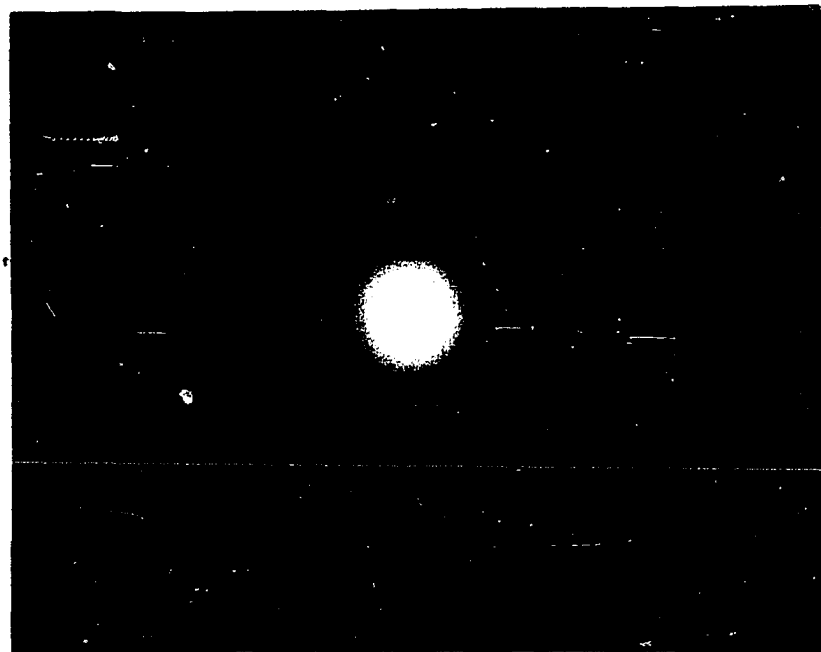
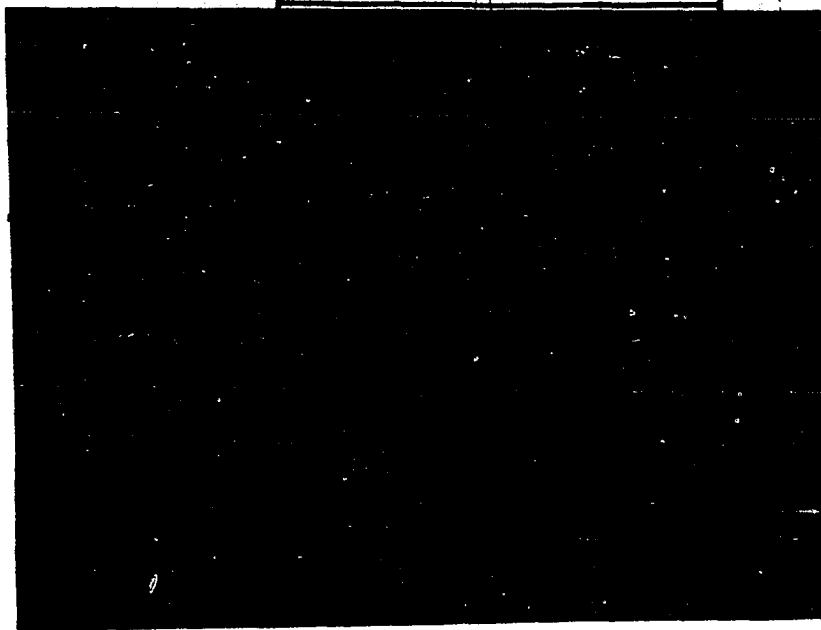


Fig. 28. Electron micrograph and diffraction pattern from $\text{Ca}(\text{OH})_2$: Otay bentonite mixture

strongest, then comparing with direct ratios of the strongest d-spacings of the compounds. When compared with strong spacings of the hexagonal crystal products, no correlation is evident. The data for the pattern of Figure 28, based on assignment of the strongest line to $3.025 \overset{\circ}{\text{Å}}$, is as follows: 3.69 vw, 3.025 s sp, 2.73 w sp, 2.46 s sp, 2.32 w sp, 2.11 s sp, 1.94 sp and $1.71 \overset{\circ}{\text{Å}}$ sp. When these spacings are compared with the results of Grudemo (23), two of the lines may be attributed to impurities in CSH (I), as shown in column 3 of Table 4. Other spacings differ by $0.05 \overset{\circ}{\text{Å}}$ to $0.10 \overset{\circ}{\text{Å}}$ either side of his findings. When compared with $\text{Ca}(\text{OH})_2$, assigning the strong spacing to $2.63 \overset{\circ}{\text{Å}}$, agreement is found with the next four strongest lines but with a difference of about $0.07 \overset{\circ}{\text{Å}}$ for the second strongest. Other compounds including $\text{Mg}(\text{OH})_2$ and CaCO_3 were compared; no correlation was evident for the $\text{Mg}(\text{OH})_2$. However, except for $0.07 \overset{\circ}{\text{Å}}$ deviation from the $1.87 \overset{\circ}{\text{Å}}$ spacing for CaCO_3 , every strong spacing less than and including $3.03 \overset{\circ}{\text{Å}}$ is in agreement. The identification is uncertain but the evidence points to a CaCO_3 formation, although different in appearance from that shown in Figure 27.

Infrared Spectroscopy

Successive monochromatic bands of infrared irradiating a substance may be absorbed wholly or in part, depending upon the correspondence between the radiated frequencies and the intramolecular vibrational frequencies of the substance. The infrared spectrum is a graph showing the per cent of radiation absorbed by the substance plotted against the incident wavelength (or frequency). This graph is characteristic of a material and can be used in its identification, as in the present study.

Pure compounds

The eight strongest absorption bands in the spectra for the compounds represented in Figure 1 are shown in Table 6 in the order of diminishing absorption. Increased absorption is indicated by the downward deflection in a spectrum called a band; maxima are therefore indicated as the wavelengths at the lowest points of the bands.

Duplications occur between bands for several of these compounds. The 3.08μ band appears in both CSH Gel and crystalline tobermorite. Near duplication occurs between the 7.01μ band for C_4AH_{13} and the 6.96μ band for crystalline tobermorite; the 9.88 band for C_4AH_{13} is near that for crystalline

Table 6. Infrared absorption spectra for pure compounds

Compound	Absorption bands, μ
Bentonite	9.75, 10.20, 9.00, 2.93, 10.98, 2.76, 11.95, 6.12
C_4AH_{13} (48)	3.13, 7.01, 5.30, 13.00, 9.88, 11.45, 15.50, 10.30
C SH Gel (48)	10.64, 3.08, 2.77, 3.58, 6.77, 7.20, 4.32, 12.40
Crystalline tobermorite (48)	10.38, 9.85, 10.75, 3.07, 9.35, 3.52, 6.96, 6.77

tobermorite at 9.85μ . The 10.20μ band for bentonite is near the 10.30μ band for C_4AH_{13} . However, no duplications occur between the three strongest bands of these compounds. Patterns for the pure compounds CSH (I), CSH (II) and CSH Gel as well as tobermorite were found by other investigators to exhibit distinct infrared spectra. These will be used in conjunction with those given in Table 6 to identify the bands which appear in each mixture. Whenever the principal bands in a pure compound coincide or overlap with distinct bands in the pattern of a mixture, they are assumed to be present in the mixture. However, if one of the principal bands is missing or doubtful, then the presence of the compound in the mixture is open to

question.

Dry mixtures of lime-bentonite

Curves A in Figures 29, 30 and 31 show infrared spectra for dry mixtures of Otay bentonite with calcitic, dolomitic monohydrated and dihydrated limes, respectively. The absorption bands, which remain after accounting for the bentonite spectrum given above, may be assumed to be associated with the lime in the mixture, as follows: for Ca(OH)_2 , 10.10, 6.74, 6.95, 7.06, 11.45 and 3.43μ ; for $\text{Ca(OH)}_2 + \text{MgO}$, 10.10, 2.70, 6.75, 6.95, 11.45 and 3.42μ ; and for $\text{Ca(OH)}_2 + \text{Mg(OH)}_2$, 10.10, 2.70, 6.74, 7.00, 7.06, 11.45 and 3.45μ . The bands at 6.74 and 10.1μ are associated with MgO. Strong bands also occur for MgO near 10 and 11.6μ . Bands at 6.95, 7.06 and 11.45μ may be associated with CaCO_3 , according to Midgley's findings (48). The weakest band at 3.43μ is the only one not attributed to other compounds which all three patterns have in common. The 2.70μ band is only common to the patterns for the mixtures containing $\text{Ca(OH)}_2 + \text{MgO}$ and $\text{Ca(OH)}_2 + \text{Mg(OH)}_2$.

Room cured mixtures of lime-bentonite

Calcitic lime plus bentonite The infrared spectrograph of this cured mixture is shown as curve B in Figure 29. Broad bands appear in this pattern with maximum absorption at the

following wavelengths: 2.74, 2.90, 5.5, 6.13, 6.74, 7.07, 9.0, 9.80, 10.15, 11.00, 11.45, 12.00 and 12.65 μ . Bentonite, calcite and the following new compounds are suggested by these bands. Identification is by comparison with published spectra on the pure compounds, the sources for which are given by author and reference following each compound: C_4AH_{13} , Midgley (48); CSH (I), Kalousek and Prebus (37) and Diamond (14); CSH (II), Kalousek and Prebus (37) and Van Bemst (63). A higher crystalline form of CSH is suggested by infrared data on tobermorite by Diamond (14), although this is not indicated conclusively by Midgley's (48) data.

It will be noted that wavelengths at maximum absorption are displaced in some instances, giving a broader band. For example, the contribution of the 9.88 μ band for C_4AH_{13} in the vicinity of the 9.75 μ bentonite is accounted for by the broader 9.80 μ band. Thus the principal bands for the pure compound may not actually coincide with but will overlap with another band in the pattern for the mixture. It may be noted from Table 6 that a number of compounds contribute more or less to the absorption band around 10 μ . The most strongly absorbed wavelengths for CSH Gel and tobermorite appear at 10.64 μ (14, 48) and 10.3-10.4 μ (14, 48) respectively. In the present pattern neither are evident by significant absorption bands at

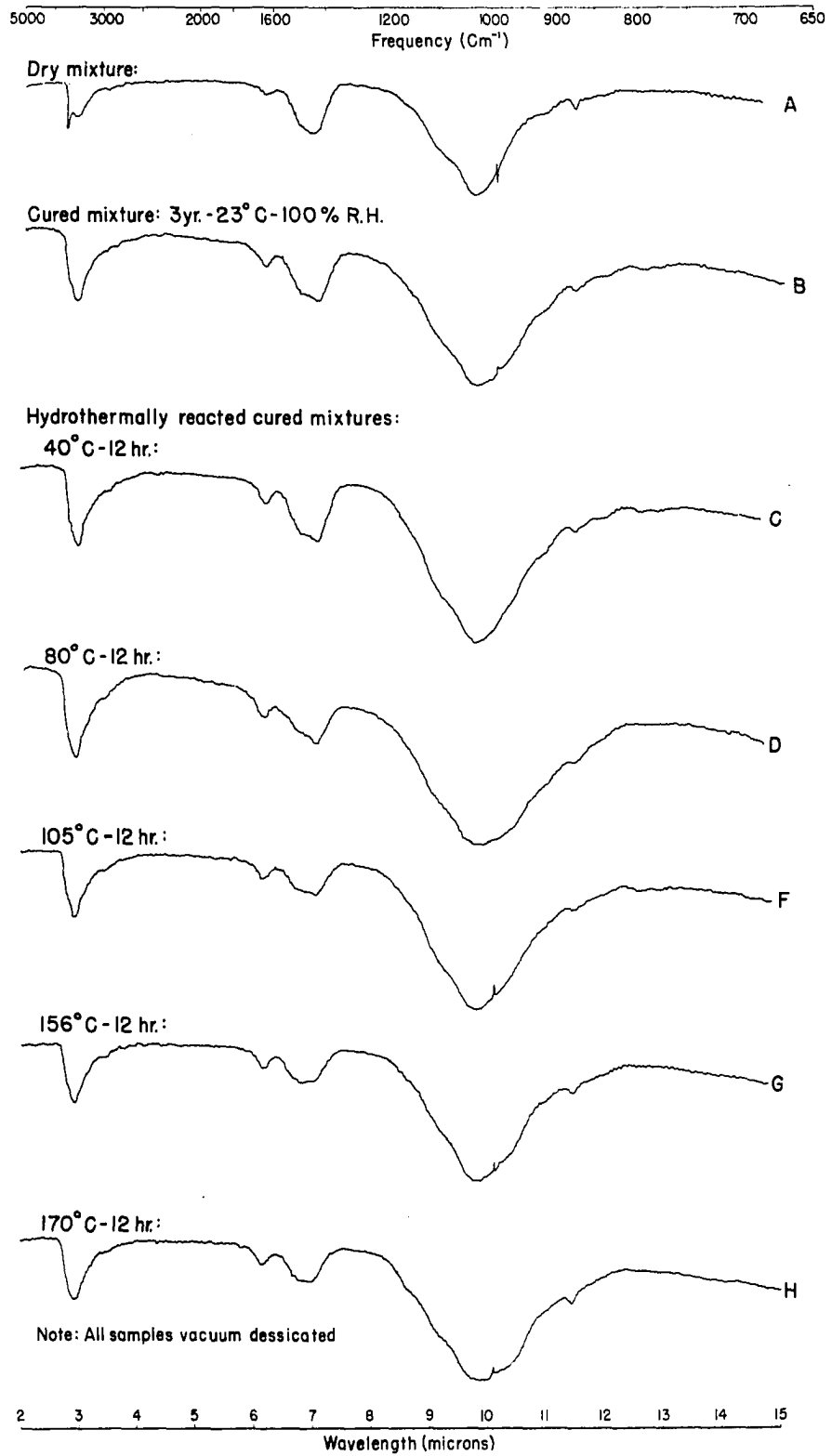


Fig. 29. Infrared spectrographs for Otay bentonite: $\text{Ca}(\text{OH})_2$: H_2O mixture (1:0.45:1.62)

their respective wavelengths. Therefore their presence in this mixture is uncertain.

Dolomitic monohydrated lime plus bentonite The infrared spectrograph for this cured mixture is shown as curve B in Figure 30. Broad bands appear in this pattern with maximum absorption at the following wavelengths: 2.72, 2.90, 3.44, 6.15, 6.70, 7.05, 8.55, 9.82, 10.40, 11.00, 11.56, 11.8 and 12.65 μ . Bentonite and calcite are indicated. The presence of the following new compounds is suggested: C_4AH_{13} , Midgley (48); CSH (I), Kalousek and Prebus (37) and Diamond (14); CSH (II), Kalousek and Prebus (37) but not by Van Bemst's (63) pattern for this compound. A higher crystalline form of CSH is suggested from data on tobermorite by Diamond (14), although this is not conclusively indicated by Midgley's (48) data. The strongest band for CSH Gel overlaps other major absorption bands; therefore, its presence is uncertain (14, 48).

Dolomitic dihydrated lime plus bentonite The infrared spectrograph for this mixture is shown as curve B in Figure 31. Broad bands appear in this pattern with maximum absorption at the following wavelengths: 2.70, 2.77, 2.91, 4.33, 5.57, 6.15, 6.84, 7.03, 8.98, 9.80, 10.10, 10.90, 11.46, 12.00, 12.60 and 14.07 μ . Bentonite and calcite are indicated. The

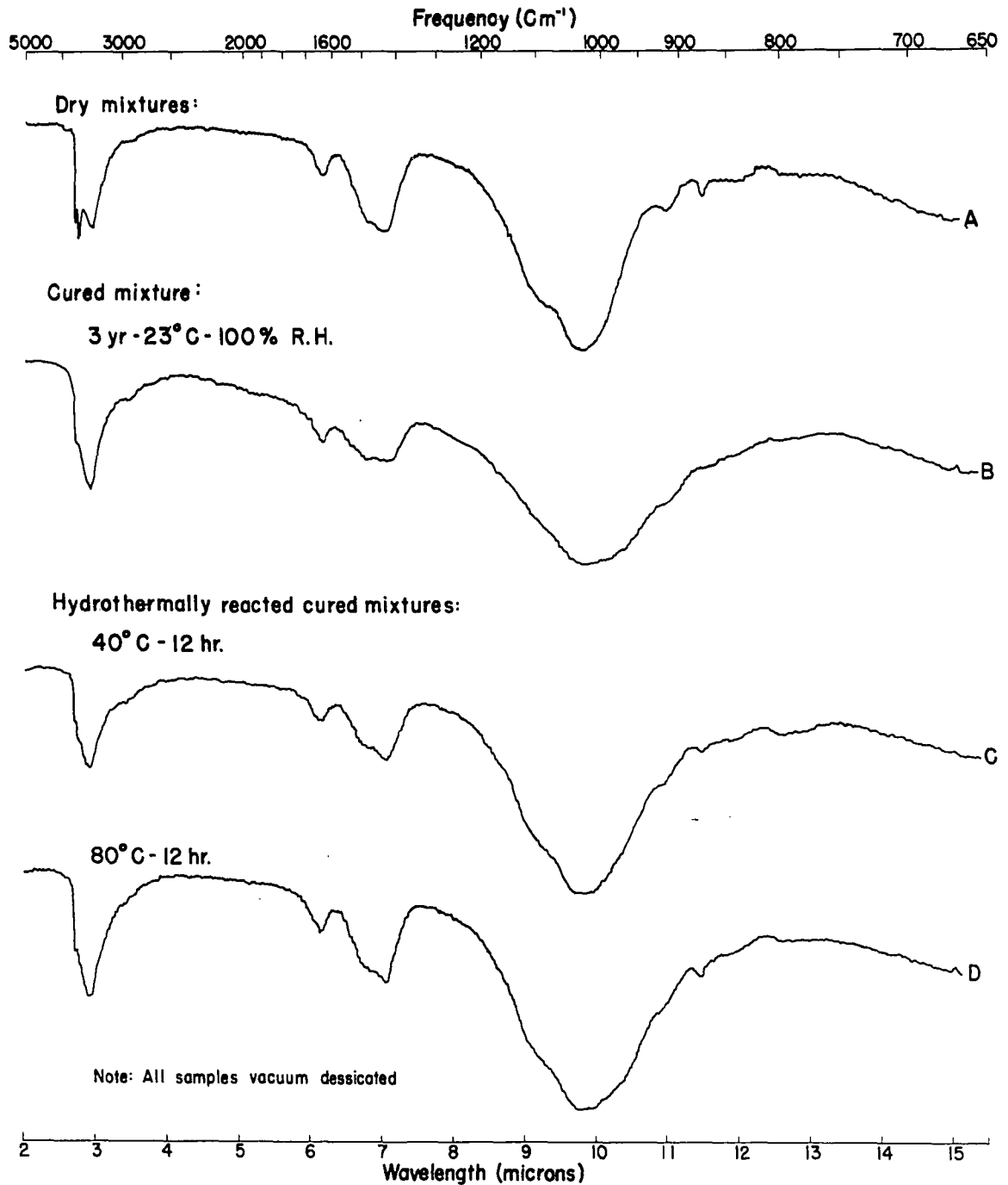


Fig. 30 Infrared spectrographs for Otay bentonite: $\text{Ca}(\text{OH})_2 \cdot \text{MgO} : \text{H}_2\text{O}$ mixture (1:0.45:1.62)

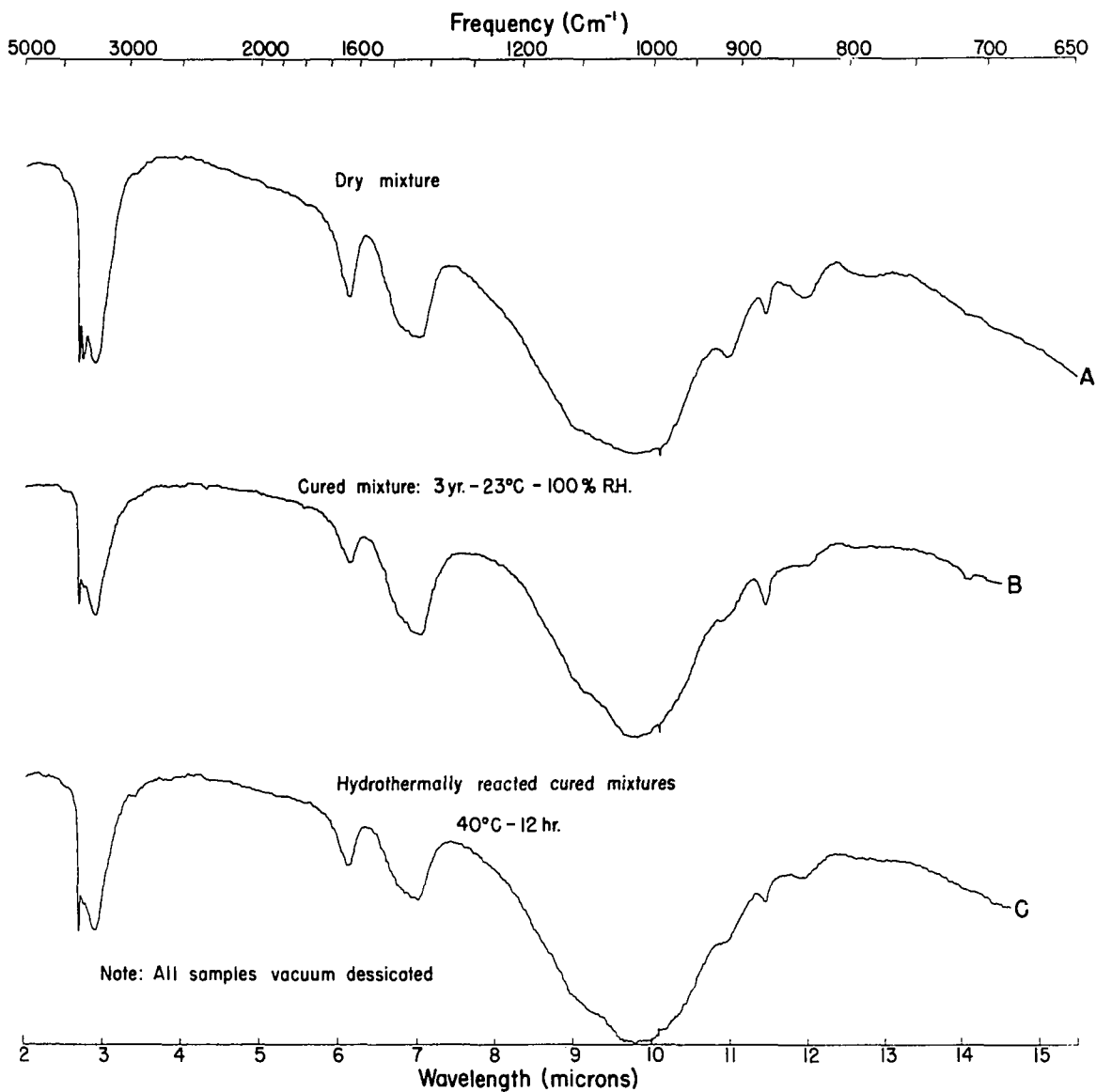


Fig. 31 Infrared spectragraphs for Otay bentonite: Ca(OH)₂ + Mg(OH)₂ : H₂O mixture (1 : 0.45 : 1.62)

presence of the following new compounds is suggested: C_4AH_{13} , Midgley (48); CSH (I), Kalousek and Prebus (37) and Diamond (14); CSH (II), Kalousek and Prebus (37) and Van Bemst (63). A higher crystalline form of CSH is suggested from data on tobermorite by Diamond (14), although this is not conclusively indicated by Midgley's (48) data. The strongest band for CSH Gel overlaps other major absorption bands; therefore its presence is uncertain (14, 48).

Hydrothermally reacted cured mixtures of lime-bentonite

The spectrographs for the cured mixtures of bentonite plus lime, after hydrothermal treatments, are shown by the types of lime used and the reaction temperatures.

Calcitic lime plus bentonite

40°C, 5 days, as shown by curve C in Figure 29

Broad bands appear in this pattern with maximum absorption at the following wavelengths: 2.74, 2.92, 3.45, 4.30, 6.15, 6.74, 7.07, 9.15, 9.74, 10.12, 10.95, 11.47, 11.98, 12.58 and 12.85 μ . Bentonite and calcite are indicated. The presence of the following new compounds is suggested: C_4AH_{13} , Midgley (48); CSH (I), Kalousek and Prebus (37) and Diamond (14); CSH (II), Kalousek and Prebus (37) and Van Bemst (63). Conclusive data for a higher crystalline form is not indicated by

the findings of Midgley (48) although pure compound studies by Diamond (14) strongly suggests tobermorite. Kalousek and Prebus (37) show only two bands, which are present here, while Kalousek and Roy (38) show bands near 2.9, 6.2, 8.3, 10 and 11.2 μ , in good agreement with Diamond (14). The principal band for CSH Gel and those of other compounds overlap. Since no definite evidence of its contribution is noted, its presence is uncertain (14, 48).

80°C, 4 days, as shown by curve D in Figure 29

Broad bands appear in this pattern with maximum absorption at the following wavelengths: 2.77, 2.90, 3.41, 6.15, 6.74, 7.05, 9.0, 9.86, 10.12, 10.40, 11.00 and 11.48 μ . Bentonite and calcite are indicated. The presence of the following new compounds is suggested: C_4AH_{13} , by three of five bands shown by Midgley (48); CSH (I), Diamond (14) and Kalousek and Prebus (37); CSH (II), by Kalousek and Prebus (37) but not by Van Bemst's (63) data. Approximately the same indications for tobermorite and CSH Gel exist in this pattern as appeared in curve C and its presence is still uncertain.

105°C, 12 hr., as shown by curve E in Figure 29

Broad bands appear in this pattern with maximum absorption at the following wavelengths: 2.77, 2.92, 3.42, 5.57, 6.15,

6.67, 7.05, 9.00, 9.80, 10.12, 11.48 and 12.60 μ . Bentonite and calcite are indicated. The presence of the following new compounds is suggested: C_4AH_{13} , Midgley (48); CSH (I), Kalousek and Prebus (37) and Diamond (14); CSH (II), by Kalousek and Prebus (37) but not by Van Bemst's (63) data. The same indications appear here for tobermorite and CSH Gel as appeared in curve C.

156°C, 12 hr., as shown by curve G in Figure 29

Broad bands appear in this pattern with maximum absorption at the following wavelengths: 2.78, 2.93, 3.48, 6.15, 6.78, 7.02, 8.60, 9.00, 9.85, 10.12, 10.4, 11.00 and 11.45 μ .

Bentonite and calcite are indicated. The presence of the following new compounds is suggested: C_4AH_{13} , Midgley (48); CSH (I), Kalousek and Prebus (37) and Diamond (14); CSH (II), by Kalousek and Prebus (37) data and possibly by that of Van Bemst (63). Presence of tobermorite in this pattern is indicated by comparison with the data of Diamond (14) and Kalousek and Prebus (37). However, only three of the four strongest bands found by Midgley (48) appear here. The intensity of the strongest tobermorite band, however, is increased slightly over that of curve E.

170°C, 12 hr., as shown by curve H in Figure 29

Broad bands appear in this pattern with maximum absorption at the following wavelengths: 2.90, 3.50, 6.12, 6.75, 6.90, 8.60, 9.16, 9.75, 10.12, 10.37 and 11.43 μ . Bentonite and calcite are indicated. The presence of the following new compounds is suggested: C_4AH_{13} , by three of the five strongest bands of Midgley's (48) pattern; CSH (I), Kalousek and Prebus (37) and Diamond (14); CSH (II), Kalousek and Prebus (37) but not by data of Van Bemst (63). The increased intensity of the strongest tobermorite band found by Midgley (48) and Diamond (14) indicates the presence of this phase. Presence of CSH Gel remains doubtful because of overlapping of its strongest line with other compounds.

Dolomitic monohydrated lime plus bentonite40°C, 5 days, as shown by curve C in Figure 30

Broad bands appear in this pattern with maximum absorption at the following wavelengths: 2.72, 2.79, 2.90, 3.43, 6.13, 6.70, 7.05, 9.00, 9.75, 11.00, 11.45, 11.85, 12.6, 12.70 and 14.0 μ . Bentonite and calcite are indicated. The presence of the following new compounds is suggested: C_4AH_{13} , Midgley (48); CSH (I), Kalousek and Prebus (37) and Diamond (14);

CSH (II), Kalousek and Prebus (37) and Van Bemst (63). Tobermorite is indicated by comparison with data of Diamond (14) and Kalousek and Prebus (37). A weak band appears for the strongest band of CSH Gel; however, it overlaps strong bands of other compounds so its presence is uncertain.

80°C, 4 days, as shown by curve D in Figure 30

Broad bands appear in this pattern with maximum absorption at the following wavelengths: 2.72, 2.77, 2.90, 5.20, 6.13, 6.80, 7.05, 9.00, 9.80, 9.90, 10.50, 10.8, 11.0, 11.45, 11.80, 12.75 and 14.0 μ . Bentonite and calcite are indicated. The presence of the following new compounds is suggested: C₄AH₁₃, Midgley (48); CSH (I), Diamond (14) and Kalousek and Prebus (37); CSH (II), Kalousek and Prebus (37) and Van Bemst (63). Very weak indications appear in the pattern for tobermorite. The strongest band for CSH Gel overlaps strong bands of other compounds; therefore, its presence cannot be definitely established. A definite change has occurred in this vicinity of the pattern, however, indicating changes related to one or more of these compounds.

105°C, 12 hr., as shown by curve E in Figure 32

Broad bands appear in this pattern with maximum absorption at the following wavelengths: 2.71, 2.76, 2.90, 6.13, 6.77, 7.05,

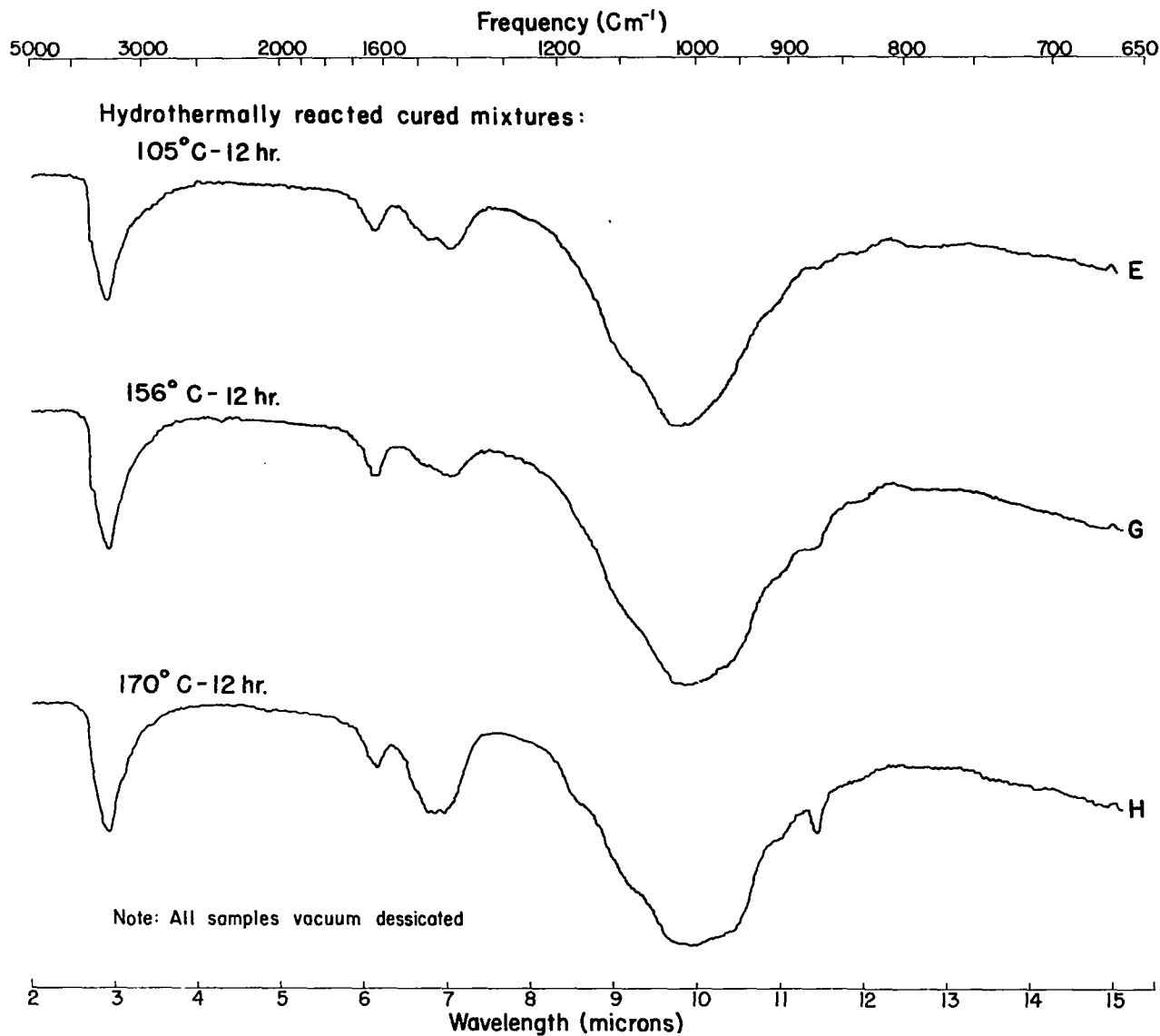


Fig. 32 Infrared spectrographs for Otay bentonite: $\text{Ca}(\text{OH})_2 + \text{MgO} : \text{H}_2\text{O}$ mixture (1 : 0.45 : 1.62)

9.10, 9.75, 9.85, 10.3, 10.95, 11.48, 12.00 and 12.75 μ .

Bentonite and calcite are indicated. The presence of the following new compounds is suggested: C_4AH_{13} , Midgley (48); CSH (I), Diamond (14) and Kalousek and Prebus (37); CSH (II), Kalousek and Prebus (37) and Van Bemst (63). Indications for CSH Gel and tobermorite are about the same here as in curve D in Figure 30 with some increased intensity noted around 10.4 μ .

156°C, 12 hr., as shown by curve G in Figure 32

Broad bands appear in this pattern with maximum absorption at the following wavelengths: 2.70, 2.92, 6.15, 6.70, 7.05, 9.1, 9.73, 9.90, 10.4, 10.50, 11.00, 11.45, 12.00 and 12.70 μ .

Bentonite and calcite are indicated. The presence of the following new compounds is suggested: C_4AH_{13} , Midgley (48); CSH (I), Kalousek and Prebus (37) and Diamond (14); CSH (II), Kalousek and Prebus (37) and Van Bemst (63). The greater intensity in the vicinity of the 10.4 μ band suggests strongly the presence of tobermorite. The strongest line for CSH Gel is not clearly indicated because of overlapping with other bands.

170°C, 12 hr., as shown by curve H in Figure 32

Broad bands appear in this pattern with maximum absorption at the following wavelengths: 2.92, 6.14, 6.75, 7.00, 8.50,

9.08, 9.70, 10.38, 11.00, 11.42, 12.0 and 12.6 μ . Bentonite and calcite are indicated. The presence of the following new compounds is suggested: C_4AH_{13} , by four of five strongest lines in Midgley's (48) pattern; CSH (I), Kalousek and Prebus (37) and Diamond (14); CSH (II), Kalousek and Prebus (37) and Van Bemst (63). Tobermorite is clearly indicated by the increased intensity of the band near 10.4 μ . Presence of CSH Gel is doubtful for the same reasons stated for curve G.

Dolomitic dihydrated lime plus bentonite

40°C, 5 days, as shown by curve C in Figure 31

Broad bands appear in this pattern with maximum absorption at the following wavelengths: 2.70, 2.78, 2.92, 3.43, 6.13, 7.02, 8.96, 9.80, 10.20, 10.95, 11.46, 11.95 and 12.75 μ . Bentonite and calcite are indicated. The presence of the following new compounds is suggested: C_4AH_{13} , Midgley (48); CSH (I), Kalousek and Prebus (37) and Diamond (14); CSH (II), Kalousek and Prebus (37) and Van Bemst (63). Absorption in this pattern near 10.5 μ is somewhat more intense here than in curve B; the relationship to CSH Gel or tobermorite is uncertain.

80°C, 4 days, as shown by curve D in Figure 33

Broad bands appear in this pattern with maximum absorption at the following wavelengths: 2.71, 2.78, 2.93, 3.40, 6.13, 7.04, 9.00, 9.80, 10.02, 10.2, 11.0, 11.45, 12.00 and 12.65 μ . Bentonite and calcite are indicated. The presence of the following new compounds is suggested: C₄AH₁₃, Midgley (48); CSH (I), Diamond (14) and Kalousek and Prebus (37); CSH (II), Kalousek and Prebus (37) and Van Bemst (63). Very weak indications appear in the pattern for tobermorite, with some reduction of the 10.4 μ band; the same indications for CSH Gel appear here as in curve C of Figure 31.

105°C, 12 hr., as shown by curve E in Figure 33

Broad bands appear in this pattern with maximum absorption at the following wavelengths: 2.71, 2.78, 2.90, 3.98, 5.15, 6.15, 6.75, 6.97, 8.98, 9.80, 10.10, 11.00, 11.45, 12.00 and 12.65 μ . Bentonite and calcite are indicated. The presence of the following new compounds is suggested: C₄AH₁₃, Midgley (48); CSH (I), Diamond (14) and Kalousek and Prebus (37); CSH (II), Kalousek and Prebus (37) and Van Bemst (63). Hardly any indication remains for the strong tobermorite band at 10.4 μ . The presence of CSH Gel remains uncertain as in curve D.

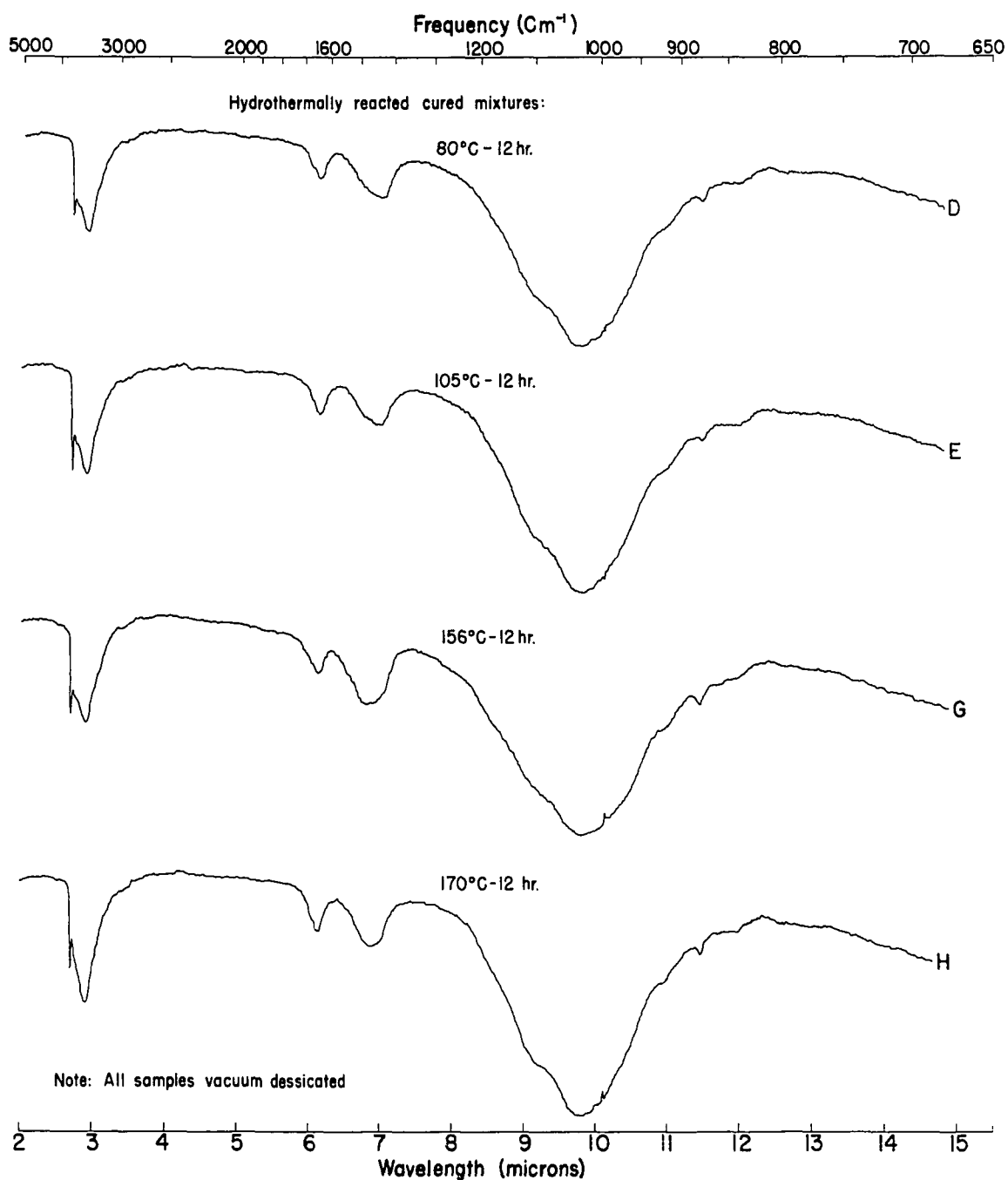


Fig. 33 Infrared spectrographs for Otoy bentonite: $\text{Ca}(\text{OH})_2 + \text{Mg}(\text{OH})_2 : \text{H}_2\text{O}$ mixture (1:0.45:1.62)

156°C, 12 hr., as shown by curve G in Figure 33

Broad bands appear in this pattern with maximum absorption at the following wavelengths: 2.71, 2.78, 2.93, 3.42, 6.13, 6.82, 9.00, 9.77, 10.15, 10.90, 11.45, 11.70, 11.95 and 12.6 μ . Bentonite and calcite are indicated. The presence of the following new compounds is suggested: C₄AH₁₃, Midgley (48); CSH (I), Kalousek and Prebus (37) and Diamond (14); CSH (II), Kalousek and Prebus (37) and Van Bemst (63). The greater intensity at 10.4 μ is apparent here somewhat more so than curve E; this indicates that tobermorite is probably also present in this mixture.

170°C, 12 hr., as shown by curve H in Figure 33

Broad bands appear in this pattern with maximum absorption at the following wavelengths: 2.70, 2.77, 2.93, 3.50, 6.16, 6.88, 9.16, 9.80, 10.11, 10.98, 11.45, 11.98 and 12.63 μ . Bentonite and calcite are indicated although band maxima have shifted somewhat. The presence of the following new compounds is suggested: C₄AH₁₃, Midgley (48); CSH (I), Kalousek and Prebus (37) and Diamond (14); CSH (II), Kalousek and Prebus (37) and Van Bemst (63). Increased intensities occur for the tobermorite band so it, too, is probably present in this mixture.

Electron Probe Analysis

Two typical single crystals were selected from a sample of the dolomitic monohydrated lime bentonite mixture which had been open to laboratory atmosphere about four months. These were hexagonal in crystal habit. A Debye-Scherrer rotating single crystal film was made by x-ray diffraction using chromium radiation. Examination of the diffraction pattern showed these to be the same compound isolated by Glenn and Handy (22). As indicated in the earlier paper, the strongest d-spacings at 7.9, 3.9 and $2.8 \overset{\circ}{\text{A}}$ correspond closely to the β form of C_4AH_{13} studied by Buttler, Glasser and Taylor (10).

The mounted crystals were noted to have a general background of calcium and silicon in the electron probe analysis. The composition and atom percentages of the crystals were as follows. Crystal number one indicated calcium (~40%), aluminum (weak) and silicon (~15%); crystal number two indicated calcium (~75-80%), aluminum (~15-20%) and silicon (weak). Relating these data, the approximate formula for the first crystal is C_3SA_7 and for the second is $\text{C}_{4-5}\text{AS}_7$.

A microscopic examination of the crystals after the examination revealed that crystal number one was completely covered by the Duco cement; the surface of crystal number two

was apparently clear of foreign material. Results on the first crystal would necessarily be open to question because of contamination by the cement. The findings on the second crystal should be reliable; the approximate composition is near that associated with the tetracalcium aluminates and it is therefore probably identified as C_4AH_{13} .

Summary of Results

The compounds formed in the lime-bentonite mixtures are tabulated according to three phases of treatment. Each table is arranged by mixture and method of analysis. Products formed in room cured mixtures are presented in Table 7. Table 8 gives the products from hydrothermal treatment of freshly prepared mixtures. The products found in the room cured mixtures after hydrothermal treatment are listed in Table 9.

Table 7. Summary of products of room cured mixtures

Method	Mixture	Bentonite: Ca(OH)_2 (C/S = 0.69)	Bentonite: $\text{Ca(OH)}_2 + \text{MgO}$ (C/S = 0.45)	Bentonite: $\text{Ca(OH)}_2 + \text{Mg(OH)}_2$ (C/S = 0.39)
X-ray diffraction		C_4AH_{13} , CSH I, II? ^a , Gel	C_4AH_{13} , CSH I, II Gel	CSH I, II?, Gel
DTA		C_4AH_{13} , CSH I	CSH I, Gel	CSH II?, Gel
Electron microscopy		Flat plates, rolled tubes	C_4AH_{13} , fibers, tubes, thin plates: CSH I	
Infrared spectroscopy		C_4AH_{13} , CSH I, II, Gel?	C_4AH_{13} , CSH I, II? Gel?	C_4AH_{13} , CSH I, CSH II, Gel?
Electron probe			C_{4-5}A	

^a? - uncertain.

Table 8. Summary of products of hydrothermal reaction of freshly prepared mixtures

Mixture	Method	X-ray diffraction	DTA
Hydrothermal, 170°C Bentonite: Ca(OH) ₂ (C/S = 0.69)		11.7 Å ^o Tob ^a CSH I, II? ^b	
Bentonite: Ca(OH) ₂ + MgO (C/S = 0.45)		11.5 Å ^o Tob CSH I, II?	CSH II?, Gel
Bentonite: Ca(OH) ₂ + Mg(OH) ₂ (C/S = 0.39)		11.2 Å ^o Tob CSH I, II?	CSH II?
Bentonite: Ca(OH) ₂ + MgO Hydrothermal, 170°C C/S = 0.22 C/S = 0.45 C/S = 1.00 C/S = 1.30 C/S = 2.00		11.5 Å ^o Tob CSH I, II? CSH I, II? CSH I, II? CSH I, II?	CSH II?, Gel CSH II?, Gel CSH II CSH II

^aTob - tobermorite.

^b? - uncertain.

Table 9. Summary of products of hydrothermal reaction of cured mixtures

Mixture	Method	X-ray Diffraction	DTA	Infrared Spectroscopy
Bentonite: Ca(OH) ₂ (C/S = 0.69) Hydrothermal, °C				
	40°	C ₄ AH ₁₃ , CSH I	CSH	C ₄ AH ₁₃ , Tob? ^a , CSH I, II, Gel?
	80°	CSH I	Al Tob? or CSH II	C ₄ AH ₁₃ ?, Tob?, CSH I, II?, Gel?
	105°	Tob?, CSH I, II?	Al Tob? or CSH I, II?	C ₄ AH ₁₃ , Tob?, CSH I, II?, Gel?
	145°		CSH I	
	156°	12.6 Tob	Al Tob? or CSH I?	C ₄ AH ₁₃ , Tob, CSH I, II?, Gel?
	164°	11.7 Tob or CSH II?	CSH I	
	170°	11.7 Tob or CSH II?	Al Tob?, CSH I	C ₄ AH ₁₃ , Tob, CSH I, II?, Gel?

^aTob - Tobermorite; ? - uncertain.

Table 9. (Continued)

Mixture	Method	X-ray Diffraction	DTA	Infrared Spectroscopy
Bentonite: Ca(OH) ₂ + MgO (C/S = 0.45) Hydrothermal, °C				
40°		C ₄ AH ₁₃ , CSH I?, Gel		C ₄ AH ₁₃ , Tob?, CSH I, II, Gel?
80°		CSH I	CSH I	C ₄ AH ₁₃ , Tob?, CSH I, II, Gel?
105°		C ₄ AH ₁₃ , CSH I	CSH I?, II?	C ₄ AH ₁₃ , Tob?, CSH I, II, Gel?
145°		C ₄ AH ₁₃ , CSH I	A1 Tob? or CSH I?	C ₄ AH ₁₃ , Tob?, CSH I, II, Gel?
156°		C ₄ AH ₁₃ ?, 11.6 Tob	A1 Tob	C ₄ AH ₁₃ , Tob, CSH I, II, Gel?
164°			A1 Tob or CSH I?	
170°		11.6 Tob, CSH II?	A1 Tob	C ₄ AH ₁₃ ?, Tob, CSH I, II, Gel?

Table 9. (Continued)

Mixture	Method	X-ray Diffraction	DTA	Infrared Spectroscopy
Bentonite: Ca(OH) ₂ + Mg(OH) ₂ (C/S = 0.39) Hydrothermal, °C				
40°		CSH I	?	C ₄ AH ₁₃ , Tob?, CSH I, II, Gel?
80°		CSH I, II?, αC ₂ SH?	?	C ₄ AH ₁₃ , Tob?, CSH I, II, Gel?
105°		CSH I, II?, αC ₂ SH	?	C ₄ AH ₁₃ , Tob?, CSH I, II, Gel?
145°		11 Tob?, CSH I, CSH II?, αC ₂ SH	Al Tob or CSH I	
156°		11.5 Tob, CSH I, CSH II?	Al Tob or CSH I	C ₄ AH ₁₃ , Tob, CSH I, II, Gel?
164°			Al Tob or CSH I	
170°		11.5 Tob, CSH I, CSH II?		C ₄ AH ₁₃ , Tob, CSH I, II, Gel?

DISCUSSION

The previous chapter related detailed experimental results to previous work whereby the products were characterized. Tables 7, 8 and 9 presented summaries of the products formed in reactions between mixtures of bentonite and three types of lime. Any uncertainty indicated there for a product was, in most instances, with reference to the particular phase of the hydrate which was present. These compounds may be classified in two groups: the calcium silicate hydrates and the calcium aluminate hydrates.

Calcium Aluminate Hydrates

Curing under room conditions for periods up to two and one-half years produces the tetracalcium aluminate hydrates in bentonite mixtures with calcitic or dolomitic monohydrated lime. Identification of C_4AH_{13} was made using x-ray diffraction, DTA and infrared spectroscopy. Slow scan x-ray diffraction techniques further indicated that another phase and lower hydrates of this compound were also present. Probable chemical composition was found by electron probe microanalysis. The absence of tetracalcium aluminates from the bentonite-dolomitic dihydrated lime mixture was indicated by x-ray diffraction and DTA but not by infrared spectroscopy. It is

extremely doubtful that the latter method, as it was employed in this study, gave reliable results for characterization of this compound in these mixtures. As indicated earlier, only one spectra for C_4AH_{13} was found in the literature for comparison.

No aluminate hydrates were produced in freshly prepared lime-bentonite mixtures, hydrothermally reacted at $170^{\circ}C$ for 12 hours.

As indicated above, only two of the three room-cured mixtures were found to contain calcium aluminate hydrates. When these three mixtures were hydrothermally reacted at various temperatures, modifications and compositional changes were indicated by x-ray diffraction. The calcium aluminate hydrate phase was noted by x-ray diffraction to persist only through the $40^{\circ}C$ reaction in the mixture containing calcitic lime. It was found to persist through the $156^{\circ}C$ reaction in the dolomitic monohydrated lime mixture. None of these phenomena were indicated by DTA. However, from x-ray diffraction and DTA, incidence of possible aluminum substitutions in the calcium silicate hydrate phase seems to be related to the apparent diminishing crystalline character of the aluminate. The C_4AH_{13} product is indicated by infrared spectroscopy in all mixtures and under every hydrothermal

condition. This result is questionable, for reasons cited earlier.

Calcium Silicate Hydrates

All methods of analysis show that the calcium silicate hydrates, CSH (I), CSH Gel and possibly CSH (II) are produced by room curing of all three lime-bentonite mixtures.

Freshly prepared mixtures of bentonite with calcitic lime (C/S ratio¹ = 0.69), dolomitic monohydrated lime (C/S ratio = 0.45) or dolomitic dihydrated lime (C/S ratio = 0.39) after hydrothermal treatment at 170°C for 12 hrs. were found by x-ray diffraction to contain well crystallized tobermorite, CSH (I) and possibly CSH (II). Results by DTA indicated calcium silicate hydrates but with uncertainty of the exact phases present.

Freshly prepared mixtures of variable C/S ratio (0.22-2.00) from dolomitic monohydrated lime and bentonite were found to produce calcium silicate hydrates in every instance. CSH Gel, CSH (I) and possibly CSH (II) were produced in the mixture at the lowest C/S ratio of 0.22. As indicated above, tobermorite was only produced in the mixture at a C/S ratio

¹C/S ratio based on chemical composition of bentonite : 52% SiO₂ (39).

of 0.45. CSH (I), and possibly CSH (II), are the only products noted in the mixtures of higher C/S ratio. The C/S ratio of 0.45 appears to be near the optimum for producing well crystallized tobermorite by this treatment.

Cured mixtures of lime-bentonite, after hydrothermal treatments at various temperatures, were found to contain several calcium silicate hydrate phases. CSH (I) was noted by x-ray diffraction in all mixtures after the 40°C treatment. The mixture containing calcitic lime was noted by DTA to contain an unidentified CSH phase after 40°C treatment; DTA results were uncertain for the other two mixtures. Indications by infrared spectroscopy of CSH Gel, CSH (II) and tobermorite in the mixtures after low temperature treatments were noted in the previous chapter to be uncertain; however, general agreement by several authors on the CSH (I) spectra lend more credence to its use for identification. CSH (I) was indicated to be present in this mixture by this method.

Mixtures of bentonite with calcitic or dolomitic monohydrated lime after the 80° and 105°C treatments were found by x-ray diffraction, DTA and infrared spectroscopy to contain CSH (I). CSH (II) and a higher crystalline form are suggested for the mixture containing calcitic lime but not by x-ray

diffraction. DTA results for the mixture containing dolomitic dihydrated lime are uncertain; x-ray diffraction indicated CSH (I) and possibly CSH (II) and $\alpha\text{C}_2\text{SH}$. The 80° and 105°C treatments have apparently modified the cured mixtures as follows. The CSH Gel is no longer present; the CSH (I) has persisted to an unknown extent. Conversion of one or both compounds or production of new phases is suggested.

Higher temperature treatments caused more noticeable changes. Highly crystalline CSH (I) or tobermorite definitely appears in all cured mixtures after treatments at 156°C . This is indicated by DTA in the mixtures containing the dolomitic monohydrated or dihydrated lime after 145°C but only by x-ray diffraction for the dihydrated lime mixture. Both x-ray diffraction and DTA indicate that these CSH phases have intermediate lime contents ($\sim 1.2-1.4$). X-ray diffraction and DTA gave evidence for aluminum substitution in the CSH lattice; it appears in all mixtures containing dolomitic lime after the 156° treatment. After the 164°C treatment, x-ray diffraction indicates conclusively the presence in all mixtures of well crystallized tobermorite with aluminum lattice substitutions. Persistence of other CSH compounds is inconclusive because identification criteria overlap. The probability that most

of the CSH compounds have been modified to produce tobermorite and that aluminum substitution has occurred are suggested by x-ray diffraction and DTA; tobermorite is more clearly indicated by infrared spectroscopy as well.

CONCLUSIONS

Calcitic or dolomitic monohydrated lime mixed with bentonite and water (weight ratio of 0.45 : 1.00 : 1.62) produce the tetracalcium aluminate hydrates during two and one-half years curing at room temperature.

Calcitic, dolomitic monohydrated or dihydrated lime mixed with bentonite and water (weight ratio of 0.45 : 1.00 : 1.62) produce the lower crystalline forms of the calcium silicate hydrates, namely, CSH Gel, CSH (I) and possibly CSH (II), during two and one-half years curing at room temperature.

The reaction products formed by curing at room temperature for periods up to two and one-half years have no apparent influence on the subsequent production of well crystallized tobermorite by hydrothermal treatment (170°C, 12 hours). Hydrothermal treatments at lower temperatures indicate that these phases may be utilized in the reactions with other components at intermediate and higher temperatures to produce the highly crystalline form of tobermorite above 155°C. Substitutions by aluminum in the tobermorite lattice are also indicated.

X-ray diffraction was found to be the most effective and

versatile method for identification of the products of the lime-bentonite-water reaction, either from room curing condition or hydrothermal treatment. DTA provided clarification at certain points in the investigation. Infrared spectroscopy results were generally inconclusive because of limited and conflicting data in the literature with which to correlate. Electron microscopy and electron probe microanalysis were used only to a limited extent; therefore, evaluations are not made. Whether or not these and DTA and infrared spectroscopy methods can be made more effective awaits the outcome from their use in further studies of the pure compounds found in these mixtures. Standardization of technique is strongly suggested so that the results may be used in correlation studies for identification.

The schematic in Figure 34 was suggested by the results of this study.

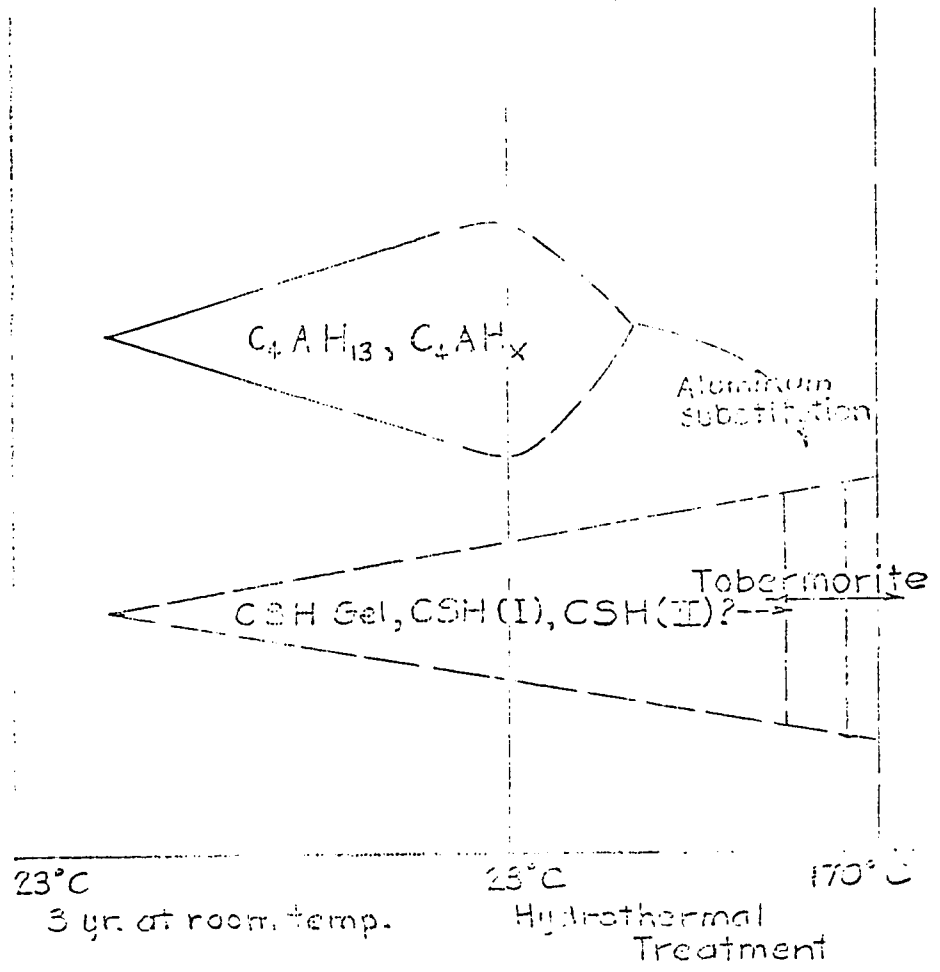


Fig. 34 Schematic of reaction product formation

REFERENCES

1. American Society for Testing Materials. Standard on hydraulic cement, designation C 219-55. Book of Standards 4: 195. 1958.
2. Anday, M. C. Accelerated curing for lime-stabilized soils. Highway Research Board. Bulletin 304: 1-13. 1962.
3. _____. Curing lime stabilized soils. [To be published in Highway Research Board 1963 Proceedings. ca. 1963]
4. Aruja, E. The unit cell and space group of $4\text{CaO}\cdot\text{Al}_2\text{O}_3\cdot 19\text{H}_2\text{O}$ polymorphs. Acta Crystallographica 14: 1213-1216. 1961.
5. Bernal, J. D. The structures of cement hydration compounds. The Third International Symposium on The Chemistry of Cement, London, 1952, Proceedings 1: 216-260. 1952.
6. Bogue, Robert Herman. The chemistry of Portland cement. Second edition. New York, New York, Reinhold Publishing Corporation. 1955.
7. Brunauer, Stephen. Tobermorite gel--the heart of concrete. American Scientist 50: 210-229. 1962.
8. _____, Copeland, L. E., and Bragg, R. H. The stoichiometry of the hydration of tricalcium silicate at room temperature. II. Hydration in paste form. Journal of Physical Chemistry 60: 116-120. 1956.
9. _____ and Greenberg, S. A. The hydration of tricalcium silicate and β -dicalcium silicate at room temperature. The Fourth International Symposium on the Chemistry of Cement, Washington, 1960, Proceedings 1: 135-165. 1962.

10. Buttler, F. G., Glasser, L. S. Dent, and Taylor H. F. W. Studies on $4\text{CaO}\cdot\text{Al}_2\text{O}_3\cdot 13\text{H}_2\text{O}$ and the related natural mineral hydrocalumite. American Ceramic Society Journal 42: 121-126. 1959.
11. Carlson, Elmer T. and Berman, Horace A. Some observations on the calcium aluminate carbonate hydrates. National Bureau of Standards. Journal of Research 64A: 333-341. 1960.
12. Claringbull, G. F. and Hey, M. H. A re-examination of tobermorite. Mineralogical Magazine 29: 960-962. 1952.
13. D'Ans, J. and Eick, H. Das System $\text{CaO}-\text{Al}_2\text{O}_3-\text{H}_2\text{O}$ bei 20°C und das Erhärten der Tonerdezemente. Zement-Kalk-Gips 6: 197-210. 1953.
14. Diamond, Sidney. Tobermorite and tobermorite-like calcium silicate hydrates: their properties and relationships to clay minerals. Unpublished Ph.D. thesis. Lafayette, Indiana, Library, Purdue University. 1963.
15. Eades, James L. and Grim, Ralph E. The reaction of hydrated lime with pure clay minerals in soil stabilization. National Academy of Sciences-National Research Council Publication 771: 51-63. 1960.
16. _____, Nichols, F. P., Jr. and Grim, Ralph E. Formation of new minerals with lime stabilization as proven by field experiments in Virginia. Highway Research Board Bulletin 335: 32-39. 1962.
17. Flint, E. P., Mc Murdie, H. F. and Wells, L. S. Formation of hydrated calcium silicates at elevated temperatures and pressures. National Bureau of Standards. Journal of Research 21: 617-638. 1938.
18. Gard, J. A., Howison, J. W. and Taylor, H. F. W. Synthetic compounds related to tobermorite: an electron microscope, x-ray, and dehydration study. Mineralogical Magazine 11: 151-158. 1959.

19. _____ and Taylor, H. F. W. A further investigation of tobermorite from Loch Eynort, Scotland. *Mineralogical Magazine* 31: 361-370. 1957.
20. Gaze, R. and Robertson, Robert H. S. Some observations on calcium silicate hydrate (I)-tobermorite. *Magazine of Concrete Research* 22: 7-12. 1956.
21. _____ and _____. Unbroken tobermorite crystals from hydrated cement. *Magazine of Concrete Research* 22: 25-26. 1957.
22. Glenn, G. R. and Handy, R. L. Lime-clay mineral reaction products. [To be published in Highway Research Board 1963 Proceedings. ca. 1963].
23. Grudemo, A. An electronographic study of the morphology and crystallization properties of calcium silicate hydrates. (In English). Svenska Forskningsinstitutet för cement och Betong vid Kungl. Stockholm. 26: 1-103. 1955.
24. _____. The microstructure of hardened cement paste. The Fourth International Symposium on the Chemistry of Cement, Washington, 1960, Proceedings 2: 615-647. 1962.
25. Heller, L. and Taylor, H. F. W. Crystallographic data for the calcium silicates. First edition. London. Her Majesty's Stationery Office. 1956.
26. _____ and _____. Hydrated calcium silicates. IV. Hydrothermal reactions: lime:silica ratios 2:1 and 3:1. *Chemical Society London Journal*. 2535-2541. 1952.
27. _____ and _____. Hydrated calcium silicates. II. Hydrothermal reactions: lime:silica ratio 1:1. *Chemical Society London Journal*. 2397-2401. 1951.
28. Hilt, G. H. and Davidson, D. T. Isolation and investigation of lime-montmorillonite-crystalline reaction product. Highway Research Board. Bulletin 304: 51-65. 1961.
29. _____ and _____. Lime fixation in clayey soils. Highway Research Board Bulletin 262: 20-32. 1960.

30. Ho, C. and Handy, R. L. Characteristics of lime retention by montmorillonitic soils. [To be published in Highway Research Board, 1963 Proceedings. ca. 1963].
31. _____ and _____. The effect of lime on electrokinetic properties of bentonites. [To be published in 1963 Clays and Clay Minerals. ca. 1964].
32. Hunt, Charles M. Infrared absorption of some compounds in the CaO-SiO₂-H₂O system. The Fourth International Symposium on the Chemistry of Cement, Washington, 1960, Proceedings 1: 297-305. 1962.
33. Jones, F. E. Hydration of calcium aluminates and ferrites. The Fourth International Symposium on the Chemistry of Cement, Washington, 1960, Proceedings 1: 204-242. 1962.
34. Kalousek, George L. Crystal chemistry of hydrous calcium silicates: I, substitution of aluminum in lattice of tobermorite. American Ceramic Society Journal 40: 74-80. 1957.
35. _____. Tobermorite and related phases in the system CaO-SiO₂-H₂O. American Concrete Institute Journal 26: 989-1011. 1955.
36. _____, Davis, C. W. and Schmertz, W. E. An investigation of hydrating cements and related hydrous solids by differential thermal analysis. American Concrete Institute Journal 20: 693-713. 1949.
37. _____ and Prebus, Albert F. Crystal chemistry of hydrous calcium silicates. III. Morphology and other properties of tobermorite and related phases. American Ceramic Society Journal 41: 124-132. 1958.
38. _____ and Roy, Rustum. Crystal chemistry of hydrous calcium silicates. II. Characterization of interlayer water. American Ceramic Society Journal 40: 236-239. 1957.

39. Kerr, Paul F., Director. Analytical data on reference clay materials. American Petroleum Institute Project 49, Preliminary Report 7: 1-160. 1950.
40. _____. Infrared spectra of reference clay minerals. American Petroleum Institute Project 49, Preliminary Report 8: 1-146. 1950.
41. Lea, F. M. The chemistry of pozzolanas. Symposium on the Chemistry of Cement, Stockholm, 1938, Proceedings 1: 460-490. 1939.
42. McCaleb, Stanley B. Hydrothermal products formed from montmorillonite clay systems. Ninth National Conference on Clays and Clay Minerals. Proceedings. 1962: 276-294. 1962.
43. McConnell, J. D. C. The hydrated calcium silicates riversideite, tobermorite, and plombierite. Mineralogical Magazine 30: 293-305. 1954.
44. Mackenzie, Robert C. The differential thermal investigation of clays. First edition. London. The Central Press. 1957.
45. Majumdar, A. J. and Roy, R. The system $\text{CaO-Al}_2\text{O}_3\text{-H}_2\text{O}$. American Ceramic Society Journal 39: 434-442. 1956.
46. Megaw, H. D. and Kelsey, C. H. Crystal structure of tobermorite. Nature 177: 390-391. 1956.
47. Midgley, H. G. A compilation of x-ray powder diffraction data of cement minerals. Magazine of Concrete Research 9: 17-24. 1957.
48. _____. The mineralogical examination of set Portland cement. The Fourth International Symposium on the Chemistry of Cement, Washington, 1960, Proceedings 1: 479-490. 1962.
49. Miller, L. B. Electron diffraction research. Rock Products 42, Number 9: 41-42. 1939.

50. Percival, A. and Taylor, H. F. W. Monocalcium aluminate hydrate in the system $\text{CaO-Al}_2\text{O}_3\text{-H}_2\text{O}$ at 21° . Chemical Society London Journal 2629-2631. 1959.
51. Roberts, M. H. New calcium aluminate hydrates. Journal of Applied Chemistry 7: 543-546. 1957.
52. Smith, Joseph V., Editor. Index to the x-ray powder data file. Philadelphia, Pennsylvania, American Society for Testing Materials. 1961.
53. Steinour, Harold H. The reactions and thermochemistry of cement hydration at ordinary temperature. Portland Cement Association 44: 1-32. 1953.
54. Taylor, H. F. W. Hydrated calcium silicates. I. Compound formation at ordinary temperatures. Chemical Society London Journal. 3682-3690. 1950.
55. _____. Hydrothermal reactions in the system $\text{CaO-SiO}_2\text{-H}_2\text{O}$ and the steam curing of cement and cement-silica products. The Fourth International Symposium on the Chemistry of Cement, Washington, 1960, Proceedings 1: 167-190. 1962.
56. _____. The chemistry of cement hydration. In Burke, J. E., editor. Progress in ceramic science. Vol. 1: 89-145. New York, New York, Pergamon Press. 1961.
57. _____ and Bessey, G. E. A review of hydrothermal reactions in the system $\text{CaO-SiO}_2\text{-H}_2\text{O}$. Magazine of Concrete Research 4: 15-26. 1950.
58. Thompson, G. P. The diffraction of cathode rays by thin film of platinum. Nature 120: 802. 1927.
59. Tilley, C. E., Megaw, H. D. and Hey, M. H. Hydrocalumite ($4\text{CaO}\cdot\text{Al}_2\text{O}_3\cdot 12\text{H}_2\text{O}$), a new mineral from Scawt Hill, Co., Antrim. Mineralogical Magazine 23: 607-615. 1934.
60. Toropov, N. A., Borisenko, A. I., and Shirokova, P. V. Gydsilikaty Kaltsiya. Akademia nauk S.S.S.R. Doklady. Otdelenie Khimicheskikh Nauk. 1: 65-69. 1953.

61. Turriziani, Renato. Prodotti di reazione dell'idrato di calcio con la pozzolana. *La Ricerca Scientifica*. 24: 1709-1717. 1954.
62. U. S. Patent No. 2, 665, 996. Hydrous calcium silicates and method of preparation. George L. Kalousek, Assignor to Owens-Illinois Glass Co., Toledo, Ohio. 1954.
63. Van Bemst, A. Contribution a l'edude de l'hydratation des silicates de calcium purs. *Societee Chemique Belges Bulletin* 64: 333-351. 1955.
64. Wells, Lansing S., Clarke, W. F. and McMurdie, H. F. Study of the system $\text{CaO-Al}_2\text{O}_3\text{-H}_2\text{O}$ at temperatures of 21° and 90°C . *National Bureau of Standards Journal of Research* 30: 367-409. 1943.

ACKNOWLEDGMENTS

It is with deep sincerity that I write these words of....
thanks to the faculty and staff of a really great university for assisting me, personally, professionally and financially to achieve the overall program of work and study; among those specially helpful were Dr. George Burnet and Dr. Elmer Rosauer;

appreciation to the members of my committee, Dr. Turgut Demirel, Dr. Donald Fitzwater, Dr. John Lemish and Dr. R. E. Untrauer for their guidance, encouragement and inspiration in my graduate program;

special tribute to my major professor, Dr. R. L. Handy, for his help and encouragement to begin this task and his continued personal interest, concern and recommendation, and without whom none of the activities culminating in this thesis would have been possible;

gratitude to my daughter Beth, who shared in special ways, and to my wife and family for their encouragement and forbearance.

I deeply regret that two of my committee have passed from this life since this work was begun three years ago. Dr. Donald Davidson and Dr. Robert Rundle gave unselfishly to me and to others. To show appreciation, I can only strive to do as well.